



The genomic landscape, causes, and consequences of extensive phylogenomic discordance in murine rodents

Journal:	<i>Genome Biology and Evolution</i>
Manuscript ID	GBE-241028
Manuscript Type:	Article
Date Submitted by the Author:	16-Oct-2024
Complete List of Authors:	Thomas, Gregg; Harvard University, Informatics Group; University of Montana, Biological Sciences Hughes, Jonathan; Cornell University, Department of Ecology and Evolutionary Biology Kumon, Tomohiro; University of Pennsylvania, Department of Biology Berv, Jacob; Cornell University, Department of Ecology and Evolutionary Biology; University of Michigan, Department of Ecology and Evolutionary Biology Nordgren, C. Erik; University of Pennsylvania, Department of Biology Lampson, Michael; University of Pennsylvania, Department of Biology Levine, Mia; University of Pennsylvania, Department of Biology Searle, Jeremy; Cornell University, Ecology and Evolutionary Biology Good, Jeffrey; University of Montana, Biological Sciences
Keywords:	phylogenetic discordance, murine rodents, molecular evolution, recombination, genomics, mouse

SCHOLARONE™
Manuscripts

1 **The genomic landscape, causes, and consequences of extensive phylogenomic discordance**
2 **in murine rodents**

3

4 Gregg W. C. Thomas^{1,2,*}, Jonathan J. Hughes^{3,4}, Tomohiro Kumon⁵, Jacob S. Berv^{3,6}, C. Erik
5 Nordgren⁵, Michael Lampson⁵, Mia Levine⁵, Jeremy B. Searle³, Jeffrey M. Good¹

6

7 ¹*Division of Biological Sciences, University of Montana, Missoula, MT, 59801.*

8 ²*Informatics Group, Harvard University, Cambridge, MA, 02138*

9 ³*Department of Ecology and Evolutionary Biology, Cornell University, Ithaca, NY, 14853.*

10 ⁴*Department of Evolution, Ecology, and Organismal Biology, University of California Riverside,
11 Riverside, CA, 92521*

12 ⁵*Department of Biology, University of Pennsylvania, Philadelphia, PA, 19104*

13 ⁶*Department of Ecology and Evolutionary Biology, University of Michigan, Ann Arbor, MI,
14 48109*

15

16 *Corresponding author

17 E-mail: gthomas@fas.harvard.edu

18

19 Abstract

20 A species tree is a central concept in evolutionary biology whereby a single branching phylogeny
21 reflects relationships among species. However, the phylogenies of different genomic regions often
22 differ from the species tree. Although tree discordance is widespread in phylogenomic studies, we
23 still lack a clear understanding of how variation in phylogenetic patterns is shaped by genome
24 biology or the extent to which discordance may compromise comparative studies. We
25 characterized patterns of phylogenomic discordance across the murine rodents – a large and
26 ecologically diverse group that gave rise to the laboratory mouse and rat model systems.
27 Combining recently published linked-read genome assemblies for seven murine species with other
28 available rodent genomes, we first used ultra-conserved elements (UCEs) to infer a robust time-
29 calibrated species tree. We then used whole genomes to examine finer-scale patterns of
30 discordance across 12 million years of divergence. We found that proximate chromosomal regions
31 tended to have more similar phylogenetic histories, but no clear relationship between local tree
32 similarity and recombination rates in house mice. However, we did observe a correlation between
33 recombination rates and average similarity to the species tree. We also detected a strong influence
34 of linked selection whereby purifying selection at UCEs led to appreciably less discordance.
35 Finally, we show that assuming a single species tree can result in high error rates when testing for
36 positive selection under different models. Collectively, our results highlight the complex
37 relationship between phylogenetic inference and genome biology and underscore how failure to
38 account for this complexity can mislead comparative genomic studies.

39

40 **Keywords:** *phylogenetic discordance, murine rodents, molecular evolution recombination,*
41 *genomics, mouse*

42 Significance Statement

43 Genomic data has demonstrated that when sequences from multiple species are compared,
44 different regions of the genome exhibit different phylogenetic histories. These discordant histories
45 could be due to either biological processes, such as ancestral variation or introgression, or artifacts
46 of the inference process. We use the genomes of several murine rodents to distinguish how features
47 of the genome, such as recombination rates, genes, and other conserved regions, affect this
48 discordance across the genome. Considering the prevalence of discordance across the genome, we
49 also test how using a single species tree, a common practice, affects inferences from tests for
50 positive selection. Our study shows that conserved genomic loci exhibit lower amounts of
51 discordance, and that discordance can negatively affect inferences of selection when the incorrect
52 species tree is used.

53 Introduction

54 Phylogenies are the unifying concept in understanding the evolution of species, traits, and genes.
55 However, extensive high-throughput sequencing data has now revealed that evolutionary
56 relationships between species may not be well represented by a single representative phylogeny
57 (Edwards 2009; Hahn and Nakhleh 2016). While a dominant signal of bifurcating speciation
58 usually exists (*i.e.*, a species tree), phylogenetic signal that may disagree with species relationships
59 can arise from ancestral polymorphisms (incomplete lineage sorting; ILS), gene flow
60 (introgression), and gene duplication and loss (Maddison 1997). The theoretical prediction of
61 phylogenetic discordance has long been appreciated (Hudson 1983; Pamilo and Nei 1988;
62 Maddison 1997; Rosenberg 2002), but empirical evidence now emphasizes just how extensive
63 discordance can be among a set of species (Feng, et al. 2022; Gable, et al. 2022; Smith, et al. 2023).
64 For example, studies of birds (Jarvis, et al. 2014), mammals (Ferreira, et al. 2021; Lopes, et al.
65 2021; Foley, et al. 2024), plants (Pease, et al. 2016), and insects (Sun, et al. 2021; He, et al. 2023)
66 have found that with extensive taxon sampling and genomic data, highly supported species tree
67 topologies are rarely or never recovered in the underlying locus trees. Whereas these examples
68 highlight the prevalence of phylogenetic discordance across the tree of life, we still lack a clear
69 understanding of how phylogenetic patterns are shaped by the details of genome biology or the
70 extent to which discordance may compromise inferences from comparative studies that assume a
71 singular species history.

72 In practice, failure to acknowledge and account for phylogenetic discordance could
73 severely affect biological inference. Analyses of molecular evolution are usually performed on a
74 gene-by-gene basis (Pond, et al. 2005; Yang 2007; Hu, et al. 2019; Kowalczyk, et al. 2019), but it
75 is still common practice to assume a single genome-wide species tree for each locus. For gene-
76 based analyses, using the wrong tree may cause erroneous inferences of positive directional
77 selection, convergent evolution, and genome-wide inferences of correlated rate variation (Mendes,
78 et al. 2016). Phylogenetic discordance can also affect how continuous traits are reconstructed
79 across phylogenies, as the genes that underly these traits may not follow the species history (Avise
80 and Robinson 2008; Hahn and Nakhleh 2016; Mendes, et al. 2018; Hibbins, et al. 2023). In these
81 instances, phylogenetic discordance may need to be characterized and incorporated into the
82 experimental and analytical design. Alternatively, if a researcher's primary questions are focused
83 on reconstructing the evolutionary history of speciation (*i.e.*, the species tree), then phylogenetic
84 discordance may obscure the true signal of speciation (Fontaine, et al. 2015; Foley, et al. 2024). In
85 this case, knowledge about patterns of discordance across genomes could inform decisions about
86 locus selection, data filtering, and model parameters during species tree reconstruction.

87 Given these considerations, a better understanding of the genomic context of phylogenetic
88 discordance is warranted. Although often conceptualized primarily as a stochastic consequence of
89 population history (Maddison 1997), patterns of phylogenetic discordance are likely to be non-
90 random and dependent on localized patterns of genetic drift, natural selection, recombination, and
91 mutation. Discordance due to ILS ultimately depends on effective population sizes across the
92 branches of the phylogeny (Pamilo and Nei 1988; Degnan and Rosenberg 2006) and, therefore,

93 should covary with any process that influences local patterns of genetic diversity (e.g., linked
94 negative or positive selection). Likewise, discordance due to introgression may be influenced by
95 selection against incompatible alleles or positive selection for beneficial variants (Lewontin and
96 Birch 1966; Jones, et al. 2018). Selection, ILS, and introgression, are expected to leave different
97 genomic signals that should allow us to test hypotheses about both the cause and the scale of
98 phylogenetic discordance (Huson, et al. 2005; Kulathinal, et al. 2009; Green, et al. 2010;
99 Vanderpool, et al. 2020). Yet the genomic context of phylogenetic discordance has remained
100 elusive. For example, localized patterns of phylogenetic discordance should be influenced by
101 patterns of recombination (Hudson and Kaplan 1988) and simulation studies confirm that the
102 closer two regions are in the genome, the more history they share (Slatkin and Pollack 2006;
103 McKenzie and Eaton 2020). However, empirical studies have been inconclusive regarding the
104 relationship between discordance and recombination rates, ranging from no relationship in great
105 apes (Hobolth, et al. 2007), a weak positive correlation in house mice (White, et al. 2009), a strong
106 positive correlation broadly across primates (Rivas-Gonzalez, et al. (2023)), or increased
107 discordance in regions of lower recombination (Scally, et al. 2012; Pease and Hahn 2013). Thus,
108 it remains unclear how phylogenetic discordance scales locally across the genome as a function of
109 recombination and the strength of linked selection, pointing to the need for empirical studies in
110 systems with sufficient genomic resources to explore the causes of discordance.

111 To investigate the causes and consequences of phylogenetic discordance, we took
112 advantage of genomic resources available for house mice (*Mus musculus*). This rodent species is
113 one of the most important mammalian model systems for biological and biomedical research and
114 is embedded within a massive radiation of rats and mice (Murinae). This ecologically diverse and
115 species-rich group is comprised of over 600 species and makes up >10% of all mammalian species,
116 and yet is only about 15 million years old, making this system an excellent choice for phylogenetic
117 studies over both short and long timescales. Despite the power of evolution-guided functional and
118 biomedical analysis (Christmas, et al. 2023), relatively few murine genomes have been sequenced
119 outside of *Mus* and *Rattus*.

120 We analyze recently sequenced genomes for seven murine species (*Mastomys natalensis*,
121 *Hylomyscus allenii*, *Praomys delectorum*, *Rhabdomys dilectus*, *Grammoys dolichurus*, *Otomoys*
122 *typus*, and *Rhynchosomys soricoides*) sampled from across this radiation (Kumon, et al. 2021). We
123 combine these new genomes with previously sequenced genomes and genomic resources from the
124 *M. musculus* model system to study phylogenetic relationships within Murinae as well as the
125 landscape of discordance along rodent chromosomes. We first inferred a species tree for these and
126 other sequenced rodent genomes, focusing on signals derived from commonly used ultra-
127 conserved elements (UCEs). We used these UCE data to infer a robust, time-calibrated phylogeny
128 of sequenced murine rodents, providing a useful resource for future comparative studies within
129 this important group. Using this species tree, we then used a subset of whole genomes to study
130 how phylogenetic discordance is related to species-level inferences of relatedness, recombination
131 rate, and patterns of molecular evolution. Using genetic maps and functional annotation from the
132 powerful house mouse system, we test several hypotheses linking spatial patterns of discordance

133 to genetic drift, natural selection, and recombination. Finally, we show how the use of a single
134 species-tree impacts gene-level inferences from common molecular evolution tests for natural
135 selection in these species. Collectively, our results advance our understanding of how core features
136 of genome biology influence underlying phylogenetic patterns, the extent to which established
137 model system resources can be leveraged for broader phylogenetic studies, and the consequences
138 of ignoring phylogenetic uncertainty.

139

140 Results

141 *Estimation of a murine species tree*

142 Using a concatenated dataset of 2,632 aligned ultra conserved elements (UCEs), we inferred a
143 species tree of 18 murine rodent species (Figure 1; Table S1) that recovered the same relationships
144 as previous reconstructions of Murinae using a small number of loci (Lecompte, et al. 2008;
145 Steppan and Schenk 2017). The species tree inferred from a quartet-based summary of the gene
146 tree topologies was identical to the concatenated tree (Figure S1). While bootstrap and SH-aLRT
147 values provided high support to our inferred species trees (Figure 1), we found evidence for
148 considerable discordance across individual UCE phylogenies. The five shortest branches in the
149 concatenated tree had a site concordance factor (sCF) of less than 50%, suggesting that alternate
150 resolutions of the quartet had equivocal support (Figure S2). Gene concordance factors (gCF) for
151 each branch in the species tree were on aggregate much higher, with all but four branches
152 supported by almost every gene tree in the analysis and with the lowest values likely being driven
153 by a several short internal branches (Figure S2). This pattern was recapitulated using a quartet-
154 based summary method (Figs. S1 and S3). At the two most discordant nodes (E and J in Figure 1),
155 the recovered topology was supported by approximately one third of all gene trees.

156 We estimated divergence times for the inferred concatenated phylogeny (Figure 1; Table
157 S2) using four fossil calibration points (Table S3). The murid and cricetid groups had an estimated
158 divergence time of 22.66 Ma (node A in Figure 1) followed by the Murinae and the Gerbillinae at
159 21.34 Ma (B), albeit with wide confidence intervals (CI) in both cases. The core Murinae (C) *sensu*
160 Steppan et al. (2005) are inferred to have arisen 13.11 Ma (CI: 11.42 – 15.10). Hydromyini then
161 split off at 12.15 Ma (D, CI: 11.10 – 13.51) followed by Otomyini and Arvicanthini at 11.70 Ma
162 (E, fossil calibration from Kimura, et al 2015). The remaining Murine tribes evolved in rapid
163 succession, with Apodemini diverging from Murini and Praomyini at 10.84 Ma (F). Murini and
164 Praomyini then split at 10.19 Ma (H). The two *Rattus* species in our dataset were inferred to have
165 diverged 2.01 Ma (Q, CI: 1.26 – 2.30). Although congruent with previous works (Lecompte, et al.
166 2008; Steppan and Schenk 2017), this dated UCE phylogeny provides context on the evolutionary
167 timescale upon which we next describe the genomic landscape of phylogenetic discordance across
168 a collection of murine genomes.

169

170 *The landscape of phylogenetic discordance along murine genomes*

171 We analyzed genome-wide phylogenetic histories of six recently sequenced murine rodent
172 genomes and the *M. musculus* reference genome spanning approximately 12 million years of
173 divergence (see Figure 1). Using the *M. musculus* coordinate system, we partitioned and aligned
174 263,389 non-overlapping 10 kb windows from these seven species (Table S1). After filtering
175 windows in repetitive regions or with low phylogenetic signal, we recovered 163,765 trees with
176 an average of 616 informative sites per window (Figure S4).

177 Phylogenetic discordance was pervasive within and between chromosomes. We inferred
178 597 of the 945 possible unique rooted topologies among six species (when specifying *R. soricoides*
179 as the outgroup) across all chromosomes. The number of unique topologies per chromosome
180 ranged from 75 to 218 (mean = 141). However, just four different topologies were ranked in the
181 top three per chromosome. (Fig 2A; File S1) and only nine trees were present at a frequency above
182 1%. Among these, the top three topologies only differed in the ordering of the clade containing
183 *Hylomyscus allenii*, *Mastomys natalensis*, and *Praomys delectorum* (HMP clade). This clade also
184 showed the second lowest concordance in the species tree inferred from UCEs (Figure 1, node J).
185 These three topologies comprise between 13-15% of all recovered topologies (Figure 2).
186 Interestingly, the least common of these three trees (13.1%) matched the topology recovered via
187 concatenation of all coding regions and the species tree recovered from UCEs (Figure 1). That is,
188 the robustly inferred species tree did not match the evolutionary relationships inferred for over
189 85% of the genome.

190 While visual inspection revealed no clear partitioning of topological structures along
191 chromosomes (e.g., Figure 2C), we found that phylogenies were not randomly distributed across
192 mouse chromosomes. Using the weighted Robinson-Foulds metric, we found that tree similarity
193 between windows decayed logarithmically along chromosomes (Figure 3A and B), and the
194 distance at which tree similarity appeared random varied considerably among chromosomes
195 ranging from 0.15 Megabases (Mb) on chromosome 17 to 141.29 Mb on the chromosome 2 (Figure
196 3C, Figure S5). While chromosomes 2, 7, 9, and 11 were autosomal outliers with distances between
197 windows to random-like trees exceeding 25 Mb, the average distance among all other autosomes
198 was only 2.1 Mb. The rates at which phylogenetic similarity decayed tended to be inversely
199 proportional to the distance at which two randomly drawn phylogenies lost similarity (Figure 3D).

200 Next, we performed a pairwise alignment of the reference mouse and rat genomes to assess
201 how large structural variations, such as inversions and translocations, may influence our inferences
202 of phylogenetic relatedness along the genome. These species span the deepest divergence of the
203 sample for which we assessed genome-wide discordance, so the level of large structural variation
204 present among them should give us an idea of the amount of ancestral variation in our sample. The
205 mouse and rat genomes were mostly co-linear for large, aligned chunks, with large translocations
206 and inversions on mouse chromosomes 5, 8, 10, 13, and 16 (Figure S6). We also observe large-
207 scale inversions on chromosome 16. We found that, while most chromosomes were co-linear
208 between mouse and rat, the average size of the 307,275 contiguously aligned chunks averages
209 under 10 kb, with the average distance between aligned segments being between 2,380 bp on the
210 mouse genome and 4,927 bp on the rat chromosome (Figure S7). This pattern presents two major

211 implications for our analyses. First, we could not transpose the coordinate system from mouse to
212 rat with enough resolution to use genetic maps from rat. Second, most other structural variations
213 in our sample appear likely to be small insertions of transposable elements (e.g., SINEs ~150-500
214 bp, LINEs ~4-7kb; Platt, et al. 2018) that should have a negligible effect on discordance analyses
215 since our window size is much larger and we excluded windows that were made up of mostly
216 repeats.

217

218 *Discordance with recombination rate and other genomic features*

219 Using markers from genetic crosses within *M. musculus* (Shifman, et al. 2006; Cox, et al. 2009)
220 we examined whether regions with high recombination also showed more phylogenetic
221 discordance over short genetic distances when compared to regions with low recombination.
222 Specifically, we calculated recombination rates within 5 Mb windows (Figure S8) and then
223 measured tree similarity between the first and last 10 kb window ($R^2 = 3.0e-9$; $p = 0.99$; Figure
224 4A) and the rate at which tree similarity changes between the first 10 kb window and every other
225 10 kb window ($R^2 = 0.003$; $p = 0.11$; Figure 4B). Surprisingly, we found no relationship between
226 tree similarity and recombination rates measured at this scale. However, we did observe a slight
227 positive correlation between recombination rate and dissimilarity to the species tree when
228 averaging wRF over all 10 kb window trees within a 5 Mb recombination window ($R^2 = 0.05$; $p =$
229 $7.6e-8$; Figure 4C). We also examined regions of the genome centered on recombination hotspots
230 identified in *M. musculus* (Smagulova, et al. 2011) and found that these regions had significantly
231 slower rates of decay in similarity over genomic distance compared to windows that were not
232 centered on hotspots ($p = 0.019$; Figure 5A), and that they were also significantly more
233 phylogenetically similar over short distances ($p = 0.015$; Figure 5B). Thus, when taken as a whole,
234 we found that regions of higher recombination rates in house mice did not show more local
235 phylogenetic discordance per se but did tend to show more discordance relative to the genome-
236 wide species tree.

237 Evolutionary relationships around certain conserved genomic features may also be shaped
238 by locally reduced effective population sizes due to a history of pervasive linked negative or
239 positive selection. To test for this, we measured tree similarity in 10 kb windows around all
240 annotated protein-coding genes, ultra-conserved elements (UCEs), and protein-coding genes
241 identified as evolving rapidly (*i.e.*, significantly elevated d_N/d_S) due to positive directional selection
242 and compared these patterns relative to chromosome-wide trends (*i.e.*, windows without annotated
243 features). In general, UCEs showed more local phylogenetic similarity among adjacent windows
244 (*i.e.*, less discordance) than regions surrounding recombination hotspots ($p = 2.42e-12$), coding
245 genes ($p = 4.65e-14$), rapidly evolving coding genes ($p = 1.56e-6$), and windows that did not
246 include any of these features ($p = 5.02e-14$; Figure 5A). In contrast, protein-coding genes
247 (including rapidly evolving genes) were indistinguishable from background rates of discordance
248 observed in windows without annotated genomic features (Figure 5A). Likewise, UCEs were also
249 much more similar to the overall species tree when compared to any other feature (Figure 5B).
250 Unlike our test of local discordance, protein-coding genes also showed less species tree

251 discordance than windows containing no features or recombination hotspots, but the effect was
252 much less pronounced than observed at UCEs.

253

254 *Consequences of tree misspecification on analyses of molecular evolution*

255 Next, we examined how phylogenetic discordance influenced inferences on the evolution of
256 protein-coding sequences. Among a set of 22,261 *M. musculus* protein-coding transcripts, the
257 average distance between the start and end of the coding sequence was 37.02 kb, or roughly 4 non-
258 overlapping 10 kb windows. At this distance, tree similarity is predicted to diminish considerably
259 (e.g., by 0.10 wRF units), such that the phylogenetic history of individual genes may often contain
260 some phylogenetic discordance (Mendes and Hahn 2016; Mendes, et al. 2019). We also found that
261 out of the 67,566 times the coding sequence in a gene overlapped with a 10 kb window, the inferred
262 topology of the gene tree exactly matched the topology of the corresponding window tree only
263 11% of the time. Thus, the common practice of inferring gene trees on concatenated coding exons
264 from a single transcript is still likely averaging over multiple possible albeit correlated histories.

265 Finally, we tested how tree misspecification might impact standard d_N/d_S based
266 phylogenetic analyses for positive directional selection. Specifically, we used the still common
267 practice of assuming a single species tree for all genes and compared that to using individually
268 inferred gene trees in three common statistical tests for positive selection: PAML's M1a vs. M2a
269 test (Yang 2007), HyPhy's BUSTED test (Murrell, et al. 2015), and HyPhy's aBSREL test (Smith,
270 Wertheim, et al. 2015). We found evidence that tree misspecification likely induces both false
271 positive (type I) and false negative (type II) errors. For example, many genes were inferred as
272 having experienced positive directional selection when using a single species tree, but not when
273 using local gene trees and vice versa (Figure 6). Assuming the locally inferred gene tree is more
274 accurate than the single tree inferred from concatenation of all gene sequences, this resulted in
275 varying rates and types of error (Table 1). For BUSTED, we observe that 28% of genes inferred
276 as having evolved under positive directional selection when using the gene tree were not inferred
277 when using the concatenated species tree (likely false negatives). The opposite was true for M1a
278 vs. M2a, where, among genes showing inconsistent evidence for positive selection across the two
279 scenarios, 76% do so when using the concatenated species tree but not individual gene trees (likely
280 false positives). In general, genes found to be evolving under positive selection using both tree
281 types tended to be more concordant with the species tree than those that had evidence for positive
282 selection either using only the concatenated tree or the gene tree (Figure 6).

283

284 **Discussion**

285 Phylogenies provide insight into the relationships of species and serve as a framework for asking
286 questions about molecular and trait evolution. However, phylogenetic histories can vary
287 extensively across regions of a genome, and evolutionary relationships between species may not
288 often be well represented by a single representative species-level phylogeny. Here, we combine
289 the resources of the house mouse (*Mus musculus*) with new and recently published (Kumon et al.

290 2021) genomes from seven species to understand the systematics of murine rodents and causes
291 and consequences of phylogenetic discordance along murine genomes. These new analyses help
292 to place this important model system in a stronger evolutionary context and begin to fill the gap in
293 genome sampling of murine rodents, which, despite their exceptional morphological and
294 ecological diversity and species richness, have had relatively few whole genomes sequenced. They
295 further provide us with the resources to study the landscape of phylogenetic discordance across
296 the genome, understand how recombination and natural selection shape phylogenetic histories, and
297 evaluate how assuming a single evolutionary history can compromise the study of molecular
298 evolution in an important biomedical model system.

299

300 *Phylogenomic relationships of murine rodent lineages from conserved genomic regions*

301 The extraordinary species richness of murine rodents complicates phylogenetic analyses because
302 of the resources required to sample, sequence, and analyze such widely distributed taxa. Earlier
303 work either attempted to resolve specific groups such as *Mus* (Lundrigan, et al. 2002; Suzuki, et
304 al. 2004) and *Apodemus* (Serizawa, et al. 2000; Liu, et al. 2004), or to uncover broader
305 relationships across the subfamily (Martin, et al. 2000; Steppan, et al. 2005) based on a few genetic
306 markers. Lecompte et al. (2008) provided one of the earliest well-supported phylogenetic
307 reconstructions from across Murinae and the tribal classifications they proposed remain generally
308 supported. More recent work has increased the number of taxa sampled, both for analyses of
309 Murinae specifically (Pagès, et al. 2016) and for their placement within Muridae and Muroidea
310 (Schenk, et al. 2013; Steppan and Schenk 2017; Rowe, et al. 2019), but the number of loci used
311 for phylogenetic inference remained limited. Other recent studies have greatly expanded the
312 number of loci used for phylogenetic inference (Mikula, et al. 2021), including the use of 1,245
313 exons (Roycroft, et al. 2020) and 1,360 exons (Roycroft, et al. 2021), but have focused on specific
314 tribes within Murinae.

315 Our inferred species tree based on 2,632 UCEs from 18 species across the radiation (Figure
316 1) is consistent with previous studies (Lecompte, et al. 2008; Steppan and Schenk 2017; Aghova,
317 et al. 2018). Branch support was uniformly high, and gene trees unambiguously support the tribal
318 classification of Lecompte, et al. (2008). However, four shorter branches show more substantial
319 gene tree discordance (Figure 1, branches D, E, H, and J), with two recovered clades (E and J)
320 being supported by less than half of all gene trees. We also estimated divergence times on our
321 inferred species tree using four fossil calibration points (Table S3), recovering times that are
322 roughly consistent with the relatively young estimates found by (Steppan and Schenk 2017) (see
323 Supplement). This dated species tree provides an evolutionary timescale to evaluate the genomic
324 landscape of phylogenetic discordance across ~12 my of murine evolution.

325

326 *The genomic landscape of phylogenetic discordance*

327 Limiting the number and nature of the loci used to resolve species relationships is often useful to
328 get an initial picture of the history of speciation across many taxa. However, such targeted

approaches may fail to capture the degree of discordance driven by incomplete lineage sorting and introgression (Alexander, et al. 2017; Chan, et al. 2020; Vanderpool, et al. 2020; Alda, et al. 2021). Our results highlight the limitations of a reduced marker-based approach and the general relationships between phylogenetic patterns and functional attributes of the genome in several interesting ways. Using the house mouse genome annotation, we found that the species tree inferred from only genes or UCEs did not match evolutionary relationships inferred for over 85% of the genome. Although similar frequencies were observed among these three most common trees (Figure 2), the topology robustly inferred from genes or UCEs was not that common overall and only the third most frequent topology among 10 kb windows genome-wide. This result was driven mainly by discordance among three more closely related (Praomyini) species sampled for this study, which had nodes with low concordance in the UCE species tree (Fig 1, node J). In the window analysis, each alternate topology of this clade occurred at a frequency of ~14% while the rest of the topology remained consistent with the species tree (Figure 2), indicating that the alternate topologies are caused by high levels of ILS at these nodes. Increased discordance at unresolved nodes is a common feature of phylogenomic datasets. These patterns illustrate how extensive discordance can arise even in a small sample of species and underscores that a single inferred species tree often may not capture the history of individual regions of the genome.

Given the fundamental role that recombination should play in shaping patterns of genetic variation within genomes, it is reasonable to assume that patterns of ILS should be broadly shaped by local recombination rate. We did not observe a clear relationship between local recombination rates in mice (*M. musculus*) and the degree of local phylogenetic discordance (i.e., phylogenetic similarity over 5 Mb intervals). However, we did find that regions of high recombination rate tended to be more discordant with the inferred species tree, in line with findings in mammals (Pease and Hahn 2013; Foley, et al. 2023; Rivas-Gonzalez, et al. 2023) and *Drosophila* (Pease and Hahn 2013). Recombination rates evolve fairly rapidly both within (Kong, et al. 2002; Cox, et al. 2009; Stapley, et al. 2017) and between mammalian species (Jensen-Seaman, et al. 2004; Ptak, et al. 2005; Steviston, et al. 2016; Stapley, et al. 2017) due, in part, to the high turnover of hotspots due to the changing landscape of binding sites for PRDM9 (Baudat, et al. 2010; Singhal, et al. 2015). Similar to findings in great apes (Hobolth, et al. 2007), our results suggest that high-resolution genetic maps from a single species provide some weak predictive value for understanding broader patterns of species tree discordance. However, these limited estimates may not be predictive of finer-scale patterns in a sample spanning over 12 million years of mammalian evolution (but see Foley, et al. 2023). Overall, the evolution of recombination landscapes across closely related species remains an important empirical question in evolutionary genetics (Dapper and Payseur 2017), especially as the generation of chromosome-scale genome assemblies continues to greatly outpace estimates of patterns of recombination within those genomes.

One source of evolution in the recombination map may be changes in synteny. Our reference-guided analyses assume collinearity between *Mus* and the other lineages we are comparing (i.e., no karyotype variation), at least at the window-based scale we are comparing variation. Structural variation, including substantial variation in chromosome numbers, is likely to

369 be widespread in rodents (Stanyon, et al. 1999; Yalcin, et al. 2011; Romanenko, et al. 2012; Keane,
370 et al. 2014) and has the potential to skew our results when comparing tree similarity between
371 regions of the genome using multiple species. Generating chromosome-scale assemblies for many
372 non-*Mus* and *Rattus* species may prove limiting given that most tissue resources for this group are
373 derived from natural history collections that often lack high molecular weight DNA. Nonetheless,
374 whole genome alignments between mouse and rat indicate high degrees of chromosomal synteny
375 and co-linearity (Fig S6), suggesting that many regions will be colinear in our sample.

376 Natural selection reduces the effective population size (N_e) of genomic regions through
377 genetic hitchhiking of variation linked to the fixation of positively selected mutations (i.e.,
378 selective sweeps; Smith and Haigh 1974; Kaplan, et al. 1989) and the purging of deleterious
379 mutations (i.e., background selection; Charlesworth, et al. 1993; Hudson and Kaplan 1995). Thus,
380 variation in parameters dependent on N_e – such as standing levels of nucleotide variation and
381 patterns of incomplete lineage sorting – should be reduced by linkage to functional elements
382 subject to selection. Consistent with this, we observed the lowest rates of local discordance (Figure
383 5A) and overall gene tree/species tree discordance (Figure 5B) near UCEs when compared to all
384 other genomic features we studied. These results suggest that a history of recurrent purifying
385 selection on UCEs (Katzman, et al. 2007) strongly reduces patterns of discordance through a
386 persistent local reduction in N_e . In contrast, protein coding genes showed rates of local discordance
387 that were similar to background levels, even when considering genes rapidly evolving due to
388 positive directional selection (Figure 5A). However, both classes of genes did show less species
389 tree discordance than background consistent with previous results (Scally, et al. 2012; Rivas-
390 Gonzalez, et al. 2023), but this effect was much weaker than as observed at UCEs (Figure 5B).
391 Collectively, these data suggest that the frequency and strength of selection plays an important role
392 in structuring patterns of incomplete lineage sorting across the genome over deeper evolutionary
393 timescales.

394 One practical consequence of this is that phylogenetic inferences based on UCE markers
395 would seem less prone to discordance and may provide cleaner estimates of species tree history
396 than randomly chosen or protein-coding regions. Indeed, windows centered on UCEs have a higher
397 degree of similarity to the species tree than other genomic features (i.e., 17% concordance with
398 the species tree, versus 13% genome-wide or 15% for protein-coding genes). However, it is worth
399 noting that UCEs are also more likely to provide a potentially misleading underestimate of
400 genome-wide levels of discordance. Given this relationship, species tree inferences based on UCEs
401 should likely not, for example, be extended to related population genetic parameters of interest
402 (e.g., ancestral population sizes, estimates population genetic diversity), and could mislead the
403 reconstruction of trait evolution across phylogenies (Avise and Robinson 2008; Hahn and Nakhleh
404 2016; Mendes, et al. 2018; Hibbins, et al. 2023). Finally, despite the relative ease of generating
405 UCE data, such markers are likely unsuitable for genetic inferences within populations given the
406 pervasive effects of linked selection.

407

408 *Discordance and Molecular Evolution*

409 We also found that the choice of tree topology drastically affects the results from various common
410 tests for positive selection. Previous studies have used simulations to show that tree
411 misspecification can lead to incorrect placement of substitutions on branches, possibly leading to
412 spurious results for tests of positive directional selection within empirical datasets (Mendes and
413 Hahn 2016). Here, we use empirical data in mice to show that these errors result in false positive
414 (detected signal for selection only when using the gene tree) and false negative results (detected
415 signal for selection only when using the species tree).

416 For each of the three selection tests run, HyPhy's BUSTED and aBSREL and PAML's
417 M1a vs. M2a, some genes showed evidence of positive selection whether the species tree or gene
418 tree was used. In contrast, many other genes had signatures of positive selection restricted only to
419 a single tree. The genes unique to the type of tree used were often discordant with the species tree
420 while the genes that showed evidence of positive selection regardless of the tree used had levels
421 of discordance comparable to all genes (85%, Figure 6, numbers in parentheses). This suggests
422 that mis-mapping substitutions by supplying these tests with the wrong tree (*i.e.*, the species tree
423 when gene trees are discordant) can lead to inflated false positive and false negative rates when
424 inferring genes under positive selection. The magnitude and direction of these biases were
425 dependent on the underlying model. So-called branch-site models that allow substitution rates to
426 vary among both branches and codon sites, such as HyPhy's BUSTED and aBSREL models,
427 resulted in more genes inferred with evidence for positive selection when using the inferred gene
428 tree (*i.e.*, the correct tree, assuming no errors in gene tree reconstruction). This means that using a
429 single species tree for these tests reduces the power to detect positive selection. On the other hand,
430 models that only allow rates to vary among sites, such as PAML's M1a vs. M2a test, showed an
431 increase in the number of putative false positives inferred when using the wrong tree. That is, tree
432 mis-specification results in spurious increases in dN/dS that mimics positive directional selection.

433 These results have wide-ranging implications for phylogenetics and comparative genomic
434 analysis. First, it is imperative that when testing a specific locus for positive selection, discordance
435 among loci must be accounted for. This is most easily achieved by simply using the gene tree (or
436 other locus type) as input to the test for selection (Good, et al. 2013; Mendes and Hahn 2016;
437 Roycroft, et al. 2021). However, as Mendes and Hahn (2016) pointed out, this may not completely
438 mask the effects of discordance on substitution rates, as sites within a single gene may still have
439 evolved under different histories because of within-gene recombination. Indeed, we found that tree
440 similarity diminished at scales that were less than the average genomic distance between the
441 beginning and end of a coding sequence in mice (~37 kb in this data set). Nevertheless, starting
442 with an inferred gene tree is advisable whenever possible, followed by a secondary analysis of
443 evidence for within-gene variation in phylogenetic history. Our results also imply that studies of
444 molecular evolution may benefit from approaches that reduce genome-wide levels of discordance,
445 such as through *post hoc* pruning of species that disproportionately contribute to unresolved nodes.

446 Incorporating discordance into a comparative framework is not trivial and many
447 comparative genomic methods assume a single species tree that test for changes in substitution
448 rates in a phylogeny (Pollard, et al. 2010; Hu, et al. 2019; Partha, et al. 2019). Even methods that

allow the use of different trees for different loci (like PAML and HyPhy) are still commonly applied with a single species tree across loci (Carbone, et al. 2014; Foote, et al. 2015; van der Valk, et al. 2021; Treaster, et al. 2023). While we used the simplifying assumption that the results from the gene tree are more likely to be correct, this may not always be the case given that errors can also occur during gene tree inference. Still, our results confirm that the use of a single tree for all loci for such tests that rely on accurate estimation of substitution rates are likely to lead to both inaccurate inferences of positive selection. We strongly encourage the use of individual gene trees for such analyses.

457

458 *Conclusions*

Murine rodents as a study system allow us to use the high-quality *M. musculus* genome to examine fine-scale patterns and effects of phylogenetic discordance along chromosomes. Our analysis reveals how discordance varies with genome biology across evolutionary timescales, as well as the limits of inference inherent to extrapolating information from a single model system to a phylogenetic sample. We also demonstrate how phylogenetic discordance can mislead common tests for selection if only a single species tree is used. Overall, our results emphasize that progress in comparative genomics requires a detailed understanding of the heterogeneous biological signals in phylogenomic datasets. Through these results, we can better understand the complexities of phylogenomic datasets and the effects of underlying biological processes on large-scale analyses and ensure that steps are taken to accommodate and study these details.

469

470 Materials & Methods

471 *Sample collection and assembly*

We collected genomes from 16 murine species and two other rodents from several sources, including NCBI and several recently sequenced in Kumon, et al. (2021) (see Table S1 for full list of samples and sources). We also report the genome of *Otomys typus* (FMNH 230007) from Ethiopia in 2015. While DNA extraction and sequencing on the 10x Genomics platform for *O. typus* is the same as described in (Kumon, et al. 2021), the library quality for this sample was too low for chromosome level assembly. Here, we instead assembled it into scaffolds with the express purpose of obtaining UCEs for phylogenetic analysis. Adapters and low-quality bases were trimmed from the reads using illumiprocessor (Faircloth 2013), which makes use of functions from trimomatic (Bolger, et al. 2014). All cleaned reads were de novo assembled using ABySS 2.3.1 (Jackman, et al. 2017) with a Bloom filter (Bloom 1970) de Bruijn graph. The final *O. typus* scaffold assembly was 2.14GB (N50=9,211; L50=64,014; E-size=12,790).

In parallel, for six of these species (see Figure 1; Table S1), we generated reference-based pseudo-assemblies with iterative mapping using an updated version pseudo-it v3.1.1 (Sarver, et al. 2017) that incorporates insertion-deletion variation to minimize reference bias in our genome-wide phylogenetic analyses and to maintain collinearity between assemblies (<https://github.com/goodest-goodlab/pseudo-it>). We used the *Mus musculus* (mm10) genome as

488 the reference for our pseudo-assembly approach. Briefly, pseudo-it maps reads from each sample
489 to the reference genome with BWA (Li 2013), calls variants with GATK HaplotypeCaller (Poplin,
490 et al. 2018), and filters SNPs and indels and generates a consensus assembly with bcftools
491 (Danecek, et al. 2021). The process is repeated, each time using the previous iteration's consensus
492 assembly as the new reference genome to which reads are mapped. In total, we did three iterations
493 of mapping for each sample.

494

495 *Ultraconserved element (UCE) retrieval and alignment*

496 We first set out to reconstruct a phylogeny of sequenced murine rodents to provide both a general
497 resource for future comparative genomic studies within this important group as well as a time-
498 calibrated phylogeny to frame an in-depth analysis of phylogenetic discordance across a subset of
499 murine whole genomes (see below). We combined our seven recently sequenced genomes with
500 nine publicly available murine genomes as well as the genomes of two non-murine rodents, the
501 great gerbil (*Rhombomys opimus*; (Nilsson, et al. 2020) and the Siberian hamster (*Phodopus*
502 *sungorus*; (Moore, et al. 2022) as outgroups. We extracted UCEs from each species, plus 1000
503 flanking bases from each side of the element using the protocols for harvesting loci from genomes
504 and the *M. musculus* UCE probe set provided with phyluce v1.7.1 (Faircloth, et al. 2012; Faircloth
505 2016). In total, we recovered 2,632 unique UCE loci, though not all UCE loci were found in all
506 taxa (Table S1).

507 We brought the extracted UCE sequences for each species into a consistent orientation
508 using MAFFT v7 (Katoh and Standley 2013) and then aligned them using FSA (Bradley, et al.
509 2009) with the default settings. We trimmed UCE alignments with TrimAl (Capella-Gutierrez, et
510 al. 2009) with a gap threshold of 0.5 and otherwise default parameters. We performed alignment
511 quality checks using AMAS (Borowiec 2016). We processed all alignments in parallel with GNU
512 Parallel (Tange 2018).

513

514 *Species tree reconstruction from UCEs*

515 We constructed a species-level rodent phylogeny with two approaches. First, using the alignments
516 of all UCEs found in four or more taxa (2,632), we reconstructed a maximum-likelihood (ML)
517 species tree with IQ-TREE v2.2.1 (Minh, Schmidt, et al. 2020). Each UCE alignment was
518 concatenated and partitioned (Chernomor, et al. 2016) such that optimal substitution models were
519 inferred for individual UCE loci with ModelFinder (Kalyaanamoorthy, et al. 2017). We also
520 reconstructed individual gene trees for each UCE alignment. For all IQ-TREE runs (concatenated
521 or individual loci), we assessed branch support with ultrafast bootstrap approximation (UFBoot)
522 (Hoang, et al. 2018) and the corrected approximate likelihood ratio test (SH-aLRT) (Guindon, et
523 al. 2010). We collapsed branches in each UCE tree exhibiting less than 10% approximated
524 bootstrap support using the nw_ed function from Newick Utilities (Junier and Zdobnov 2010). We
525 used these trees as input to the quartet summary method ASTRAL-III v5.7.8 (Zhang, et al. 2018)
526 to infer a species tree. We generated visualizations of phylogenies with R v4.1.1 (R Core Team

527 2021) using phytools v1.9-16 (Revell 2012) and the ggtree package v3.14 (Yu, et al. 2017; Yu
528 2020) and its imported functions from ape v5.0 (Paradis and Schliep 2019) and treeio v1.16.2
529 (Wang, et al. 2020).

530 We then used two methods to assess phylogenetic discordance across the reconstructed
531 species tree. First, we calculated site and gene concordance factors (sCF and gCF) with IQ-TREE
532 2 (Minh, Hahn, et al. 2020; Minh, Schmidt, et al. 2020) to assess levels of phylogenetic discordance
533 between the inferred UCE trees and the concatenated species tree. gCF is calculated for each
534 branch in the species tree as the proportion of UCE trees in which that branch also appears (Baum
535 2007). sCF represents the proportion of alignment sites concordant with a given species tree branch
536 in a randomized subset of quartets of taxa (Minh, Hahn, et al. 2020). We visualized gCF and sCF
537 (Lanfear 2018) for each branch in each species tree using methods in R v4.3.0 (Lanfear 2018; R
538 Core Team 2021). Next, we used PhyParts (Smith, Moore, et al. 2015) to identify topological
539 conflict between the UCE trees and the species tree from ASTRAL-III. For this analysis, we rooted
540 all trees with *Phodopus sungorus* as the outgroup using the nw_reroot function in the Newick
541 Utilities (Junier and Zdobnov 2010) package and excluded 204 UCE trees that did not contain the
542 outgroup.

543

544 *Divergence time estimation*

545 We used IQ-TREE 2's (Minh, Schmidt, et al. 2020) implementation of least square dating to
546 estimate branch lengths of our species trees in units of absolute time (To, et al. 2016). To improve
547 divergence-time estimation, we used SortaDate (Smith, et al. 2018) to identify a set of 100 UCE
548 loci that exhibit highly clocklike behavior and minimized topological conflict with the
549 concatenated species tree. We applied four node age calibrations (Table S3) as described in
550 Kimura, et al. (2015) and Aghova, et al. (2018). The origin of core Murinae (Node E) was
551 constrained to between 11.1 and 12.3 Ma, following Kimura, et al. (2015). Maximum ages were
552 set for Otomyini+Arvicanthini (9.2 Ma, Kimura, et al. 2015), *Apodemus* (9.6 Ma, Daxner-Höck
553 2002), and *Mus* (8.0 Ma, Kimura, et al. 2013). Branch lengths were resampled 100 times to produce
554 confidence intervals.

555

556 *Genome window-based phylogenetic analysis*

557 For the second part of our work, we wanted to quantitatively infer phylogenetic discordance across
558 a subset of the murine genomes used to infer the species tree and relate that discordance to other
559 features of the genome, such as recombination rate, proximity to genes, and rates of molecular
560 evolution. To assess the distribution of phylogenetic discordance across rodent genomes, we
561 limited subsequent analyses to *M. musculus* and the pseudo-assemblies (see above) of six of the
562 genomes (*Mastomys natalensis*, *Hylomyscus allenii*, *Praomys delectorum*, *Rhabdomys dilectus*,
563 *Grammomys dolichurus*, and *Rhynchomys soricoides*). *Otomys typus* was excluded from these
564 analyses due to the inadequacy of the library outlined above.

565 We partitioned these genomes into 10 kilobase (kb) windows based on the coordinates in
566 the reference *M. musculus* genome (mm10; Mouse Genome Sequencing, et al. 2002) using
567 bedtools makewindows (Quinlan and Hall 2010). These coordinates were converted between the
568 reference and the consensus sequence for each genome using liftOver (Hinrichs, et al. 2006). Note
569 that this method assumes both collinearity of all genomes and similar karyotypes (see Discussion).
570 We then removed windows from the subsequent analyses if (1) 50% or more of the window
571 overlapped with repeat regions from the *M. musculus* reference RepeatMasker (Smit, et al. 2013-
572 2015) file downloaded from the UCSC Genome Browser's table browser (Hinrichs, et al. 2006)
573 or (2) 50% or more of the window contained missing data in three or more samples. Overlaps with
574 repeat regions were determined with bedtools coverage (Quinlan and Hall 2010). We then aligned
575 the 10kb windows with MAFFT (Katoh and Standley 2013), trimmed alignments with trimAl
576 (Capella-Gutierrez, et al. 2009), and inferred phylogenies for each with IQ-TREE 2 (Minh,
577 Schmidt, et al. 2020) which uses ModelFinder to determine the best substitution model for each
578 window (Kalyaanamoorthy, et al. 2017).

579 To assess patterns of tree similarity between windows on the same chromosome, we used
580 the weighted Robinson-Foulds (wRF) (Robinson and Foulds 1981; Böcker, et al. 2013) distance
581 measure implemented in the phangorn library (Schliep 2011) in R (R Core Team 2021), which
582 compares two trees by finding clades or splits present in one tree but not the other weighted by the
583 missing branch length in each tree for each mismatch and differences in branch length between the
584 co-occurring branches in both trees (Robinson and Foulds 1979). Consequently, the resulting
585 measure of wRF is in units of branch length (i.e., expected number of substitutions per site for
586 maximum likelihood trees). We compared wRF between trees from windows on the same
587 chromosome to characterize (1) heterogeneity in patterns discordance along the chromosome and
588 (2) whether tree similarity is correlated with distance between windows. For the second question,
589 we sampled every window on a chromosome at increasing distance (in 10kb windows) until the
590 distribution of wRF scores for all pairs of windows at that distance was not significantly different
591 (Wilcox test, $p > 0.01$) than that of a sample of 12,000 measures of wRF between randomly
592 selected trees on different chromosomes. We selected 12,000 as the random sample size because
593 it roughly matched the number of windows on the largest chromosome (chromosome 1, $n =$
594 12,113). We used Snakemake 7 (Mölder, et al. 2021) to compute window alignments and trees in
595 parallel.

596

597 Whole genome alignment between mouse and rat

598

599 To assess how un-accounted for large-scale structural variation may impact our conclusions, we
600 compared the reference mouse and rat genomes. We used minimap2 (Li 2018) to align the mouse
601 (mm10) and rat (rnor6) (Gibbs, et al. 2004) genomes to assess the impact of structural variation
602 that spans the divergence of our subset of species used in the discordance analyses. We
603 downloaded the rat reference genome (rnor6) from the UCSC genome browser and for both
604 genomes removed the Y chromosome and all smaller unplaced scaffolds. We then used minimap2

605 in whole genome alignment mode (-x asm20) to generate a pairwise alignment file from which we
606 calculated alignment segment sizes and the distances between alignment segments. We visualized
607 the alignment as a dot plot using the pafr package in R (<https://github.com/dwinter/pafr>).
608

609 *Recombination rate and functional annotation*

610 We retrieved 10,205 genetic markers generated from a large heterogenous stock of outbred mice
611 (Shifman, et al. 2006; Cox, et al. 2009) to assess whether phylogenetic discordance along
612 chromosomes was correlated with mouse recombination rates. We converted the physical
613 coordinates of these markers from build 37 (mm9) to build 38 (mm10) of the *M. musculus* genome
614 using liftOver (Hinrichs, et al. 2006). We then partitioned the markers into 5Mb windows and
615 estimated local recombination rates defined as the slope of the correlation between the location on
616 the *M. musculus* genetic and physical maps for all markers in the window (White, et al. 2009;
617 Kartje, et al. 2020). Within each 5Mb window, we calculated wRF distances between the first 10kb
618 window and every other 10kb window.

619 We also compared the chromosome-wide wRF distances to those based on phylogenies
620 from regions around several types of adjacent to genomic features. We retrieved coordinates from
621 25,753 protein coding genes annotated in *M. musculus* from Ensembl (release 99; Cunningham, et
622 al. 2022), all 3,129 UCEs from the *M. musculus* UCE probe set provided with PHYLUCE
623 (Faircloth, et al. 2012; Faircloth 2016), and 9,865 recombination hotspots from Smagulova, et al.
624 (2011). The recombination hotspot coordinates were converted between build 37 and build 38
625 using the liftOver tool (Hinrichs, et al. 2006). For each feature, the starting window was the 10kb
626 window containing the feature's midpoint coordinate. We then calculated wRF between this
627 window and all windows within 5Mb in either direction and for each chromosome compared the
628 slope and wRF distance of windows adjacent to the feature with the same metrics for the whole
629 chromosome. We compared distributions of these measures for each genomic feature with an
630 ANOVA (aov(feature.measure ~ feature.label)) followed by Tukey's range test
631 (TukeyHSD(anova.result)) to assess differences in means, as implemented in R v4.1.1 (R Core
632 Team 2021).

633 *Molecular evolution*

634 To test how tree misspecification affects common model-based analyses of molecular evolution,
635 we retrieved 22,261 coding sequences from *M. musculus* using the longest coding transcript of
636 each gene. Coding coordinates from the *M. musculus* coding sequences were transposed to the new
637 assemblies via liftOver (Hinrichs, et al. 2006) and sequences retrieved with bedtools getfasta
638 (Quinlan and Hall 2010). We recovered 17,216 genes that were present in all seven species. Using
639 MACSE (Ranwez, et al. 2018), we trimmed non-homologous regions from each ortholog using
640 trimNonHomologousFragments, aligned the orthologs using alignSequences, and trimmed the
641 aligned sequences with trimAlignment to remove unaligned flanking regions. Finally, we manually
642 filtered the alignments using the following (non-mutually exclusive) criteria: 3,368 alignments
643 were removed during filtering for gapped sites, 3,132 alignments had a premature stop codon in at

644 least one species, 1,571 alignments had only three or fewer unique sequences among the seven
645 species, and 78 alignments were shorter than 100 bp. After filtering, 12,559 total alignments for
646 tree reconstruction and inference of selection.

647 We then used IQ-TREE 2 (Minh, Schmidt, et al. 2020) to reconstruct a single species tree
648 from concatenation of all gene alignments, as well as gene-trees for each individual alignment.
649 This species tree from coding regions matches the topologies of these species inferred by
650 concatenation of UCEs in the previous section. Next we ran several tests that use both coding
651 alignments and a tree to infer positive selection: PAML's M1a vs. M2a test (Yang 2007), HyPhy's
652 aBSREL model (Smith, Wertheim, et al. 2015), and HyPhy's BUSTED model (Murrell, et al.
653 2015). We ran each test twice on each gene, once using the species tree derived from concatenated
654 data, and once using the tree estimated for that gene. For the HyPhy models, no target branch was
655 selected, meaning all branches in the input phylogeny were tested.

656 The end point of each of these three tests is a p-value, which lets us assess whether a model
657 that allows for positively selected sites fits better than a model that does not. For M1a vs. M2a, we
658 obtained the p-value manually by first performing a likelihood ratio test to determine genes under
659 selection by calculating $2 * (lnl\ M1a - lnl\ M2a)$. The p-value of this likelihood ratio is then
660 retrieved from a one-tailed chi-square distribution with two degrees of freedom (Yang 2007). For
661 BUSTED and aBSREL, p-values are computed automatically during the test using similar
662 likelihood ratios. For the M1a vs. M2a and BUSTED tests, a single p-value is computed for each
663 gene. P-values were adjusted by correcting for false discovery rates (Benjamini and Hochberg
664 1995; Yekutieli and Benjamini 1999) using the "fdr" method in the p.adjust() function in R (R
665 Core Team 2021) and we categorized a gene as being positively selected if its adjusted p-value
666 was < 0.01 . For the aBSREL test, a p-value is generated for each branch in the input gene tree.
667 aBSREL corrects for multiple testing internally across branches using the Holm-Bonferroni
668 procedure (Holm 1979; Pond, et al. 2005). We further correct the p-values across genes with the
669 Bonferroni method and classify a gene as having experienced positive selection if one or more
670 branches has a p-value < 0.01 after all corrections. We used Snakemake 7 (Mölder, et al. 2021) to
671 compute coding alignments, trees, and selection tests in parallel.
672

673 Data availability

674 For the six previously assembled genomes (see Table S1), all raw reads and assemblies are
675 available as an NCBI BioProject (Accession Number PRJNA669840). The reads and assembly
676 for *Otomys typus*, pseudo-assemblies for the six other new samples, and locus alignments
677 (UCEs, genes, and genomic windows) are available on Dryad
678 (<https://doi.org/10.5061/dryad.866t1g1wq>). All code and summary data for this project are
679 deposited on github (<https://github.com/gwct/murine-discordance>).
680

681 Acknowledgments

We thank Jake Esselstyn and Kevin Rowe for helpful comments and discussion on the murine species tree and Matt Hahn and the Hahn lab for feedback on the manuscript. We also thank Brant Faircloth and Trevor Sless for advice on using phyluce. We are grateful for tissue samples provided by Chris Conroy at the Museum of Vertebrate Zoology, Berkeley, CA (MVZ) and Adam Ferguson at the Field Museum of Natural History, Chicago, IL (FMNH), and to the original collectors. This work was supported by the National Science Foundation (DEB-1754096 to J.M.G), the Eunice Kennedy Shriver National Institute of Child Health and Human Development of the National Institutes of Health (R01-HD094787 to J.M.G.). J.J.H. received financial support from the Cornell Center for Vertebrate Genomics. J.S.B. was supported by the University of Michigan Life Sciences Fellows Program and the Jean Wright Cohn Endowment Fund at the University of Michigan Museum of Zoology. Computations for species tree reconstruction were performed using the computer clusters and data storage resources of the University of California Riverside HPCC, which were funded by grants from NSF (MRI-2215705, MRI-1429826) and NIH (1S10OD016290-01A1), and the Cornell University Biotechnology Resource Center BioHPC (RRID:SCR_021757) with help from Qi Sun. Bioinformatic analyses for genomic discordance and selection tests were conducted using the University of Montana Griz Shared Computing Cluster supported by grants from the NSF (CC-2018112 and OAC-1925267, J.M.G. co-PI). Any opinions, findings, and conclusions or recommendations expressed in this material are those of the authors and do not necessarily reflect the views of the NSF or the NIH.

701

702

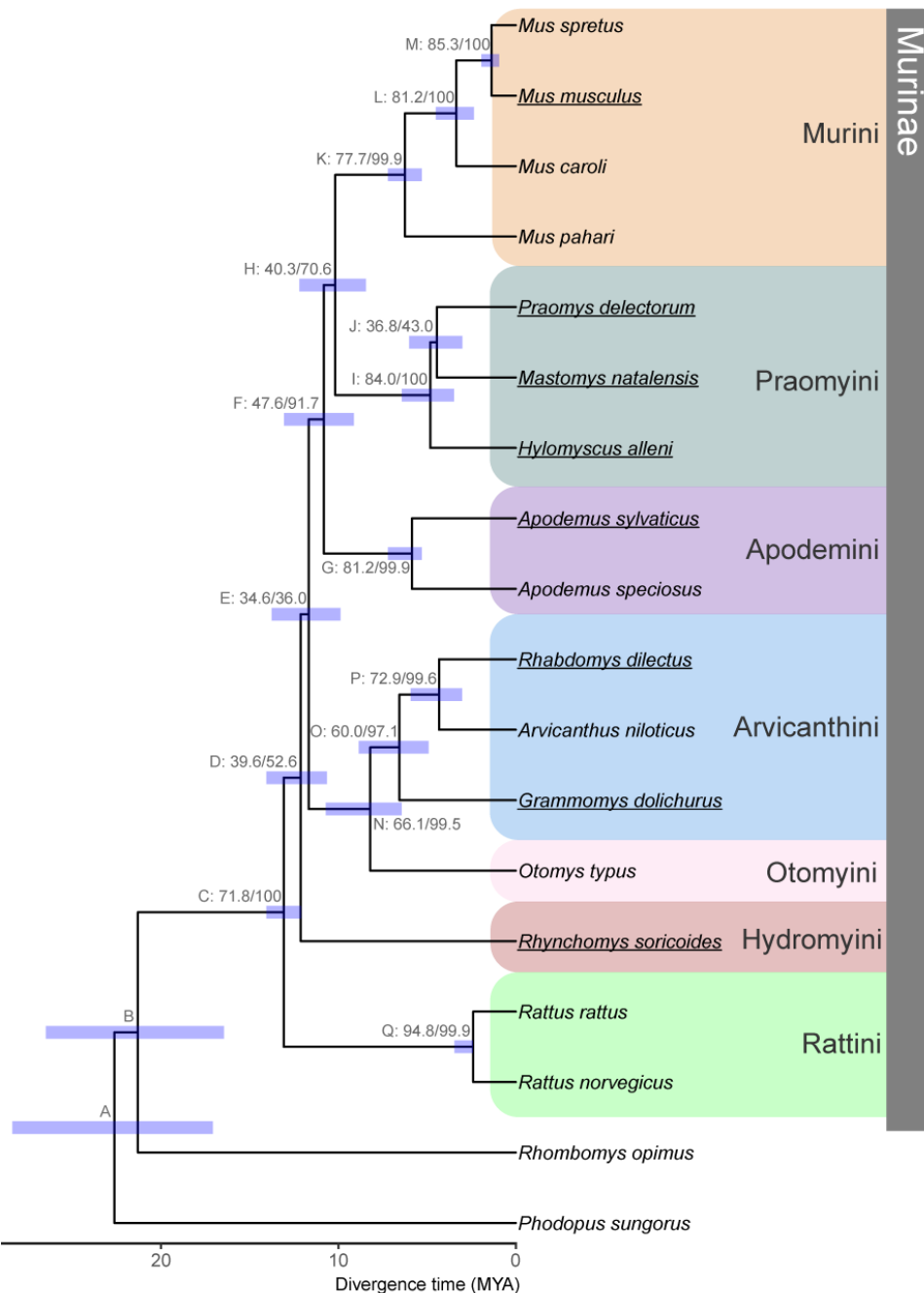
703 **Tables**

704 **Table 1. Rates and types of error when using a single species tree for gene-based selection**
705 **tests (Assuming the gene tree topology is the correct topology).**

Test	False positive rate	False negative rate
BUSTED	0.45%	28.10%
aBSREL	0.41%	10.60%
M1a vs. M2a	2.66%	3.20%

706

For Peer Review

707 **Figures**708 **Figure 1**

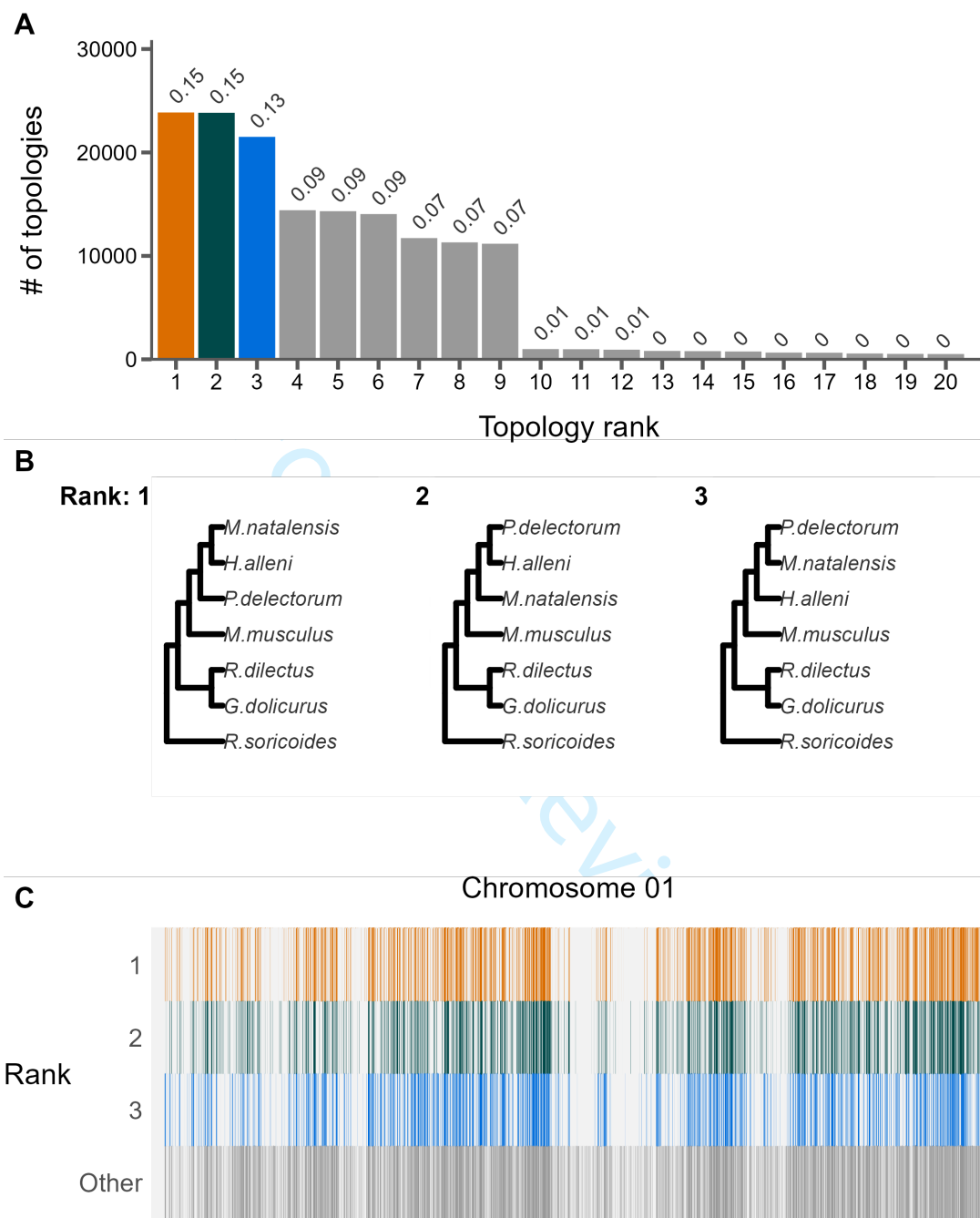
709

710 **Figure 1.** Species trees inferred from concatenation of ultra-conserved elements (UCEs) from 18
 711 rodent species. Internal nodes are labeled by a letter identifier referenced in the text and site and
 712 gene concordance factors (*i.e.*, Label: sCF/gCF) as well as a bar indicating the confidence interval
 713 for divergence time estimation. Ultrafast bootstrap/SH-aLRT values were all 100. Bottom scale
 714 represents time in millions of years before present. Fossil calibrations are described in Tables S2

715 and S3. Tribes within sub-family Murinae are highlighted on the right following the classifications
716 used by Lecompte, et al. (2008). Genomes used for the genome-wide phylogenetic discordance
717 analyses are underlined.

718

For Peer Review

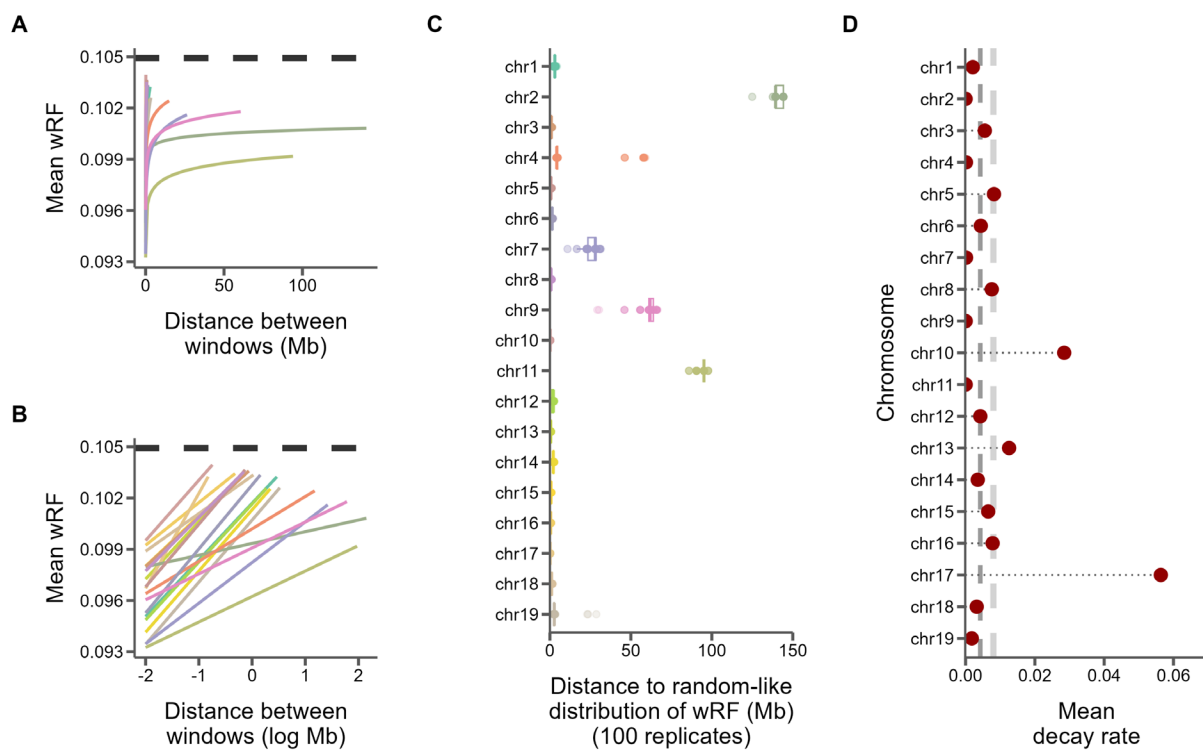
719 **Figure 2**

720

721 **Figure 2.** The landscape and profile of phylogenetic discordance across non-overlapping 10kb
 722 windows in murine genomes. A) Distribution of the 20 most frequent topologies recovered across
 723 all windows. Numbers above bars indicate proportion of each topology. B) The top three
 724 topologies recovered across all chromosomes 1. C) Distribution of the topologies recovered along

725 chromosome 1. The x-axis is scaled to the length of the chromosome and each vertical bar
726 represents one 10kb window. The three most frequent topologies occupy the first three rows while
727 all other topologies are shown in the bottom row. See Supplemental File S1 for individual
728 chromosome plots.

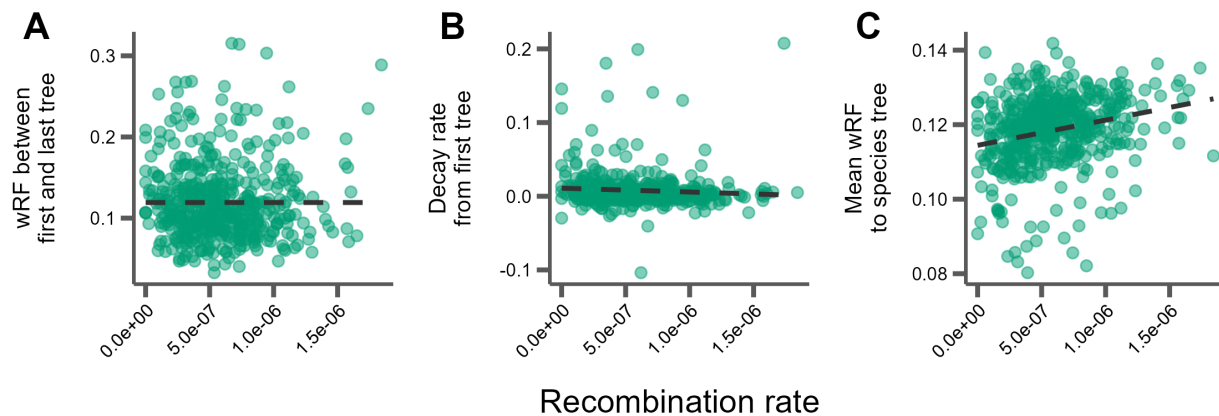
For Peer Review

729 **Figure 3**

730

731 **Figure 3.** Similarity between 10kb windows decays as genomic distance between windows
 732 increases. A) The log fit to the mean of distributions of weighted Robinson-Foulds distances
 733 between trees of windows at increasing genomic distance (10kb steps). Each line represents one
 734 chromosome. B) The same, but on a log scale with a linear fit. C) For every window on each
 735 chromosome, the genomic distance between windows at which tree distance becomes random for
 736 100 replicates of random window selection. D) Points represent the slopes of the correlation
 737 between genomic distance and tree distance (lines from panel B), which is the rate at which tree
 738 similarity decays across the genome. Dark grey dashed line is median slope and light grey dashed
 739 line is mean.

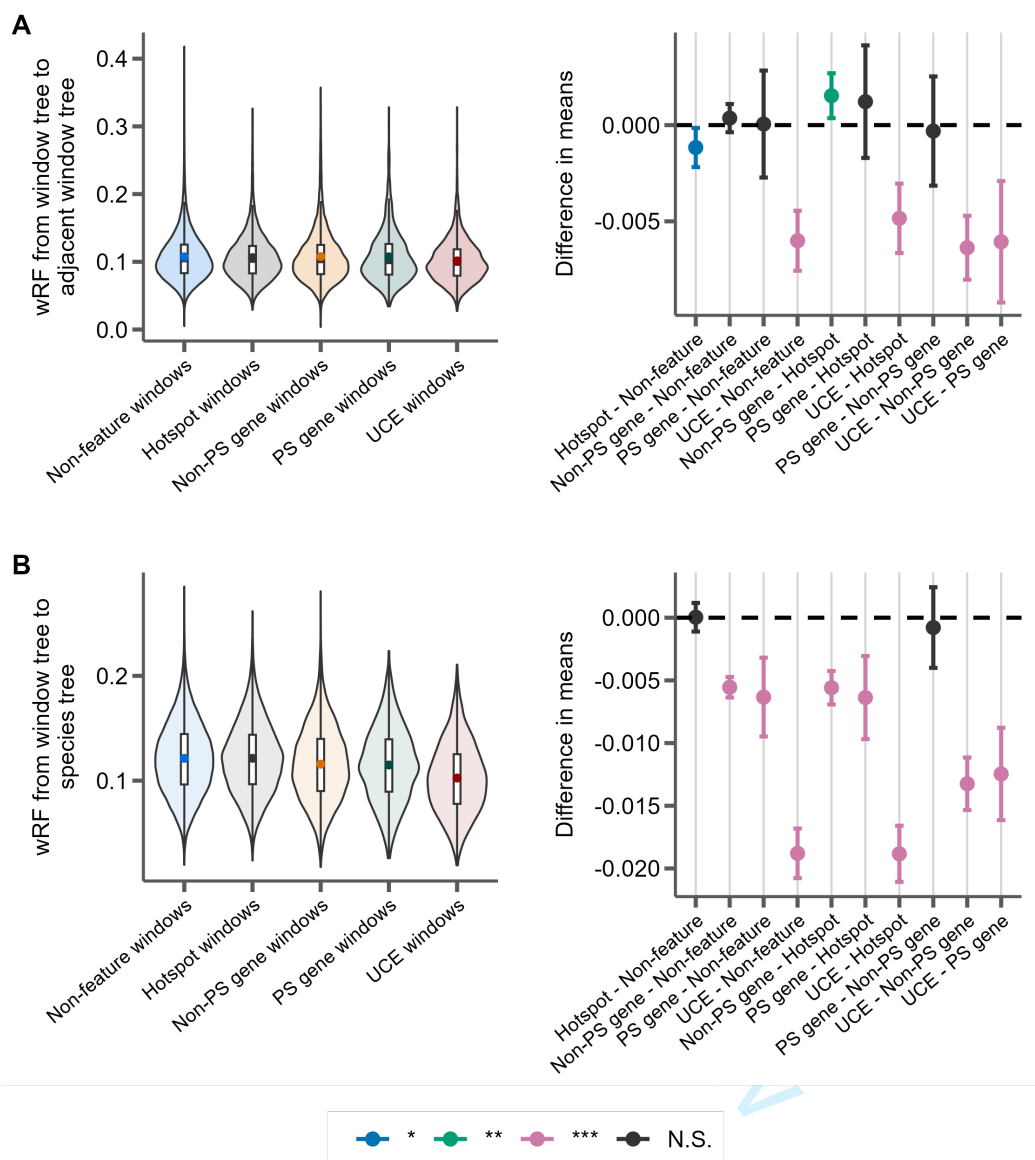
740

741 **Figure 4**

742

743 **Figure 4.** Correlations between tree similarity and recombination rate in 5 Mb windows. A) Tree
 744 similarity as measured by the weighted Robinson-Foulds distance between the first and last 10 kb
 745 windows within the 5 Mb window. B) The slopes of the linear correlation between the weighted
 746 Robinson-Foulds distances between the first 10 kb window and every other 10 kb window within
 747 a 5 Mb window represent the rate at which tree similarity decays over each 5 Mb window. C) The
 748 mean wRF of all 10 kb window trees within each 5Mb window compared to the species tree.

749

750 **Figure 5**

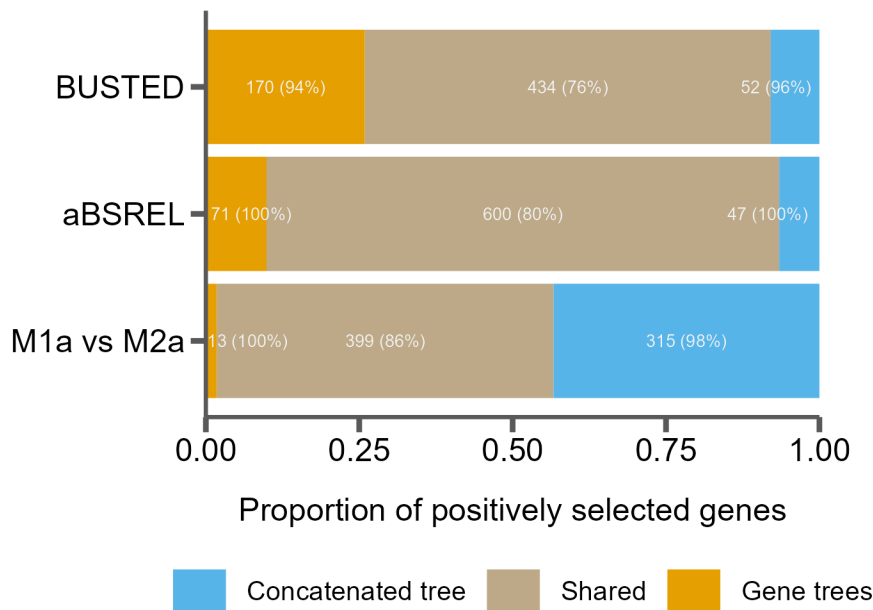
751

752 **Figure 5.** Distributions of weighted Robinson-Foulds distance from trees constructed from 10kb
 753 windows either centered on recombination hotspots (Hotspot), protein-coding genes without
 754 evidence for positive selection (Non-PS genes), protein coding genes with evidence for positive
 755 selection (PS genes), UCEs, or containing none of these features (Non-feature). For each panel,
 756 the left portion shows the distributions of the measure for each feature type and the right panel
 757 shows the differences in means for each pairwise comparison of features with significance assessed
 758 with Tukey's range test. The labels on the x-axis indicate the feature pairs being compared, with
 759 the first feature being the reference (*i.e.* points above 0 indicate this feature has a higher mean). *P*-
 760 value thresholds: * < 0.05, ** < 0.01, *** < 0.001. A) The phylogenetic similarity of windows

761 immediately adjacent to feature windows. B) The phylogenetic similarity between the species tree
762 inferred from protein-coding gene trees and the feature window.

763

For Peer Review

764 **Figure 6**

765

766 **Figure 6.** Tree misspecification leads to erroneous results in tests for positive selection. The
 767 proportion of genes inferred to be under positive selection for three tests using either a single
 768 species tree (concatenated tree) or individual gene trees, as well as those found in both cases
 769 (shared). Numbers in the bars indicate raw counts, and percentages indicate the percent of genes
 770 in that category that are discordant from the species tree.

771

772

773

774 **References**

- 775 Aghova T, Kimura Y, Bryja J, Dobigny G, Granjon L, Kergoat GJ. 2018. Fossils know it best:
776 Using a new set of fossil calibrations to improve the temporal phylogenetic framework of murid
777 rodents (Rodentia: Muridae). *Mol Phylogenet Evol* 128:98-111.
- 778
- 779 Alda F, Ludt WB, Elias DJ, McMahan CD, Chakrabarty P. 2021. Comparing Ultraconserved
780 Elements and Exons for Phylogenomic Analyses of Middle American Cichlids: When Data Agree
781 to Disagree. *Genome Biol Evol* 13:evab161.
- 782
- 783 Alexander AM, Su YC, Oliveros CH, Olson KV, Travers SL, Brown RM. 2017. Genomic data
784 reveals potential for hybridization, introgression, and incomplete lineage sorting to confound
785 phylogenetic relationships in an adaptive radiation of narrow-mouth frogs. *Evolution* 71:475-488.
- 786
- 787 Avise JC, Robinson TJ. 2008. Hemiplasy: a new term in the lexicon of phylogenetics. *Syst Biol*
788 57:503-507.
- 789
- 790 Baudat F, Buard J, Grey C, Fledel-Alon A, Ober C, Przeworski M, Coop G, de Massy B. 2010.
791 PRDM9 is a major determinant of meiotic recombination hotspots in humans and mice. *Science*
792 327:836-840.
- 793
- 794 Baum DA. 2007. Concordance trees, concordance factors, and the exploration of reticulate
795 genealogy. *TAXON* 56:417-426.
- 796
- 797 Benjamini Y, Hochberg Y. 1995. Controlling the false discovery rate: a practical and powerful
798 approach to multiple testing. *Journal of the Royal statistical society: series B (Methodological)*
799 57:289-300.
- 800
- 801 Bloom BH. 1970. Space/time trade-offs in hash coding with allowable errors. *Commun. ACM*
802 13:422–426.
- 803
- 804 Böcker S, Canzar S, Gunnar WK. 2013. The Generalized Robinson-Foulds Metric. In: Darling A,
805 Stoye J, editors. *Algorithms in Bioinformatics*. Berlin, Heidelberg: Springer.
- 806
- 807 Bolger AM, Lohse M, Usadel B. 2014. Trimmomatic: a flexible trimmer for Illumina sequence
808 data. *Bioinformatics* 30:2114-2120.
- 809
- 810 Borowiec ML. 2016. AMAS: a fast tool for alignment manipulation and computing of summary
811 statistics. *PeerJ* 4:e1660.

- 812
813 Bradley RK, Roberts A, Smoot M, Juvekar S, Do J, Dewey C, Holmes I, Pachter L. 2009. Fast
814 statistical alignment. *PLoS Comput Biol* 5:e1000392.
- 815
816 Capella-Gutierrez S, Silla-Martinez JM, Gabaldon T. 2009. trimAl: a tool for automated alignment
817 trimming in large-scale phylogenetic analyses. *Bioinformatics* 25:1972-1973.
- 818
819 Carbone L, Harris RA, Gnerre S, Veeramah KR, Lorente-Galdos B, Huddleston J, Meyer TJ,
820 Herrero J, Roos C, Aken B, et al. 2014. Gibbon genome and the fast karyotype evolution of small
821 apes. *Nature* 513:195-201.
- 822
823 Chan KO, Hutter CR, Wood PL, Jr., Grismer LL, Brown RM. 2020. Target-capture phylogenomics
824 provide insights on gene and species tree discordances in Old World treefrogs (Anura:
825 Rhacophoridae). *Proc Biol Sci* 287:20202102.
- 826
827 Charlesworth B, Morgan MT, Charlesworth D. 1993. The effect of deleterious mutations on
828 neutral molecular variation. *Genetics* 134:1289-1303.
- 829
830 Chernomor O, von Haeseler A, Minh BQ. 2016. Terrace Aware Data Structure for Phylogenomic
831 Inference from Supermatrices. *Syst Biol* 65:997-1008.
- 832
833 Christmas MJ, Kaplow IM, Genereux DP, Dong MX, Hughes GM, Li X, Sullivan PF, Hindle AG,
834 Andrews G, Armstrong JC, et al. 2023. Evolutionary constraint and innovation across hundreds of
835 placental mammals. *Science* 380:eabn3943.
- 836
837 Cox A, Ackert-Bicknell CL, Dumont BL, Ding Y, Bell JT, Brockmann GA, Wergedal JE, Bult C,
838 Paigen B, Flint J, et al. 2009. A new standard genetic map for the laboratory mouse. *Genetics*
839 182:1335-1344.
- 840
841 Cunningham F, Allen JE, Allen J, Alvarez-Jarreta J, Amode MR, Armean IM, Austine-Orimoloye
842 O, Azov AG, Barnes I, Bennett R, et al. 2022. Ensembl 2022. *Nucleic Acids Res* 50:D988-D995.
- 843
844 Danecek P, Bonfield JK, Liddle J, Marshall J, Ohan V, Pollard MO, Whitwham A, Keane T,
845 McCarthy SA, Davies RM, et al. 2021. Twelve years of SAMtools and BCFtools. *Gigascience*
846 10:giab008.
- 847
848 Dapper AL, Payseur BA. 2017. Connecting theory and data to understand recombination rate
849 evolution. *Philos Trans R Soc Lond B Biol Sci* 372.

- 850
851 Daxner-Höck G. 2002. Cricetodon meini and other rodents from Mühlbach and Grund, Lower
852 Austria (Middle Miocene, late MN5). Annalen des Naturhistorischen Museums in Wien. Serie A
853 für Mineralogie und Petrographie, Geologie und Paläontologie, Anthropologie und
854 Prähistorie:267-291.
- 855
856 Degnan JH, Rosenberg NA. 2006. Discordance of species trees with their most likely gene trees.
857 PLoS Genet 2:e68.
- 858
859 Edwards SV. 2009. Is a new and general theory of molecular systematics emerging? Evolution
860 63:1-19.
- 861
862 Faircloth BC. 2013. illumiprocessor: a trimmomatic wrapper for parallel adapter and quality
863 trimming.
- 864
865 Faircloth BC. 2016. PHYLUCE is a software package for the analysis of conserved genomic loci.
866 Bioinformatics 32:786-788.
- 867
868 Faircloth BC, McCormack JE, Crawford NG, Harvey MG, Brumfield RT, Glenn TC. 2012.
869 Ultraconserved elements anchor thousands of genetic markers spanning multiple evolutionary
870 timescales. Syst Biol 61:717-726.
- 871
872 Feng S, Bai M, Rivas-Gonzalez I, Li C, Liu S, Tong Y, Yang H, Chen G, Xie D, Sears KE, et al.
873 2022. Incomplete lineage sorting and phenotypic evolution in marsupials. Cell 185:1646-1660
e1618.
- 875
876 Ferreira MS, Jones MR, Callahan CM, Farelo L, Tolesa Z, Suchentrunk F, Boursot P, Mills LS,
877 Alves PC, Good JM, et al. 2021. The Legacy of Recurrent Introgression during the Radiation of
878 Hares. Syst Biol 70:593-607.
- 879
880 Foley NM, Harris AJ, Bredemeyer KR, Ruedi M, Puechmaille SJ, Teeling EC, Criscitiello MF,
881 Murphy WJ. 2024. Karyotypic stasis and swarming influenced the evolution of viral tolerance in
882 a species-rich bat radiation. Cell Genom 4:100482.
- 883
884 Foley NM, Mason VC, Harris AJ, Bredemeyer KR, Damas J, Lewin HA, Eizirik E, Gatesy J,
885 Karlsson EK, Lindblad-Toh K, et al. 2023. A genomic timescale for placental mammal evolution.
886 Science 380:eabl8189.
- 887

- 888 Fontaine MC, Pease JB, Steele A, Waterhouse RM, Neafsey DE, Sharakhov IV, Jiang X, Hall AB,
889 Catteruccia F, Kakani E, et al. 2015. Mosquito genomics. Extensive introgression in a malaria
890 vector species complex revealed by phylogenomics. *Science* 347:1258524.
- 891
- 892 Foote AD, Liu Y, Thomas GW, Vinar T, Alföldi J, Deng J, Dugan S, van Elk CE, Hunter ME,
893 Joshi V, et al. 2015. Convergent evolution of the genomes of marine mammals. *Nat Genet* 47:272-
894 275.
- 895
- 896 Gable SM, Byars MI, Literman R, Tollis M. 2022. A Genomic Perspective on the Evolutionary
897 Diversification of Turtles. *Syst Biol* 71:1331-1347.
- 898
- 899 Gibbs RA, Weinstock GM, Metzker ML, Muzny DM, Sodergren EJ, Scherer S, Scott G, Steffen
900 D, Worley KC, Burch PE, et al. 2004. Genome sequence of the Brown Norway rat yields insights
901 into mammalian evolution. *Nature* 428:493-521.
- 902
- 903 Good JM, Wiebe V, Albert FW, Burbano HA, Kircher M, Green RE, Halbwax M, Andre C,
904 Atencia R, Fischer A, et al. 2013. Comparative population genomics of the ejaculate in humans
905 and the great apes. *Mol Biol Evol* 30:964-976.
- 906
- 907 Green RE, Krause J, Briggs AW, Maricic T, Stenzel U, Kircher M, Patterson N, Li H, Zhai W,
908 Fritz MH, et al. 2010. A draft sequence of the Neandertal genome. *Science* 328:710-722.
- 909
- 910 Guindon S, Dufayard JF, Lefort V, Anisimova M, Hordijk W, Gascuel O. 2010. New algorithms
911 and methods to estimate maximum-likelihood phylogenies: assessing the performance of PhyML
912 3.0. *Syst Biol* 59:307-321.
- 913
- 914 Hahn MW, Nakhleh L. 2016. Irrational exuberance for resolved species trees. *Evolution* 70:7-17.
- 915
- 916 He B, Zhao Y, Su C, Lin G, Wang Y, Li L, Ma J, Yang Q, Hao J. 2023. Phylogenomics reveal
917 extensive phylogenetic discordance due to incomplete lineage sorting following the rapid radiation
918 of alpine butterflies (Papilionidae: Parnassius). *Syst Entomol*.
- 919
- 920 Hibbins MS, Breithaupt LC, Hahn MW. 2023. Phylogenomic comparative methods: Accurate
921 evolutionary inferences in the presence of gene tree discordance. *Proc Natl Acad Sci U S A*
922 120:e2220389120.
- 923
- 924 Hinrichs AS, Karolchik D, Baertsch R, Barber GP, Bejerano G, Clawson H, Diekhans M, Furey
925 TS, Harte RA, Hsu F, et al. 2006. The UCSC Genome Browser Database: update 2006. *Nucleic
926 Acids Res* 34:D590-598.

- 927
928 Hoang DT, Chernomor O, von Haeseler A, Minh BQ, Vinh LS. 2018. UFBoot2: Improving the
929 Ultrafast Bootstrap Approximation. *Mol Biol Evol* 35:518-522.
- 930
931 Hobolth A, Christensen OF, Mailund T, Schierup MH. 2007. Genomic relationships and speciation
932 times of human, chimpanzee, and gorilla inferred from a coalescent hidden Markov model. *PLoS*
933 *Genet* 3:e7.
- 934
935 Holm S. 1979. A simple sequentially rejective multiple test procedure. *Scandinavian journal of*
936 *statistics*:65-70.
- 937
938 Hu Z, Sackton TB, Edwards SV, Liu JS. 2019. Bayesian Detection of Convergent Rate Changes
939 of Conserved Noncoding Elements on Phylogenetic Trees. *Mol Biol Evol* 36:1086-1100.
- 940
941 Hudson RR. 1983. Testing the Constant-Rate Neutral Allele Model with Protein Sequence Data.
942 *Evolution* 37:203-217.
- 943
944 Hudson RR, Kaplan NL. 1988. The coalescent process in models with selection and
945 recombination. *Genetics* 120:831-840.
- 946
947 Hudson RR, Kaplan NL. 1995. Deleterious background selection with recombination. *Genetics*
948 141:1605-1617.
- 949
950 Huson DH, Klöpper T, Lockhart PJ, Steel MA. 2005. Reconstruction of Reticulate Networks from
951 Gene Trees. In: Miyano S, Mesirov J, Kasif S, Istrail S, Pevzner PA, Waterman M, editors.
952 *Research in Computational Molecular Biology. RECOMB 2005. Lecture Notes in Computer*
953 *Science*: Springer, Berlin, Heidelberg.
- 954
955 Jackman SD, Vandervalk BP, Mohamadi H, Chu J, Yeo S, Hammond SA, Jahesh G, Khan H,
956 Coombe L, Warren RL, et al. 2017. ABySS 2.0: resource-efficient assembly of large genomes
957 using a Bloom filter. *Genome Res* 27:768-777.
- 958
959 Jarvis ED, Mirarab S, Aberer AJ, Li B, Houde P, Li C, Ho SY, Faircloth BC, Nabholz B, Howard
960 JT, et al. 2014. Whole-genome analyses resolve early branches in the tree of life of modern birds.
961 *Science* 346:1320-1331.
- 962
963 Jensen-Seaman MI, Furey TS, Payseur BA, Lu Y, Roskin KM, Chen CF, Thomas MA, Haussler
964 D, Jacob HJ. 2004. Comparative recombination rates in the rat, mouse, and human genomes.
965 *Genome Res* 14:528-538.

- 966
967 Jones MR, Mills LS, Alves PC, Callahan CM, Alves JM, Lafferty DJR, Jiggins FM, Jensen JD,
968 Melo-Ferreira J, Good JM. 2018. Adaptive introgression underlies polymorphic seasonal
969 camouflage in snowshoe hares. *Science* 360:1355-1358.
- 970
971 Junier T, Zdobnov EM. 2010. The Newick utilities: high-throughput phylogenetic tree processing
972 in the UNIX shell. *Bioinformatics* 26:1669-1670.
- 973
974 Kalyaanamoorthy S, Minh BQ, Wong TKF, von Haeseler A, Jermiin LS. 2017. ModelFinder: fast
975 model selection for accurate phylogenetic estimates. *Nat Methods* 14:587-589.
- 976
977 Kaplan NL, Hudson RR, Langley CH. 1989. The "hitchhiking effect" revisited. *Genetics* 123:887-
978 899.
- 979
980 Kartje ME, Jing P, Payseur BA. 2020. Weak Correlation between Nucleotide Variation and
981 Recombination Rate across the House Mouse Genome. *Genome Biol Evol* 12:293-299.
- 982
983 Katoh K, Standley DM. 2013. MAFFT multiple sequence alignment software version 7:
984 improvements in performance and usability. *Mol Biol Evol* 30:772-780.
- 985
986 Katzman S, Kern AD, Bejerano G, Fewell G, Fulton L, Wilson RK, Salama SR, Haussler D. 2007.
987 Human genome ultraconserved elements are ultraselected. *Science* 317:915.
- 988
989 Keane TM, Wong K, Adams DJ, Flint J, Reymond A, Yalcin B. 2014. Identification of structural
990 variation in mouse genomes. *Front Genet* 5:192.
- 991
992 Kimura Y, Hawkins MT, McDonough MM, Jacobs LL, Flynn LJ. 2015. Corrected placement of
993 Mus-Rattus fossil calibration forces precision in the molecular tree of rodents. *Sci Rep* 5:14444.
- 994
995 Kimura Y, Jacobs LL, Cerling TE, Uno KT, Ferguson KM, Flynn LJ, Patnaik R. 2013. Fossil mice
996 and rats show isotopic evidence of niche partitioning and change in dental ecomorphology related
997 to dietary shift in Late Miocene of Pakistan. *PLoS One* 8:e69308.
- 998
999 Kong A, Gudbjartsson DF, Sainz J, Jonsdottir GM, Gudjonsson SA, Richardsson B, Sigurdardottir
1000 S, Barnard J, Hallbeck B, Masson G, et al. 2002. A high-resolution recombination map of the
1001 human genome. *Nat Genet* 31:241-247.
- 1002

- 1003 Kowalczyk A, Meyer WK, Partha R, Mao W, Clark NL, Chikina M. 2019. RERconverge: an R
1004 package for associating evolutionary rates with convergent traits. *Bioinformatics* 35:4815-4817.
- 1005
1006 Kulathinal RJ, Steviston LS, Noor MA. 2009. The genomics of speciation in *Drosophila*: diversity,
1007 divergence, and introgression estimated using low-coverage genome sequencing. *PLoS Genet*
1008 5:e1000550.
- 1009
1010 Kumon T, Ma J, Akins RB, Stefanik D, Nordgren CE, Kim J, Levine MT, Lampson MA. 2021.
1011 Parallel pathways for recruiting effector proteins determine centromere drive and suppression. *Cell*
1012 184:4904-4918 e4911.
- 1013
1014 Calculating and interpreting gene- and site-concordance factors in phylogenomics [Internet]. The
1015 Lanfear Lab @ ANU2018 September 20, 2021]. Available from:
1016 http://www.robertlanfear.com/blog/files/concordance_factors.html
- 1017
1018 Lecompte E, Aplin K, Denys C, Catzeflis F, Chades M, Chevret P. 2008. Phylogeny and
1019 biogeography of African Murinae based on mitochondrial and nuclear gene sequences, with a new
1020 tribal classification of the subfamily. *BMC Evol Biol* 8:199.
- 1021
1022 Lewontin RC, Birch LC. 1966. Hybridization as a Source of Variation for Adaptation to New
1023 Environments. *Evolution* 20:315-336.
- 1024
1025 Li H. 2013. Aligning sequence reads, clone sequences and assembly contigs with BWA-MEM.
1026 arXiv preprint arXiv:1303.3997.
- 1027
1028 Li H. 2018. Minimap2: pairwise alignment for nucleotide sequences. *Bioinformatics* 34:3094-
1029 3100.
- 1030
1031 Liu X, Wei F, Li M, Jiang X, Feng Z, Hu J. 2004. Molecular phylogeny and taxonomy of wood
1032 mice (genus *Apodemus* Kaup, 1829) based on complete mtDNA cytochrome b sequences, with
1033 emphasis on Chinese species. *Mol Phylogenetic Evol* 33:1-15.
- 1034
1035 Lopes F, Oliveira LR, Kessler A, Beux Y, Crespo E, Cardenas-Alayza S, Majluf P, Sepulveda M,
1036 Brownell RL, Franco-Trecu V, et al. 2021. Phylogenomic Discordance in the Eared Seals is best
1037 explained by Incomplete Lineage Sorting following Explosive Radiation in the Southern
1038 Hemisphere. *Syst Biol* 70:786-802.
- 1039
1040 Lundrigan BL, Jansa SA, Tucker PK. 2002. Phylogenetic relationships in the genus *mus*, based on
1041 paternally, maternally, and biparentally inherited characters. *Syst Biol* 51:410-431.

- 1042
1043 Maddison WP. 1997. Gene Trees in Species Trees. *Systematic Biology* 46:523-536.
- 1044
1045 Martin Y, Gerlach G, Schlotterer C, Meyer A. 2000. Molecular phylogeny of European muroid
1046 rodents based on complete cytochrome b sequences. *Mol Phylogenet Evol* 16:37-47.
- 1047
1048 McKenzie PF, Eaton DAR. 2020. The Multispecies Coalescent in Space and Time.
1049 bioRxiv:2020.2008.2002.233395.
- 1050
1051 Mendes FK, Fuentes-Gonzalez JA, Schraiber JG, Hahn MW. 2018. A multispecies coalescent
1052 model for quantitative traits. *Elife* 7:e36482.
- 1053
1054 Mendes FK, Hahn MW. 2016. Gene Tree Discordance Causes Apparent Substitution Rate
1055 Variation. *Syst Biol* 65:711-721.
- 1056
1057 Mendes FK, Hahn Y, Hahn MW. 2016. Gene Tree Discordance Can Generate Patterns of
1058 Diminishing Convergence over Time. *Mol Biol Evol* 33:3299-3307.
- 1059
1060 Mendes FK, Livera AP, Hahn MW. 2019. The perils of intralocus recombination for inferences of
1061 molecular convergence. *Philos Trans R Soc Lond B Biol Sci* 374:20180244.
- 1062
1063 Mikula O, Nicolas V, Šumbera R, Konečný A, Denys C, Verheyen E, Bryjová A, Lemmon AR,
1064 Lemmon EM, Bryja J. 2021. Nuclear phylogenomics, but not mitogenomics, resolves the most
1065 successful Late Miocene radiation of African mammals (Rodentia: Muridae: Arvicanthini).
1066 *Molecular Phylogenetics and Evolution* 157:107069.
- 1067
1068 Minh BQ, Hahn MW, Lanfear R. 2020. New Methods to Calculate Concordance Factors for
1069 Phylogenomic Datasets. *Mol Biol Evol* 37:2727-2733.
- 1070
1071 Minh BQ, Schmidt HA, Chernomor O, Schrempf D, Woodhams MD, von Haeseler A, Lanfear R.
1072 2020. IQ-TREE 2: New Models and Efficient Methods for Phylogenetic Inference in the Genomic
1073 Era. *Mol Biol Evol* 37:1530-1534.
- 1074
1075 Mölder F, Jablonski KP, Letcher B, Hall MB, Tomkins-Tinch CH, Sochat V, Forster J, Lee S,
1076 Twardziok SO, Kanitz A, et al. 2021. Sustainable data analysis with Snakemake. *F1000Res* 10:33.
- 1077

- 1078 Moore EC, Thomas GWC, Mortimer S, Kopania EEK, Hunnicutt KE, Clare-Salzler ZJ, Larson
1079 EL, Good JM. 2022. The Evolution of Widespread Recombination Suppression on the Dwarf
1080 Hamster (*Phodopus*) X Chromosome. *Genome Biol Evol* 14:evac080.
- 1081
- 1082 Mouse Genome Sequencing C, Waterston RH, Lindblad-Toh K, Birney E, Rogers J, Abril JF,
1083 Agarwal P, Agarwala R, Ainscough R, Andersson M, et al. 2002. Initial sequencing and
1084 comparative analysis of the mouse genome. *Nature* 420:520-562.
- 1085
- 1086 Murrell B, Weaver S, Smith MD, Wertheim JO, Murrell S, Aylward A, Eren K, Pollner T, Martin
1087 DP, Smith DM, et al. 2015. Gene-wide identification of episodic selection. *Mol Biol Evol* 32:1365-
1088 1371.
- 1089
- 1090 Nilsson P, Solbakken MH, Schmid BV, Orr RJS, Lv R, Cui Y, Song Y, Zhang Y, Baalsrud HT,
1091 Torresen OK, et al. 2020. The Genome of the Great Gerbil Reveals Species-Specific Duplication
1092 of an MHCII Gene. *Genome Biol Evol* 12:3832-3849.
- 1093
- 1094 Pagès M, Fabre P-H, Chaval Y, Mortelliti A, Nicolas V, Wells K, Michaux JR, Lazzari V. 2016.
1095 Molecular phylogeny of South-East Asian arboreal murine rodents. *Zoologica Scripta* 45:349-364.
- 1096
- 1097 Pamilo P, Nei M. 1988. Relationships between gene trees and species trees. *Mol Biol Evol* 5:568-
1098 583.
- 1099
- 1100 Paradis E, Schliep K. 2019. ape 5.0: an environment for modern phylogenetics and evolutionary
1101 analyses in R. *Bioinformatics* 35:526-528.
- 1102
- 1103 Partha R, Kowalczyk A, Clark NL, Chikina M. 2019. Robust Method for Detecting Convergent
1104 Shifts in Evolutionary Rates. *Mol Biol Evol* 36:1817-1830.
- 1105
- 1106 Pease JB, Haak DC, Hahn MW, Moyle LC. 2016. Phylogenomics Reveals Three Sources of
1107 Adaptive Variation during a Rapid Radiation. *PLoS Biol* 14:e1002379.
- 1108
- 1109 Pease JB, Hahn MW. 2013. More accurate phylogenies inferred from low-recombination regions
1110 in the presence of incomplete lineage sorting. *Evolution* 67:2376-2384.
- 1111
- 1112 Platt RN, 2nd, Vandewege MW, Ray DA. 2018. Mammalian transposable elements and their
1113 impacts on genome evolution. *Chromosome Res* 26:25-43.
- 1114

- 1115 Pollard KS, Hubisz MJ, Rosenbloom KR, Siepel A. 2010. Detection of nonneutral substitution
1116 rates on mammalian phylogenies. *Genome Res* 20:110-121.
- 1117
- 1118 Pond SL, Frost SD, Muse SV. 2005. HyPhy: hypothesis testing using phylogenies. *Bioinformatics*
1119 21:676-679.
- 1120
- 1121 Poplin R, Ruano-Rubio V, DePristo MA, Fennell TJ, Carneiro MO, Auwera GAVd, Kling DE,
1122 Gauthier LD, Levy-Moonshine A, Roazen D, et al. 2018. Scaling accurate genetic variant
1123 discovery to tens of thousands of samples. *bioRxiv*:201178.
- 1124
- 1125 Ptak SE, Hinds DA, Koehler K, Nickel B, Patil N, Ballinger DG, Przeworski M, Frazer KA, Paabo
1126 S. 2005. Fine-scale recombination patterns differ between chimpanzees and humans. *Nat Genet*
1127 37:429-434.
- 1128
- 1129 Quinlan AR, Hall IM. 2010. BEDTools: a flexible suite of utilities for comparing genomic
1130 features. *Bioinformatics* 26:841-842.
- 1131
- 1132 R Core Team. 2021. R: A language and environment for statistical computing. Vienna, Austria.
- 1133
- 1134 Ranwez V, Douzery EJP, Cambon C, Chantret N, Delsuc F. 2018. MACSE v2: Toolkit for the
1135 Alignment of Coding Sequences Accounting for Frameshifts and Stop Codons. *Mol Biol Evol*
1136 35:2582-2584.
- 1137
- 1138 Revell LJ. 2012. phytools: an R package for phylogenetic comparative biology (and other things).
1139 *Methods in Ecology and Evolution* 3:217-223.
- 1140
- 1141 Rivas-Gonzalez I, Rousselle M, Li F, Zhou L, Dutheil JY, Munch K, Shao Y, Wu D, Schierup
1142 MH, Zhang G. 2023. Pervasive incomplete lineage sorting illuminates speciation and selection in
1143 primates. *Science* 380:eabn4409.
- 1144
- 1145 Robinson DF, Foulds LR. 1981. Comparison of phylogenetic trees. *Mathematical Biosciences*
1146 53:131-147.
- 1147
- 1148 Robinson DF, Foulds LR editors.; 1979 Berlin, Heidelberg.
- 1149
- 1150 Romanenko SA, Perelman PL, Trifonov VA, Graphodatsky AS. 2012. Chromosomal evolution in
1151 Rodentia. *Heredity (Edinb)* 108:4-16.
- 1152

- 1153 Rosenberg NA. 2002. The probability of topological concordance of gene trees and species trees.
1154 *Theor Popul Biol* 61:225-247.
- 1155
1156 Rowe KC, Achmadi AS, Fabre P-H, Schenk JJ, Steppan SJ, Esselstyn JA. 2019. Oceanic islands
1157 of Wallacea as a source for dispersal and diversification of murine rodents. *Journal of*
1158 *Biogeography* 46:2752-2768.
- 1159
1160 Roycroft E, Achmadi A, Callahan CM, Esselstyn JA, Good JM, Moussalli A, Rowe KC. 2021.
1161 Molecular Evolution of Ecological Specialisation: Genomic Insights from the Diversification of
1162 Murine Rodents. *Genome Biol Evol* 13:evab103.
- 1163
1164 Roycroft EJ, Moussalli A, Rowe KC. 2020. Phylogenomics Uncovers Confidence and Conflict in
1165 the Rapid Radiation of Australo-Papuan Rodents. *Syst Biol* 69:431-444.
- 1166
1167 Sarver BA, Keeble S, Cosart T, Tucker PK, Dean MD, Good JM. 2017. Phylogenomic Insights
1168 into Mouse Evolution Using a Pseudoreference Approach. *Genome Biol Evol* 9:726-739.
- 1169
1170 Scally A, Dutheil JY, Hillier LW, Jordan GE, Goodhead I, Herrero J, Hobolth A, Lappalainen T,
1171 Mailund T, Marques-Bonet T, et al. 2012. Insights into hominid evolution from the gorilla genome
1172 sequence. *Nature* 483:169-175.
- 1173
1174 Schenk JJ, Rowe KC, Steppan SJ. 2013. Ecological opportunity and incumbency in the
1175 diversification of repeated continental colonizations by muroid rodents. *Syst Biol* 62:837-864.
- 1176
1177 Schliep KP. 2011. phangorn: phylogenetic analysis in R. *Bioinformatics* 27:592-593.
- 1178
1179 Serizawa K, Suzuki H, Tsuchiya K. 2000. A phylogenetic view on species radiation in Apodemus
1180 inferred from variation of nuclear and mitochondrial genes. *Biochem Genet* 38:27-40.
- 1181
1182 Shifman S, Bell JT, Copley RR, Taylor MS, Williams RW, Mott R, Flint J. 2006. A high-resolution
1183 single nucleotide polymorphism genetic map of the mouse genome. *PLoS Biol* 4:e395.
- 1184
1185 Singhal S, Leffler EM, Sannareddy K, Turner I, Venn O, Hooper DM, Strand AI, Li Q, Raney B,
1186 Balakrishnan CN, et al. 2015. Stable recombination hotspots in birds. *Science* 350:928-932.
- 1187
1188 Slatkin M, Pollack JL. 2006. The concordance of gene trees and species trees at two linked loci.
1189 *Genetics* 172:1979-1984.
- 1190

- 1191 Smagulova F, Gregoretti IV, Brick K, Khil P, Camerini-Otero RD, Petukhova GV. 2011. Genome-
1192 wide analysis reveals novel molecular features of mouse recombination hotspots. *Nature* 472:375-
1193 378.
- 1194
- 1195 RepeatMasker Open-4.0 [Internet]. 2013-2015. Available from <http://www.repeatmasker.org>.
- 1196
- 1197 Smith BT, Merwin J, Provost KL, Thom G, Brumfield RT, Ferreira M, Mauck WM, Moyle RG,
1198 Wright TF, Joseph L. 2023. Phylogenomic Analysis of the Parrots of the World Distinguishes
1199 Artifactual from Biological Sources of Gene Tree Discordance. *Syst Biol* 72:228-241.
- 1200
- 1201 Smith JM, Haigh J. 1974. The hitch-hiking effect of a favourable gene. *Genet Res* 23:23-35.
- 1202
- 1203 Smith MD, Wertheim JO, Weaver S, Murrell B, Scheffler K, Kosakovsky Pond SL. 2015. Less is
1204 more: an adaptive branch-site random effects model for efficient detection of episodic diversifying
1205 selection. *Mol Biol Evol* 32:1342-1353.
- 1206
- 1207 Smith SA, Brown JW, Walker JF. 2018. So many genes, so little time: A practical approach to
1208 divergence-time estimation in the genomic era. *PLoS One* 13:e0197433.
- 1209
- 1210 Smith SA, Moore MJ, Brown JW, Yang Y. 2015. Analysis of phylogenomic datasets reveals
1211 conflict, concordance, and gene duplications with examples from animals and plants. *BMC Evol
1212 Biol* 15:150.
- 1213
- 1214 Stanyon R, Yang F, Cavagna P, O'Brien P, Bagga M, Ferguson-Smith M, Wienberg J. 1999.
1215 Animal Cytogenetics and Comparative Mapping-Reciprocal chromosome painting shows that
1216 genomic rearrangement between rat and mouse proceeds ten times faster than between humans
1217 and cats. *Cytogenetics and Cell Genetics* 84:150-155.
- 1218
- 1219 Stapley J, Feulner PGD, Johnston SE, Santure AW, Smadja CM. 2017. Variation in recombination
1220 frequency and distribution across eukaryotes: patterns and processes. *Philos Trans R Soc Lond B
1221 Biol Sci* 372.
- 1222
- 1223 Steppan SJ, Adkins RM, Spinks PQ, Hale C. 2005. Multigene phylogeny of the Old World mice,
1224 Murinae, reveals distinct geographic lineages and the declining utility of mitochondrial genes
1225 compared to nuclear genes. *Mol Phylogenet Evol* 37:370-388.
- 1226
- 1227 Steppan SJ, Schenk JJ. 2017. Muroid rodent phylogenetics: 900-species tree reveals increasing
1228 diversification rates. *PLoS One* 12:e0183070.

- 1229
1230 Steviston LS, Woerner AE, Kidd JM, Kelley JL, Veeramah KR, McManus KF, Great Ape Genome
1231 P, Bustamante CD, Hammer MF, Wall JD. 2016. The Time Scale of Recombination Rate
1232 Evolution in Great Apes. *Mol Biol Evol* 33:928-945.
- 1233
1234 Sun C, Huang J, Wang Y, Zhao X, Su L, Thomas GWC, Zhao M, Zhang X, Jungreis I, Kellis M,
1235 et al. 2021. Genus-Wide Characterization of Bumblebee Genomes Provides Insights into Their
1236 Evolution and Variation in Ecological and Behavioral Traits. *Mol Biol Evol* 38:486-501.
- 1237
1238 Suzuki H, Shimada T, Terashima M, Tsuchiya K, Aplin K. 2004. Temporal, spatial, and ecological
1239 modes of evolution of Eurasian *Mus* based on mitochondrial and nuclear gene sequences. *Mol*
1240 *Phylogenet Evol* 33:626-646.
- 1241
1242 Tange O. 2018. GNU Parallel.
- 1243
1244 To TH, Jung M, Lycett S, Gascuel O. 2016. Fast Dating Using Least-Squares Criteria and
1245 Algorithms. *Syst Biol* 65:82-97.
- 1246
1247 Treaster S, Deelen J, Daane JM, Murabito J, Karasik D, Harris MP. 2023. Convergent genomics
1248 of longevity in rockfishes highlights the genetics of human life span variation. *Sci Adv*
1249 9:eadd2743.
- 1250
1251 van der Valk T, Pecnerova P, Diez-Del-Molino D, Bergstrom A, Oppenheimer J, Hartmann S,
1252 Xenikoudakis G, Thomas JA, Dehasque M, Saglican E, et al. 2021. Million-year-old DNA sheds
1253 light on the genomic history of mammoths. *Nature* 591:265-269.
- 1254
1255 Vanderpool D, Minh BQ, Lanfear R, Hughes D, Murali S, Harris RA, Raveendran M, Muzny DM,
1256 Hibbins MS, Williamson RJ, et al. 2020. Primate phylogenomics uncovers multiple rapid
1257 radiations and ancient interspecific introgression. *PLoS Biol* 18:e3000954.
- 1258
1259 Wang LG, Lam TT, Xu S, Dai Z, Zhou L, Feng T, Guo P, Dunn CW, Jones BR, Bradley T, et al.
1260 2020. Treeio: An R Package for Phylogenetic Tree Input and Output with Richly Annotated and
1261 Associated Data. *Mol Biol Evol* 37:599-603.
- 1262
1263 White MA, Ane C, Dewey CN, Larget BR, Payseur BA. 2009. Fine-scale phylogenetic
1264 discordance across the house mouse genome. *PLoS Genet* 5:e1000729.
- 1265

- 1266 Yalcin B, Wong K, Agam A, Goodson M, Keane TM, Gan X, Nellaker C, Goodstadt L, Nicod J,
1267 Bhomra A, et al. 2011. Sequence-based characterization of structural variation in the mouse
1268 genome. *Nature* 477:326-329.
- 1269
1270 Yang Z. 2007. PAML 4: phylogenetic analysis by maximum likelihood. *Mol Biol Evol* 24:1586-
1271 1591.
- 1272
1273 Yekutieli D, Benjamini Y. 1999. Resampling-based false discovery rate controlling multiple test
1274 procedures for correlated test statistics. *Journal of Statistical Planning and Inference* 82:171-196.
- 1275
1276 Yu G. 2020. Using ggtree to Visualize Data on Tree-Like Structures. *Curr Protoc Bioinformatics*
1277 69:e96.
- 1278
1279 Yu G, Smith DK, Zhu H, Guan Y, Lam TT-Y. 2017. ggtree: an r package for visualization and
1280 annotation of phylogenetic trees with their covariates and other associated data. *Methods in
1281 Ecology and Evolution* 8:28-36.
- 1282
1283 Zhang C, Rabiee M, Sayyari E, Mirarab S. 2018. ASTRAL-III: polynomial time species tree
1284 reconstruction from partially resolved gene trees. *BMC Bioinformatics* 19:153.
- 1285
1286
1287

1 **The genomic landscape, causes, and consequences of extensive phylogenomic discordance**
2 **in Old World mice and rat/murine rodents**

3

4 Gregg W. C. Thomas^{1,2,*}, Jonathan J. Hughes^{3,4}, Tomohiro Kumon⁵, Jacob S. Berv^{3,6}, C. Erik
5 Nordgren⁵, Michael Lampson⁵, Mia Levine⁵, Jeremy B. Searle³, Jeffrey M. Good¹

6

7 ¹*Division of Biological Sciences, University of Montana, Missoula, MT, 59801.*

8 ²*Informatics Group, Harvard University, Cambridge, MA, 02138*

9 ³*Department of Ecology and Evolutionary Biology, Cornell University, Ithaca, NY, 14853.*

10 ⁴*Department of Evolution, Ecology, and Organismal Biology, University of California Riverside,
11 Riverside, CA, 92521*

12 ⁵*Department of Biology, University of Pennsylvania, Philadelphia, PA, 19104*

13 ⁶*Department of Ecology and Evolutionary Biology, University of Michigan, Ann Arbor, MI,
14 48109*

15

16 *Corresponding author

17 E-mail: gthomas@fas.harvard.edu

18

19 Abstract

20 A species tree is a central concept in evolutionary biology whereby a single branching phylogeny
21 reflects relationships among species. However, the phylogenies of different genomic regions often
22 differ from the species tree. Although tree discordance is widespread in phylogenomic studies, we
23 still lack a clear understanding of how variation in phylogenetic patterns is shaped by genome
24 biology or the extent to which discordance may compromise comparative studies. We
25 characterized patterns of phylogenomic discordance across the murine rodents (Old World mice
26 and rats)—a large and ecologically diverse group that gave rise to the laboratory mouse and rat
27 model systems. Combining recently published linked-read genome assemblies for seven murine
28 species with other available rodent genomes, we first used ultra-conserved elements (UCEs) to
29 infer a robust time-calibrated species tree. We then used whole genomes to examine finer-scale
30 patterns of discordance and across 12 million years of divergence. We found that proximate
31 chromosomal regions tended to have more similar phylogenetic histories. While we found, but no
32 clear relationship between local tree similarity and recombination rates in house mice. However,
33 we did observe a correlation between recombination rates and average similarity to the species
34 tree. We also detected a strong influence of linked selection whereby purifying selection at UCEs
35 led to appreciably less discordance. Finally, we show that assuming a single species tree can result
36 in high error rates when testing for positive selection under different models. Collectively, our
37 results highlight the complex relationship between phylogenetic inference and genome biology
38 and underscore how failure to account for this complexity can mislead comparative genomic
39 studies.

40

41 **Keywords:** phylogenetic discordance, murine rodents, molecular evolution recombination,
42 genomics, mouse

43 Significance Statement

44 Genomic data has demonstrated that when sequences from multiple species are compared,
45 different regions of the genome exhibit different phylogenetic histories. These discordant histories
46 could be due to either biological processes, such as ancestral variation or introgression, or artifacts
47 of the inference process. We use the genomes of several murine rodents to distinguish how features
48 of the genome, such as recombination rates, genes, and other conserved regions, affect this
49 discordance across the genome. Considering the prevalence of discordance across the genome, we
50 also test how using a single species tree, a common practice, affects inferences from tests for
51 positive selection. Our study shows that conserved genomic loci exhibit lower amounts of
52 discordance, and that discordance can negatively affect inferences of selection when the incorrect
53 species tree is used.

54 Introduction

55 Phylogenies are the unifying concept in understanding the evolution of species, traits, and genes.
56 However, with the availability of extensive high-throughput sequencing data it has become
57 apparent now revealed that evolutionary relationships between species may not be well represented
58 by a single representative phylogeny (Edwards 2009; Hahn and Nakhleh 2016). While a dominant
59 signal of bifurcating speciation may exist usually exists (*i.e.*, a species tree), phylogenetic signal
60 that may disagree with species relationships can arise from ancestral polymorphisms (incomplete
61 lineage sorting; ILS), gene flow through hybridization (introgression), and gene duplication and
62 loss (Maddison 1997). The theoretical prediction of phylogenetic discordance has long been
63 appreciated (Hudson 1983; Pamilo and Nei 1988; Maddison 1997; Rosenberg 2002), but empirical
64 evidence now emphasizes just how extensive discordance can be among a set of species. Several
65 recent studies focused on analyzing phylogenetic discordance among the genomes of specific
66 taxonomic groups (Feng, et al. 2022; Gable, et al. 2022; Smith, et al. 2023). Among others For
67 example, studies of birds (Jarvis, et al. 2014), seals mammals (Ferreira, et al. 2021; Lopes, et al.
68 2021; Foley, et al. 2024), tomatoes plants (Pease, et al. 2016), bumblebees (Pease, et al. 2016), and
69 insects (Sun, et al. 2021; He, et al. 2023), and butterflies (He, et al. 2023) have found that with
70 extensive taxon sampling and genomic data, highly supported species tree topologies are rarely or
71 never recovered in the underlying locus trees. Whereas these examples highlight the prevalence of
72 phylogenetic discordance across the tree of life, we still lack a clear understanding of how
73 phylogenetic patterns are shaped by the details of genome biology or the extent to which
74 discordance may compromise inferences from comparative studies that assume a singular species
75 history.

76 From a practical perspective In practice, failure to acknowledge and account for
77 phylogenetic discordance could severely affect biological inference. Analyses of molecular
78 evolution are usually performed on a gene-by-gene basis (Pond, et al. 2005; Yang 2007; Hu, et al.
79 2019; Kowalczyk, et al. 2019), but it is still common practice to assume a single genome-wide
80 species tree for each locus. For gene-based analyses, using the wrong tree may compromise because
81 erroneous inferences of positive directional selection, convergent evolution, and genome-wide
82 inferences of correlated rate variation (Mendes, et al. 2016). Phylogenetic discordance can also
83 affect how continuous traits are reconstructed across phylogenies, as the genes that underly these
84 traits may not follow the species history (Avise and Robinson 2008; Hahn and Nakhleh 2016;
85 Mendes, et al. 2018; Hibbins, et al. 2023). In these instances, phylogenetic discordance may need
86 to be characterized and incorporated into the experimental and analytical design. Alternatively, if
87 a researcher's primary questions are focused on reconstructing the evolutionary history of
88 speciation (*i.e.*, the species tree), then phylogenetic discordance may obscure the true signal of
89 speciation (Fontaine, et al. 2015; Foley, et al. 2024). In this case, knowledge about patterns of
90 discordance across genomes could inform decisions about locus selection, data filtering, and model
91 parameters during species tree reconstruction.

92 Given these considerations, a better understanding of the genomic context of phylogenetic
93 discordance is warranted. Although often conceptualized primarily as a stochastic consequence of

94 population history (Maddison 1997), patterns of phylogenetic discordance are likely to be non-
95 random and dependent on localized patterns of genetic drift, natural selection, recombination, and
96 mutation. Discordance due to ILS ultimately depends on effective population sizes across the
97 branches of the phylogeny (Pamilo and Nei 1988; Degnan and Rosenberg 2006) and, therefore,
98 should covary with any process that influences local patterns of genetic diversity (e.g., linked
99 negative or positive selection). Likewise, ~~the potential for~~ discordance due to introgression may
100 be influenced by selection against incompatible alleles or positive selection for beneficial variants
101 (Lewontin and Birch 1966; Jones, et al. 2018). Selection, ILS, and introgression, are expected to
102 leave ~~differing~~different genomic signals ~~across a sample of genomes~~ that should allow us to test
103 hypotheses about both the cause and the scale of phylogenetic discordance (Huson, et al. 2005;
104 Kulathinal, et al. 2009; Green, et al. 2010; Vanderpool, et al. 2020). Yet the genomic context of
105 phylogenetic discordance has remained elusive. For example, localized patterns of phylogenetic
106 discordance should be influenced by patterns of recombination (Hudson and Kaplan 1988) and
107 simulation studies ~~posit~~confirm that the closer two regions are in the genome, the more history
108 they share (Slatkin and Pollack 2006; McKenzie and Eaton 2020). However, ~~empirical~~ studies ~~of~~
109 ~~mammals~~ have been inconclusive regarding the relationship between ~~phylogenetic~~ discordance
110 and recombination rates, ranging from no ~~correlation~~relationship in great apes (Hobolth, et al.
111 2007) ~~to~~, a weak positive correlation in house mice (White, et al. 2009). ~~Some studies have also~~
112 ~~linked increased amounts of phylogenetic discordance to areas of the genome with lower~~
113 ~~recombination rates (White, et al. 2009)~~, a strong positive correlation broadly across primates
114 (Rivas-Gonzalez, et al. (2023)). ~~More recently~~, or increased discordance in regions of lower
115 recombination (Scally, et al. 2012; Pease and Hahn 2013) ~~have found a strong correlation between~~
116 ~~levels of ILS and recombination rate through a detailed study of the primate phylogeny. However,~~
117 Thus, it remains unclear how phylogenetic discordance scales locally across the genome as a
118 function of recombination and the strength of linked selection. pointing to the need for empirical
119 studies in systems with sufficient genomic resources to explore the causes of discordance.

120 To investigate the causes and consequences of phylogenetic discordance, we took
121 advantage of genomic resources available for house ~~mouse~~mice (*Mus musculus*). This rodent
122 species is one of the most important mammalian model systems for biological and biomedical
123 research and is embedded within a massive radiation of ~~Old World~~ rats and mice (Murinae). This
124 ecologically diverse and species-rich group is comprised of over 600 species and makes up >10%
125 of all mammalian species, and yet is only about 15 million years old, making this system an
126 excellent choice for phylogenetic studies over both short and long timescales. Despite the power
127 of evolution-guided functional and biomedical analysis (Christmas, et al. 2023), relatively few
128 murine genomes have been sequenced outside of *Mus* and *Rattus*.

129 In the present work, we We analyze recently sequenced ~~genome sequences~~genomes for
130 seven murine ~~rodent~~ species (*Mastomys natalensis*, *Hylomyscus allenii*, *Praomys delectorum*,
131 *Rhabdomys dilectus*, *Grammomys dolichurus*, *Otomoys typus*, and *Rhynchosomys soricoides*)
132 sampled from across this radiation (Kumon, et al. 2021). We combine these new genomes with
133 previously sequenced ~~rodent~~ genomes and genomic resources from the *M. musculus* model system

134 to study phylogenetic relationships within Murinae as well as the landscape of discordance along
135 rodent chromosomes. We first inferred a species tree for these and other sequenced rodent
136 genomes, focusing on signals derived from commonly used ultra-conserved elements (UCEs).
137 We used these UCE data to promote broader comparisons across genomes-infer a robust, time-
138 calibrated phylogeny of variable quality. We sequenced murine rodents, providing a useful
139 resource for future comparative studies within this important group. Using this species tree, we
140 then used whole genome sequences from a subset of these genomes,whole genomes to study how
141 phylogenetic discordance is related to species-level inferences of relatedness, recombination rate,
142 and patterns of molecular evolution. Using genetic maps, and functional annotation information
143 from the powerful house mice to describe the genomic context of phylogenetic discordance across
144 murine rodents and evaluate mouse system, we test several hypotheses linking spatial patterns of
145 discordance to genetic drift, natural selection, and recombination. Finally, we show how the use
146 of a single species-tree impacts gene-level inferences from common molecular evolution tests for
147 natural selection in these species. Collectively, our results advance our understanding of how core
148 features of genome biology influence underlying phylogenetic patterns, the extent to which
149 established model system resources can be leveraged for broader phylogenetic studies, and the
150 consequences of ignoring phylogenetic uncertainty.

151

152

Results

153

Estimation of a murine species tree

154 Using a concatenated dataset of 2,632 aligned ultra conserved elements (UCEs), we inferred a
155 species tree of 18 murine rodent species (Figure 1; Table S1) that recovered the same relationships
156 as previous reconstructions of Murinae using a small number of loci (Lecompte, et al. 2008;
157 Steppan and Schenk 2017). The species tree inferred from a quartet-based summary of the gene
158 tree topologies was identical to the concatenated tree (Fig. Figure S1). While bootstrap and SH-
159 aLRT values provided high support to our inferred species trees (Fig. Figure 1), we found evidence
160 for considerable discordance across individual UCE phylogenies. The five shortest branches in the
161 concatenated tree had a site concordance factor (sCF) of less than 50%, suggesting that alternate
162 resolutions of the quartet had equivocal support (Fig. Figure S2). Gene concordance factors (gCF)
163 for each branch in the species tree were on aggregate much higher, with all but four branches
164 supported by almost every gene tree in the analysis and with the lowest values likely being driven
165 by a several short internal branches (Fig. Figure S2). This pattern was recapitulated using a quartet-
166 based summary method (Figs. S1 and S3). At the two most discordant nodes (E and J in Fig. Figure
167 1), the recovered topology was supported by approximately one third of all gene trees.

168 We estimated divergence times for the inferred concatenated phylogeny (Fig. Figure 1;
169 Table S2) using four fossil calibration points (Table S3). The murid and cricetid groups had an
170 estimated divergence time of 22.66 Ma (node A in Fig. Figure 1) followed by the Murinae and the
171 Gerbillinae at 21.34 Ma (B), albeit with wide confidence intervals (CI) in both cases. The core
172 Murinae (C) *sensu* Steppan et al. (2005) are inferred to have arisen 13.11 Ma (CI: 11.42 – 15.10).

173 [Hydromyini](#) then split off at 12.15 Ma (D, CI: 11.10 – 13.51) followed by [Otomyini](#) and
174 [Arvicanthini](#) at 11.70 Ma (E, fossil calibration from Kimura, et al 2015). The remaining Murine
175 tribes evolved in rapid succession, with [Apodemini](#) diverging from [Murini](#) and [Praomyini](#) at 10.84
176 Ma (F). [Murini](#) and [Praomyini](#) then split at 10.19 Ma (H). The two *Rattus* species in our dataset
177 were inferred to have diverged 2.01 Ma (Q, CI: 1.26 – 2.30). Although congruent with previous
178 works (Lecompte, et al. 2008; Steppan and Schenk 2017), this dated UCE phylogeny provides
179 context on the evolutionary timescale upon which we next describe the genomic landscape of
180 phylogenetic discordance across a collection of murine genomes.

181

182 *The landscape of phylogenetic discordance along murine genomes*

183 We analyzed genome-wide phylogenetic histories of six recently sequenced murine rodent
184 genomes and the *M. musculus* reference genome spanning approximately 12 million years of
185 divergence (see Fig. [Figure 1](#)). Using the *M. musculus* coordinate system, we partitioned and
186 aligned 263,389 non-overlapping 10 kb windows from these seven species (Table [S1](#)). After
187 filtering windows in repetitive regions or with low phylogenetic signal, we recovered 163,765 trees
188 with an average of 616 informative sites per window (Fig. [Figure S4](#)).

189 Phylogenetic discordance was pervasive within and between chromosomes. We inferred
190 597 of the 945 possible unique rooted topologies among six species (when specifying *R. soricoides*
191 as the outgroup) across all chromosomes. The number of unique topologies per chromosome
192 ranged from 75 to 218 (mean = 141). However, just four different topologies were ranked in the
193 top three per chromosome. (Fig 2A; File S1) and only nine trees were present at a frequency above
194 1%. Among these, the top three topologies only differed in the ordering of the clade containing
195 *Hylomyscus allenii*, *Mastomys natalensis*, and *Praomys delectorum* (HMP clade). This clade also
196 showed the second lowest concordance in the species tree inferred from UCEs (Fig. [Figure 1](#), node
197 J). These three topologies comprise between 13-15% of all recovered topologies (Fig. [Figure 2](#)).
198 Interestingly, the least common of these three trees (13.1%) matched the topology recovered via
199 concatenation of all coding regions and the species tree recovered from UCEs (Fig. [Figure 1](#)). That
200 is, the robustly inferred species tree did not match the evolutionary relationships inferred for over
201 85% of the genome.

202 While visual inspection revealed no clear partitioning of topological structures along
203 chromosomes (e.g., Fig. [Figure 2C](#)), we found that phylogenies were not randomly distributed
204 across mouse chromosomes. Using the weighted Robinson-Foulds metric, we found that tree
205 similarity between windows decayed logarithmically along chromosomes (Fig. [Figure 3A and B](#)),
206 and the distance at which tree similarity appeared random varied considerably among
207 chromosomes ranging from 0.15 Megabases (Mb) on chromosome 17 to 141.29 Mb on the
208 chromosome 2 (Fig. [Figure 3C](#), Fig. [Figure S5](#)). While chromosomes 2, 7, 9, and 11 were
209 autosomal outliers with distances between windows to random-like trees exceeding 25 Mb, the
210 average distance among all other autosomes was only 2.1 Mb. The rates at which phylogenetic
211 similarity decayed tended to be inversely proportional to the distance at which two randomly
212 drawn phylogenies lost similarity (Fig. [Figure 3D](#)).

213 Next, we performed a pairwise alignment of the reference mouse and rat genomes to assess
214 how large structural variations, such as inversions and translocations, may influence our inferences
215 of phylogenetic relatedness along the genome. These species span the deepest divergence of the
216 sample for which we assessed genome-wide discordance, so the level of large structural variation
217 present among them should give us an idea of the amount of ancestral variation in our sample. The
218 mouse and rat genomes were mostly co-linear for large, aligned chunks, with large translocations
219 and inversions on mouse chromosomes 5, 8, 10, 13, and 16 (Fig. Figure S6). We also observe
220 large-scale inversions on chromosome 16. We found that, while most chromosomes were co-linear
221 between mouse and rat, the average size of the 307,275 contiguously aligned chunks averages
222 under 10 kb, with the average distance between aligned segments being between 2,380 bp on the
223 mouse genome and 4,927 bp on the rat chromosome (Fig. Figure S7). This pattern presents two
224 major implications for our analyses. First, we could not transpose the coordinate system from
225 mouse to rat with enough resolution to use genetic maps from rat. Second, most other structural
226 variations in our sample appear likely to be small insertions of transposable elements (e.g., SINEs
227 ~150-500 bp, LINEs ~4-7kb; Platt, et al. 2018) that should have a negligible effect on discordance
228 analyses since our window size is much larger and we excluded windows that were made up of
229 mostly repeats.

230

231 Discordance with recombination rate and other genomic features

232 Using markers from genetic crosses within *M. musculus* (Shifman, et al. 2006; Cox, et al. 2009)
233 we examined whether regions with high recombination also showed more phylogenetic
234 discordance over short genetic distances when compared to regions with low recombination.
235 Specifically, we calculated recombination rates within 5 Mb windows (Fig. Figure S8) and then
236 measured tree similarity between the first and last 10 kb window ($R^2 = 3.0e-9$; $p = 0.99$; Fig. Figure
237 4A) and the rate at which tree similarity changes between the first 10 kb window and every other
238 10 kb window ($R^2 = 0.003$; $p = 0.11$; Fig. Figure 4B). Surprisingly, we found no relationship
239 between tree similarity and recombination rates measured at this scale. However, we did observe
240 a slight positive correlation between recombination rate and dissimilarity to the species tree when
241 averaging wRF over all 10 kb window trees within a 5 Mb recombination window ($R^2 = 0.05$; $p =$
242 7.6e-8; Fig. Figure 4C). We also examined regions of the genome centered on recombination
243 hotspots identified in *M. musculus* (Smagulova, et al. 2011) and found that these regions had
244 significantly slower rates of decay in similarity over genomic distance compared to windows that
245 were not centered on hotspots ($p = 0.019$; Fig. Figure 5A), and that they were also significantly
246 more phylogenetically similar over short distances ($p = 0.015$; Fig. Figure 5B). Thus, when taken
247 as a whole, we found that regions of higher recombination rates in house mice did not show more
248 local phylogenetic discordance per se but did tend to show more discordance relative to the
249 genome-wide species tree.

250

Evolutionary relationships around certain conserved genomic features may also be shaped
251 by locally reduced effective population sizes due to a history of pervasive linked negative or
252 positive selection. To test for this, we measured tree similarity in 10 kb windows around all

253 annotated protein-coding genes, ultra-conserved elements (UCEs), and protein-coding genes
254 identified as evolving rapidly (*i.e.*, significantly elevated d_N/d_S) due to positive directional selection
255 and compared these patterns relative to chromosome-wide trends (*i.e.*, windows without annotated
256 features). In general, UCEs showed more local phylogenetic similarity among adjacent windows
257 (*i.e.*, less discordance) than regions surrounding recombination hotspots ($p = 2.42e-12$), coding
258 genes ($p = 4.65e-14$), rapidly evolving coding genes ($p = 1.56e-6$), and windows that did not
259 include any of these features ($p = 5.02e-14$; Fig. Figure 5A). In contrast, protein-coding genes
260 (including rapidly evolving genes) were indistinguishable from background rates of discordance
261 observed in windows without annotated genomic features (Fig. Figure 5A). Likewise, UCEs were
262 also much more similar to the overall species tree when compared to any other feature (Fig. Figure
263 5B). Unlike our test of local discordance, protein-coding genes also showed less species tree
264 discordance than windows containing no features or recombination hotspots, but the effect was
265 much less pronounced than observed at UCEs.

266

267 *Consequences of tree misspecification on analyses of molecular evolution*

268 Next, we examined how phylogenetic discordance influenced inferences on the evolution of
269 protein-coding sequences. Among a set of 22,261 *M. musculus* protein-coding transcripts, the
270 average distance between the start and end of the coding sequence was 37.02 kb, or roughly 4 non-
271 overlapping 10 kb windows. At this distance, tree similarity is predicted to diminish considerably
272 (*e.g.*, by 0.10 wRF units), such that the phylogenetic history of individual genes may often contain
273 some phylogenetic discordance (Mendes and Hahn 2016; Mendes, et al. 2019). We also found that
274 out of the 67,566 times the coding sequence in a gene overlapped with a 10 kb window, the inferred
275 topology of the gene tree exactly matched the topology of the corresponding window tree only
276 11% of the time. Thus, the common practice of inferring gene trees on concatenated coding exons
277 from a single transcript is still likely averaging over multiple possible *albeit correlated histories*.

278 Finally, we tested how tree misspecification might impact standard d_N/d_S based
279 phylogenetic analyses for positive directional selection. Specifically, we used the still common
280 practice of assuming a single species tree for all genes and compared that to using individually
281 inferred gene trees in three common statistical tests for positive selection: PAML's M1a vs. M2a
282 test (Yang 2007), HyPhy's BUSTED test (Murrell, et al. 2015), and HyPhy's aBSREL test (Smith,
283 Wertheim, et al. 2015). We found evidence that tree misspecification likely induces both false
284 positive (type I) and false negative (type II) errors. For example, many genes were inferred as
285 having experienced positive directional selection when using a single species tree, but not when
286 using local gene trees and vice versa (Fig. Figure 6). Assuming the locally inferred gene tree is
287 more accurate than the single tree inferred from concatenation of all gene sequences, this resulted
288 in varying rates and types of error (Table 1). For BUSTED, we observe that 28% of genes inferred
289 as having evolved under positive directional selection when using the gene tree were not inferred
290 when using the concatenated species tree (likely false negatives). The opposite was true for M1a
291 vs. M2a, where, among genes showing inconsistent evidence for positive selection across the two
292 scenarios, 76% do so when using the concatenated species tree but not individual gene trees (likely

293 false positives). In general, genes found to be evolving under positive selection using both tree
294 types tended to be more concordant with the species tree than those that had evidence for positive
295 selection either using only the concatenated tree or the gene tree ([Fig. Figure 6](#)).

296

297 **Discussion**

298 Phylogenies provide insight into the relationships of species and serve as a framework for asking
299 questions about molecular and trait evolution. However, phylogenetic histories can vary
300 extensively across regions of a genome, and evolutionary relationships between species may not
301 often be well represented by a single representative species-level phylogeny. Here, we combine
302 the resources of the house mouse (*Mus musculus*) with new and recently published (Kumon et al.
303 2021) genomes from seven species to understand the systematics of murine rodents and causes
304 and consequences of phylogenetic discordance along murine genomes. [These new analyses help](#)
305 [to place this important model system in a stronger evolutionary context and begin to fill the gap in](#)
306 [genome sampling of murine rodents, which, despite their exceptional morphological and](#)
307 [ecological diversity and species richness, have had relatively few whole genomes sequenced. They](#)
308 [further provide us with the resources to study the landscape of phylogenetic discordance across](#)
309 [the genome, understand how recombination and natural selection shape phylogenetic histories, and](#)
310 [evaluate how assuming a single evolutionary history can compromise the study of molecular](#)
311 [evolution in an important biomedical model system.](#)

312

313 *Phylogenomic relationships of murine rodent lineages from conserved genomic regions*

314 The extraordinary species richness of murine rodents complicates phylogenetic analyses because
315 of the resources required to sample, sequence, and analyze such widely distributed taxa. Earlier
316 work either attempted to resolve specific groups such as *Mus* ([Lundrigan, et al. 2002; Suzuki, et](#)
317 [al. 2004](#)) and *Apodemus* ([Serizawa, et al. 2000; Liu, et al. 2004](#)), or to uncover broader
318 relationships across the subfamily ([Martin, et al. 2000; Steppan, et al. 2005](#)) based on a few genetic
319 [markers](#). Lecompte et al. (2008) provided one of the earliest well-supported phylogenetic
320 reconstructions from across Murinae and the tribal classifications they proposed remain generally
321 supported. More recent work has increased the number of taxa sampled, both for analyses of
322 Murinae specifically ([Pagès, et al. 2016](#)) and for their placement within Muridae and Muroidea
323 ([Schenk, et al. 2013; Steppan and Schenk 2017; Rowe, et al. 2019](#)), but the number of loci used
324 for phylogenetic inference remained limited. Other recent studies have greatly expanded the
325 number of loci used for phylogenetic inference ([Mikula, et al. 2021](#)), including the use of 1,245
326 exons ([Roycroft, et al. 2020](#)) and 1,360 exons ([Roycroft, et al. 2021](#)), but have focused on specific
327 tribes within Murinae.

328 [Our inferred species tree based on 2,632 UCEs from 18 species across the radiation \(Fig.](#)
329 [Figure 1\) is consistent with previous studies \(Lecompte, et al. 2008; Steppan and Schenk 2017;](#)
330 [Aghova, et al. 2018\). Branch support was uniformly high, and gene trees unambiguously support](#)
331 [the tribal classification of Lecompte, et al. \(2008\). However, four shorter branches show more](#)

332 substantial gene tree discordance ([Fig. Figure 1](#), branches D, E, H, and J), with two recovered
333 clades (E and J) being supported by less than half of all gene trees. [We also estimated divergence](#)
334 [times on our inferred species tree using four fossil calibration points \(Table S3\)](#), recovering times
335 [that are roughly consistent with the relatively young estimates found by \(Steppan and Schenk](#)
336 [2017\) \(see Supplement\)](#). This dated species tree provides an evolutionary timescale to evaluate the
337 [genomic landscape of phylogenetic discordance across ~12 my of murine evolution.](#)

338

339 [*The genomic landscape of phylogenetic discordance*](#)

340 [Limiting the number and nature of the loci used to resolve species relationships is often useful to](#)
341 [get an initial picture of the history of speciation across many taxa. However, such targeted](#)
342 [approaches may fail to capture the degree of discordance driven by incomplete lineage sorting and](#)
343 [introgression \(Alexander, et al. 2017; Chan, et al. 2020; Vanderpool, et al. 2020; Alda, et al. 2021\).](#)

344 [Our results highlight the limitations of a reduced marker-based approach and the general](#)
345 [relationships between phylogenetic patterns and functional attributes of the genome in several](#)
346 [interesting ways. Using the house mouse genome annotation, we found that the species tree](#)
347 [inferred from only genes or UCEs did not match evolutionary relationships inferred for over 85%](#)
348 [of the genome. Although similar frequencies were observed among these three most common trees](#)
349 [\(\[Fig. Figure 2\]\(#\)\), the topology robustly inferred from genes or UCEs was not that common overall](#)
350 [and only the third most frequent topology among 10 kb windows genome-wide. This result was](#)
351 [driven mainly by discordance among three more closely related \(Praomyini\) species sampled for](#)
352 [this study, which had nodes with low concordance in the UCE species tree \(Fig 1, node J\). In the](#)
353 [window analysis, each alternate topology of this clade occurred at a frequency of ~14% while the](#)
354 [rest of the topology remained consistent with the species tree \(\[Fig. Figure 2\]\(#\)\), indicating that the](#)
355 [alternate topologies are caused by high levels of ILS at these nodes. Increased discordance at](#)
356 [unresolved nodes is a common feature of phylogenomic datasets. These patterns illustrate how](#)
357 [extensive discordance can arise even in a small sample of species and underscores that a single](#)
358 [inferred species tree often may not capture the history of individual regions of the genome.](#)

359 [Given the fundamental role that recombination should play in shaping patterns of genetic](#)
360 [variation within genomes, it is reasonable to assume that patterns of ILS should be broadly shaped](#)
361 [by local recombination rate. We did not observe a clear relationship between local recombination](#)
362 [rates in mice \(*M. musculus*\) and the degree of local phylogenetic discordance \(i.e., phylogenetic](#)
363 [similarity over 5 Mb intervals\). However, we did find that regions of high recombination rate](#)
364 [tended to be more discordant with the inferred species tree, in line with findings in other mammals](#)
365 [\(Pease and Hahn 2013; Foley, et al. 2023; Rivas-Gonzalez, et al. 2023\) and *Drosophila* \(Pease and](#)
366 [Hahn 2013\). Recombination rates evolve fairly rapidly both within \(Kong, et al. 2002; Cox, et al.](#)
367 [2009; Stapley, et al. 2017\) and between mammalian species \(Jensen-Seaman, et al. 2004; Ptak, et](#)
368 [al. 2005; Stevenson, et al. 2016; Stapley, et al. 2017\) due, in part, to the high turnover of hotspots](#)
369 [due to the changing landscape of binding sites for PRDM9 \(Baudat, et al. 2010; Singhal, et al.](#)
370 [2015\). Similar to findings in great apes \(Hobolth, et al. 2007\), our results suggest that high-](#)
371 [resolution genetic maps from a single species provide some weak predictive value for](#)

372 understanding broader patterns of species tree discordance. However, these limited estimates may
373 not be predictive of finer-scale patterns in a sample spanning over 12 million years of mammalian
374 evolution (but see Foley, et al. 2023). Overall, the evolution of recombination landscapes across
375 closely related species remains an important empirical question in evolutionary genetics (Dapper
376 and Payseur 2017), especially as the generation of chromosome-scale genome assemblies
377 continues to greatly outpace estimates of patterns of recombination within those genomes.

378 One source of evolution in the recombination map may be changes in synteny. Our
379 reference-guided analyses assume collinearity between *Mus* and the other lineages we are
380 comparing (*i.e.*, no karyotype variation), at least at the window-based scale we are comparing
381 variation. Structural variation, including substantial variation in chromosome numbers, is likely to
382 be widespread in rodents (Stanyon, et al. 1999; Yalcin, et al. 2011; Romanenko, et al. 2012; Keane,
383 et al. 2014) and has the potential to skew our results when comparing tree similarity between
384 regions of the genome using multiple species. Generating chromosome-scale assemblies for many
385 non-*Mus* and *Rattus* species may prove limiting given that most tissue resources for this group are
386 derived from natural history collections that often lack high molecular weight DNA. Nonetheless,
387 whole genome alignments between mouse and rat indicate high degrees of chromosomal synteny
388 and co-linearity (Fig S6), suggesting that many regions will be colinear in our sample.

389 Natural selection reduces the effective population size (N_e) of genomic regions through
390 genetic hitchhiking of variation linked to the fixation of positively selected mutations (*i.e.*,
391 selective sweeps; Smith and Haigh 1974; Kaplan, et al. 1989) and the purging of deleterious
392 mutations (*i.e.*, background selection; Charlesworth, et al. 1993; Hudson and Kaplan 1995). Thus,
393 variation in parameters dependent on N_e – such as standing levels of nucleotide variation and
394 patterns of incomplete lineage sorting – should be reduced by linkage to functional elements
395 subject to selection. Consistent with this, we observed the lowest rates of local discordance (Fig.
396 Figure 5A) and overall gene tree/species tree discordance (Fig. Figure 5B) near UCEs when
397 compared to all other genomic features we studied. These results suggest that a history of recurrent
398 purifying selection on UCEs (Katzman, et al. 2007) strongly reduces patterns of discordance
399 through a persistent local reduction in N_e . In contrast, protein coding genes showed rates of local
400 discordance that were similar to background levels, even when considering genes rapidly evolving
401 due to positive directional selection (Fig. Figure 5A). However, both classes of genes did show
402 less species tree discordance than background consistent with previous results (Scally, et al. 2012;
403 Rivas-Gonzalez, et al. 2023), but this effect was much weaker than as observed at UCEs (Fig.
404 Figure 5B). Collectively, these data suggest that the frequency and strength of selection plays an
405 important role in structuring patterns of incomplete lineage sorting across the genome over deeper
406 evolutionary timescales.

407 One practical consequence of this is that phylogenetic inferences based on UCE markers
408 would seem less prone to discordance and may provide cleaner estimates of species tree history
409 than randomly chosen or protein-coding regions. Indeed, windows centered on UCEs have a higher
410 degree of similarity to the species tree than other genomic features (*i.e.*, 17% concordance with
411 the species tree, versus 13% genome-wide or 15% for protein-coding genes). However, it is worth

412 noting that UCEs are also more likely to provide a potentially misleading underestimate of
413 genome-wide levels of discordance. Given this relationship, species tree inferences based on UCEs
414 should likely not, for example, be extended to related population genetic parameters of interest
415 (e.g., ancestral population sizes, estimates population genetic diversity), and could mislead the
416 reconstruction of trait evolution across phylogenies (Avise and Robinson 2008; Hahn and Nakhleh
417 2016; Mendes, et al. 2018; Hibbins, et al. 2023). Finally, despite the relative ease of generating
418 UCE data, such markers are likely unsuitable for genetic inferences within populations given the
419 pervasive effects of linked selection.

420

421 *Discordance and Molecular Evolution*

422 We also found that the choice of tree topology drastically affects the results from various common
423 tests for positive selection. Previous studies have used simulations to show that tree
424 misspecification can lead to incorrect placement of substitutions on branches, possibly leading to
425 spurious results for tests of positive directional selection within empirical datasets (Mendes and
426 Hahn 2016). Here, we use empirical data in mice to show that these errors result in false positive
427 (detected signal for selection only when using the gene tree) and false negative results (detected
428 signal for selection only when using the species tree).

429 For each of the three selection tests run, HyPhy's BUSTED and aBSREL and PAML's
430 M1a vs. M2a, some genes showed evidence of positive selection whether the species tree or gene
431 tree was used. In contrast, many other genes had signatures of positive selection restricted only to
432 a single tree. The genes unique to the type of tree used were often discordant with the species tree
433 while the genes that showed evidence of positive selection regardless of the tree used had levels
434 of discordance comparable to all genes (85%, Fig.-Figure 6, numbers in parentheses). This suggests
435 that mis-mapping substitutions by supplying these tests with the wrong tree (*i.e.*, the species tree
436 when gene trees are discordant) can lead to inflated false positive and false negative rates when
437 inferring genes under positive selection. The magnitude and direction of these biases were
438 dependent on the underlying model. So-called branch-site models that allow substitution rates to
439 vary among both branches and codon sites, such as HyPhy's BUSTED and aBSREL models,
440 resulted in more genes inferred with evidence for positive selection when using the inferred gene
441 tree (*i.e.*, the correct tree, assuming no errors in gene tree reconstruction). This means that using a
442 single species tree for these tests reduces the power to detect positive selection. On the other hand,
443 models that only allow rates to vary among sites, such as PAML's M1a vs. M2a test, showed an
444 increase in the number of putative false positives inferred when using the wrong tree. That is, tree
445 mis-specification results in spurious increases in dN/dS that mimics positive directional selection.

446 These results have wide-ranging implications for phylogenetics and comparative genomic
447 analysis. First, it is imperative that when testing a specific locus for positive selection, discordance
448 among loci must be accounted for. This is most easily achieved by simply using the gene tree (or
449 other locus type) as input to the test for selection (Good, et al. 2013; Mendes and Hahn 2016;
450 Roycroft, et al. 2021). However, as Mendes and Hahn (2016) pointed out, this may not completely
451 mask the effects of discordance on substitution rates, as sites within a single gene may still have

452 evolved under different histories because of within-gene recombination. Indeed, we found that tree
453 similarity diminished at scales that were less than the average genomic distance between the
454 beginning and end of a coding sequence in mice (~37 kb in this data set). Nevertheless, starting
455 with an inferred gene tree is advisable whenever possible, followed by a secondary analysis of
456 evidence for within-gene variation in phylogenetic history.

457 Our results also imply that studies of molecular evolution may benefit from approaches that reduce
458 genome-wide levels of discordance, such as through *post hoc* pruning of species that
459 disproportionately contribute to unresolved nodes.

460 Incorporating discordance into a comparative framework is not trivial and many
461 comparative genomic methods assume a single species tree that test for changes in substitution
462 rates in a phylogeny (Pollard, et al. 2010; Hu, et al. 2019; Partha, et al. 2019). Even methods that
463 allow the use of different trees for different loci (like PAML and HyPhy) are still commonly
464 applied with a single species tree across loci (Carbone, et al. 2014; Foote, et al. 2015; van der Valk,
465 et al. 2021; Treaster, et al. 2023). While we used the simplifying assumption that the results from
466 the gene tree are more likely to be correct, this may not always be the case given that errors can
467 also occur during gene tree inference. Still, our results confirm that the use of a single tree for all
468 loci for such tests that rely on accurate estimation of substitution rates are likely to lead to both
469 inaccurate inferences of positive selection. We strongly encourage the use of individual gene trees
470 for such analyses.

471

472 Conclusions

473 Murine rodents as a study system allow us to use the high-quality *M. musculus* genome to examine
474 fine-scale patterns and effects of phylogenetic discordance along chromosomes. Our analysis
475 reveals how discordance varies with genome biology across evolutionary timescales, as well as
476 the limits of inference inherent to extrapolating information from a single model system to a
477 phylogenetic sample. We also demonstrate how phylogenetic discordance can mislead common
478 tests for selection if only a single species tree is used. Overall, our results emphasize that progress
479 in comparative genomics requires a detailed understanding of the heterogeneous biological signals
480 in phylogenomic datasets. Through these results, we can better understand the complexities of
481 phylogenomic datasets and the effects of underlying biological processes on large-scale analyses
482 and ensure that steps are taken to accommodate and study these details.

483

484 Materials & Methods

485 *Sample collection and assembly*

486 We collected genomes from 16 murine species and 2two other rodents from several sources,
487 including NCBI and several recently sequenced in Kumon, et al. (2021) (see Table 4S1 for full list
488 of samples and sources). We also report the sampling genome of *Otomys typus* (FMNH 230007)
489 from Ethiopia in 2015. While DNA extraction and sequencing on the 10x Genomics platform for
490 *O. typus* is the same as described in (Kumon, et al. 2021), the library quality for this sample was

491 too low for chromosome level assembly. Here, we instead assembled it into scaffolds with the
492 express purpose of obtaining UCEs for phylogenetic analysis. Adapters and low-quality bases were
493 trimmed from the reads using illumiprocessor (Faircloth 2013), which makes use of functions from
494 trimmomatic [using the default parameters](#) (Bolger, et al. 2014). All cleaned reads were de novo
495 assembled using ABySS 2.3.1 (Jackman, et al. 2017) with a Bloom filter (Bloom 1970) de Bruijn
496 graph. The final *O. typus* scaffold assembly was 2.14GB (N50=9,211; L50=64,014; E-
497 size=12,790).

498 In parallel, for six of these species (see [Fig. Figure 1](#); [Table 1](#); [Fig. Figure 4S1](#)), we
499 generated reference-based pseudo-assemblies with iterative mapping using an updated version
500 pseudo-it v3.1.1 (Sarver, et al. 2017) that incorporates insertion-deletion variation to minimize
501 reference bias in our genome-wide phylogenetic analyses and to maintain collinearity between
502 assemblies (<https://github.com/goodest-goodlab/pseudo-it>). We used the *Mus musculus* (mm10)
503 genome as the reference for our pseudo-assembly approach. Briefly, pseudo-it maps reads from
504 each sample to the reference genome with BWA (Li 2013), calls variants with GATK
505 HaplotypeCaller (Poplin, et al. 2018), and filters SNPs and indels and generates a consensus
506 assembly with bcftools (Danecek, et al. 2021). The process is repeated, each time using the
507 previous iteration's consensus assembly as the new reference genome to which reads are mapped.
508 In total, we did three iterations of mapping for each sample.

509

510 *Ultraconserved element (UCE) retrieval and alignment*

511 ~~ToWe first set out to~~ reconstruct a ~~broad~~ phylogeny of [sequenced](#) murine rodents, ~~we to provide~~
512 ~~both a useful resource for future comparative genomic studies within this important group as well~~
513 ~~as a time-calibrated phylogeny to frame an in-depth analysis of phylogenetic discordance across a~~
514 ~~subset of murine whole genomes (see below)~~. We combined our seven recently sequenced
515 genomes with nine publicly available ~~genomes from other Old World mice and rats (subfamily~~
516 ~~Murinae) murine genomes~~ as well as the genomes of two non-murine rodents, the great gerbil
517 (*Rhombomys opimus*; (Nilsson, et al. 2020) and the Siberian hamster (*Phodopus sungorus*; (Moore,
518 et al. 2022) as outgroups. We extracted UCEs from each species, plus 1000 flanking bases from
519 each side of the element using the protocols for harvesting loci from genomes and the *M. musculus*
520 UCE probe set provided with phyluce v1.7.1 (Faircloth, et al. 2012; Faircloth 2016). In total, we
521 recovered 2,632 unique UCE loci, though not all UCE loci were found in all taxa ([Table 4S1](#)).

522 We brought the extracted UCE sequences for each species into a consistent orientation
523 using MAFFT v7 (Katoh and Standley 2013) and then aligned them using FSA (Bradley, et al.
524 2009) with the default settings. We trimmed UCE alignments with TrimAl (Capella-Gutierrez, et
525 al. 2009) with a gap threshold of 0.5 and otherwise default parameters. We performed alignment
526 quality checks using AMAS (Borowiec 2016). We processed all alignments in parallel with GNU
527 Parallel (Tange 2018).

528

529 *Species tree reconstruction from UCEs*

530 We constructed a species-level rodent phylogeny with two approaches. First, using the alignments
531 of all UCEs found in four or more taxa (2,632), we reconstructed a maximum-likelihood (ML)
532 species tree with IQ-TREE v2.2.1 (Minh, Schmidt, et al. 2020). Each UCE alignment was
533 concatenated and partitioned (Chernomor, et al. 2016) such that optimal substitution models were
534 inferred for individual UCE loci with ModelFinder (Kalyaanamoorthy, et al. 2017). We also
535 reconstructed individual gene trees for each UCE alignment. For all IQ-TREE runs (concatenated
536 or individual loci), we assessed branch support with ultrafast bootstrap approximation (UFBoot)
537 (Hoang, et al. 2018) and the corrected approximate likelihood ratio test (SH-aLRT) (Guindon, et
538 al. 2010). We collapsed branches in each UCE tree exhibiting less than 10% approximated
539 bootstrap support using the nw_ed function from Newick Utilities (Junier and Zdobnov 2010). We
540 used these trees as input to the quartet summary method ASTRAL-III v5.7.8 (Zhang, et al. 2018)
541 to infer a species tree. We generated visualizations of phylogenies with R v4.1.1 (R Core Team
542 2021) using phytools v1.9-16 (Revell 2012) and the ggtree package v3.14 (Yu, et al. 2017; Yu
543 2020) and its imported functions from ape v5.0 (Paradis and Schliep 2019) and treeio v1.16.2
544 (Wang, et al. 2020).

545 We then used two methods to assess phylogenetic discordance across the reconstructed
546 species tree. First, we calculated site and gene concordance factors (sCF and gCF) with IQ-TREE
547 2 (Minh, Hahn, et al. 2020; Minh, Schmidt, et al. 2020) to assess levels of phylogenetic discordance
548 between the inferred UCE trees and the concatenated species tree. gCF is calculated for each
549 branch in the species tree as the proportion of UCE trees in which that branch also appears (Baum
550 2007). sCF represents the proportion of alignment sites concordant with a given species tree branch
551 in a randomized subset of quartets of taxa (Minh, Hahn, et al. 2020).[\(Minh, Hahn, et al. 2020\)](#). We
552 visualized gCF and sCF (Lanfear 2018) for each branch in each species tree using methods in R
553 v4.3.0 (Lanfear 2018; R Core Team 2021). Next, we used PhyParts (Smith, Moore, et al. 2015) to
554 identify topological conflict between the UCE trees and the species tree from ASTRAL-III. For
555 this analysis, we rooted all trees with *Phodopus sungorus* as the outgroup using the nw_reroot
556 function in the Newick Utilities (Junier and Zdobnov 2010) package and excluded 204 UCE trees
557 that did not contain the outgroup.

558

559 *Divergence time estimation*

560 We used IQ-TREE 2's (Minh, Schmidt, et al. 2020) implementation of least square dating to
561 estimate branch lengths of our species trees in units of absolute time (To, et al. 2016).[To improve](#)
~~562 divergence time estimation, we used SortaDate (Smith, et al. 2018) to identify a set of 100 UCE~~
~~563 loci that exhibit highly clocklike behavior and minimized topological conflict with the~~
~~564 concatenated species tree. We applied node age calibrations (Table 2) from Schenk et al. (2013)~~
~~565 and Steppan and Schenk (2017), which in turn were sourced from fossil calibrations described on~~
~~566 Paleobiology Database (2011). As *Rattus* is paraphyletic, the maximum age is taken from the~~
~~567 earliest crown group fossil on Paleobiology Database (2011). In contrast, the estimated *Rattus*~~
~~568 node age from Schenk et al (2013) was used as the minimum age. Branch lengths were resampled~~
~~569 100 times to produce confidence intervals. To return a single solution, least square dating typically~~

570 requires that one calibration be fixed and not a range. We selected one calibration node (here, the
571 branch leading to Murinae) and estimated dates across the tree when this node is set to its
572 minimum, its maximum, and its midpoint ages. On the midpoint calibrated tree, we plot confidence
573 intervals for each node representing the lowest minimum and highest maximum ages estimated
574 across the three dating analyses. To improve divergence-time estimation, we used SortaDate
575 (Smith, et al. 2018) to identify a set of 100 UCE loci that exhibit highly clocklike behavior and
576 minimized topological conflict with the concatenated species tree. We applied four node age
577 calibrations (Table S3) as described in Kimura, et al. (2015) and Aghova, et al. (2018). The origin
578 of core Murinae (Node E) was constrained to between 11.1 and 12.3 Ma, following Kimura, et al.
579 (2015). Maximum ages were set for Otomyini+Arvicanthini (9.2 Ma, Kimura, et al. 2015),
580 *Apodemus* (9.6 Ma, Daxner-Höck 2002), and *Mus* (8.0 Ma, Kimura, et al. 2013). Branch lengths
581 were resampled 100 times to produce confidence intervals.

582

583 *Genome window-based phylogenetic analysis*

584 For the second part of our work, we wanted to quantitatively infer phylogenetic discordance across
585 a subset of the murine genomes used to infer the species tree and relate that discordance to other
586 features of the genome, such as recombination rate, proximity to genes, and rates of molecular
587 evolution. To assess the distribution of phylogenetic discordance across the rodent
588 genomegenomes, we limited subsequent analyses to *M. musculus* and the pseudo-assemblies (see
589 above) of six of the genomes (*Mastomys natalensis*, *Hylomyscus allenii*, *Praomys delectorum*,
590 *Rhabdomys dilectus*, *Grammomys dolichurus*, and *Rhynchomys soricoides*). *Otomys typus* was
591 excluded from these analyses due to the inadequacy of the library outlined above.

592 We partitioned these genomes into 10 kilobase (kb) windows based on the coordinates in
593 the reference *M. musculus* genome (mm10; Mouse Genome Sequencing, et al. 2002) using
594 bedtools makewindows (Quinlan and Hall 2010). These coordinates were converted between the
595 reference and the consensus sequence for each genome using liftOver (Hinrichs, et al. 2006). Note
596 that this method assumes both collinearity of all genomes and similar karyotypes (see Discussion).
597 We then removed windows from the subsequent analyses if (1) 50% or more of the window
598 overlapped with repeat regions from the *M. musculus* reference RepeatMasker (Smit, et al. 2013-
599 2015) file downloaded from the UCSC Genome Browser's table browser (Hinrichs, et al. 2006)
600 or (2) 50% or more of the window contained missing data in 3three or more samples. Overlaps
601 with repeat regions were determined with bedtools coverage (Quinlan and Hall 2010). We then
602 aligned the 10kb windows with MAFFT (Katoh and Standley 2013), trimmed alignments with
603 trimAl (Capella-Gutierrez, et al. 2009), and inferred phylogenies for each with IQ-TREE 2 (Minh,
604 Schmidt, et al. 2020) which uses ModelFinder to determine the best substitution model for each
605 window (Kalyaanamoorthy, et al. 2017).

606 To assess patterns of tree similarity between windows on the same chromosome, we used
607 the weighted Robinson-Foulds (wRF) (Robinson and Foulds 1981; Böcker, et al. 2013) distance
608 measure implemented in the phangorn library (Schliep 2011) in R (R Core Team 2021), which
609 compares two trees by finding clades or splits present in one tree but not the other weighted by the

missing branch length in each tree for each mismatch and differences in branch length between the co-occurring branches in both trees (Robinson and Foulds 1979). Consequently, the resulting measure of wRF is in units of branch length (i.e., expected number of substitutions per site for maximum likelihood trees). We compared wRF between trees from windows on the same chromosome to characterize (1) heterogeneity in patterns discordance along the chromosome and (2) whether tree similarity is correlated with distance between windows. For the second question, we sampled every window on a chromosome at increasing distance (in 10kb windows) until the distribution of wRF scores for all pairs of windows at that distance was not significantly different (Wilcox test, $p > 0.01$) than that of a sample of 12,000 measures of wRF between randomly selected trees on different chromosomes. We selected 12,000 as the random sample size because it roughly matched the number of windows on the largest chromosome (chromosome 1, $n = 12,113$). We used Snakemake 7 (Mölder, et al. 2021) to compute window alignments and trees in parallel.

623

624 *Whole genome alignment between mouse and rat*

625

626 To assess how un-accounted for large-scale structural variation may impact our conclusions, we
627 compared the reference mouse and rat genomes. We used minimap2 (Li 2018) to align the mouse
628 (mm10) and rat (rnor6) (Gibbs, et al. 2004) genomes to assess the impact of structural variation
629 that spans the divergence of our subset of species used to-in the discordance analyses. We
630 downloaded the rat reference genome (rnor6) from the UCSC genome browser and for both
631 genomes removed the Y chromosome and all smaller unplaced scaffolds. We then used minimap2
632 in whole genome alignment mode (-x asm20) to generate a pairwise alignment file from which we
633 calculated alignment segment sizes and the distances between alignment segments. We visualized
634 the alignment as a dot plot using the pafr package in R (<https://github.com/dwinter/pafr>).

635

636 *Recombination rate and functional annotation*

637 We retrieved 10,205 genetic markers generated from a large heterogenous stock of outbred mice
638 (Shifman, et al. 2006; Cox, et al. 2009) to assess whether phylogenetic discordance along
639 chromosomes was correlated with mouse recombination rates. We converted the physical
640 coordinates of these markers from build 37 (mm9) to build 38 (mm10) of the *M. musculus* genome
641 using liftOver (Hinrichs, et al. 2006). We then partitioned the markers into 5Mb windows and
642 estimated local recombination rates defined as the slope of the correlation between the location on
643 the *M. musculus* genetic and physical maps for all markers in the window (White, et al. 2009;
644 Kartje, et al. 2020). Within each 5Mb window, we calculated wRF distances between the first 10kb
645 window and every other 10kb window.

646 We also compared the chromosome-wide wRF distances to those based on phylogenies
647 from regions around several types of adjacent to genomic features. We retrieved coordinates from
648 25,753 protein coding genes annotated in *M. musculus* from Ensembl (release 99; Cunningham, et
649 al. 2022), all 3,129 UCEs from the *M. musculus* UCE probe set provided with PHYLUCE

|650 (Faircloth, et al. 2012; Faircloth 2016), and 9,865 recombination hotspots from Smagulova, et al.
|651 (2011). The recombination hotspot coordinates were converted between build 37 and build 38
|652 using the liftOver tool (Hinrichs, et al. 2006). For each feature, the starting window was the 10kb
|653 window containing the feature's midpoint coordinate. We then calculated wRF between this
|654 window and all windows within 5Mb in either direction and for each chromosome compared the
|655 slope and wRF distance of windows adjacent to the feature with the same metrics for the whole
|656 chromosome. We compared distributions of these measures for each genomic feature with an
|657 ANOVA (`aov(feature.measure ~ feature.label)`) followed by Tukey's range test
|658 (`TukeyHSD(anova.result)`) to assess differences in means, as implemented in R v4.1.1 (R Core
|659 Team 2021).

660 *Molecular evolution*

661 To test how tree misspecification affects common model-based analyses of molecular evolution,
662 we retrieved 22,261 coding sequences from *M. musculus* using the longest coding transcript of
663 each gene. Coding coordinates from the *M. musculus* coding sequences were transposed to the new
664 assemblies via liftOver (Hinrichs, et al. 2006) and sequences retrieved with bedtools getfasta
665 (Quinlan and Hall 2010). We recovered 17,216 genes that were present in all 7seven species. Using
666 MACSE (Ranwez, et al. 2018), we trimmed non-homologous regions from each ortholog using
667 trimNonHomologousFragments, aligned the orthologs using alignSequences, and trimmed the
668 aligned sequences with trimAlignment to remove unaligned flanking regions. Finally, we manually
669 filtered the alignments using the following (non-mutually exclusive) criteria: 3,368 alignments
670 were removed during filtering for gapped sites, 3,132 alignments had a premature stop codon in at
|671 least one species, 1,571 alignments had only 3three or fewer unique sequences among the 7seven
672 species, and 78 alignments were shorter than 100 bp. After filtering, 12,559 total alignments for
673 tree reconstruction and inference of selection.

674 We then used IQ-TREE 2 (Minh, Schmidt, et al. 2020) to reconstruct a single species tree
675 from concatenation of all gene alignments, as well as gene-trees for each individual alignment.
676 This species tree from coding regions matches the topologies of these species inferred by
677 concatenation of UCEs in the previous section. Next we ran several tests that use both coding
678 alignments and a tree to infer positive selection: PAML's M1a vs. M2a test (Yang 2007), HyPhy's
|679 aBSREL model (Smith, Wertheim, et al. 2015), and HyPhy's BUSTED model (Murrell, et al.
680 2015). We ran each test twice on each gene, once using the species tree derived from concatenated
681 data, and once using the tree estimated for that gene. For the HyPhy models, no target branch was
682 selected, meaning all branches in the input phylogeny were tested.

|683 The end point of each of these three tests is a p-value, which lets us assess whether
684 a model that allows for positively selected sites fits better than a model that does not. For M1a vs.
685 M2a, we obtained the p-value manually by first performing a likelihood ratio test to determine
686 genes under selection by calculating $2 * (lnl\ M1a - lnl\ M2a)$. The p-value of this likelihood
|687 ratio is then retrieved from a one-tailed chi-square distribution with 2two degrees of freedom
688 (Yang 2007). For BUSTED and aBSREL, p-values are computed automatically during the test

689 using similar likelihood ratios. For the M1a vs. M2a and BUSTED tests, a single p-value is
690 computed for each gene. P-values were adjusted by correcting for false discovery rates (Benjamini
691 and Hochberg 1995; Yekutieli and Benjamini 1999) using the “fdr” method in the p.adjust()
692 function in R (R Core Team 2021) and we categorized a gene as being positively selected if its
693 adjusted p-value was < 0.01. For the aBSREL test, a p-value is generated for each branch in the
694 input gene tree. aBSREL corrects for multiple testing internally across branches using the Holm-
695 Bonferroni procedure (Holm 1979; Pond, et al. 2005). We further correct the p-values across genes
696 with the Bonferroni method and classify a gene as having experienced positive selection if one or
697 more branches has a p-value < 0.01 after all corrections. We used Snakemake 7 (Mölder, et al.
698 2021) to compute coding alignments, trees, and selection tests in parallel.

699

700 Data availability

701 For the six previously assembled genomes (see Table S1), all raw reads and assemblies are
702 available as an NCBI BioProject (Accession Number PRJNA669840). The reads and assembly
703 for *Otomys typus*, pseudo-assemblies for the six other new samples, and locus alignments
704 (UCEs, genes, and genomic windows) are available on Dryad
705 (<https://doi.org/10.5061/dryad.866t1g1wq>). All code and summary data for this project are
706 deposited on github (<https://github.com/gwct/murine-discordance>).

707

708

709 Acknowledgments

710 We thank Jake Esselstyn and Kevin Rowe for helpful comments and discussion on the
711 murine species tree and Matt Hahn and the Hahn lab for feedback on the manuscript. We also
712 thank Brant Faircloth and Trevor Sless for advice on using phyluce. We are grateful for tissue
713 samples provided by Chris Conroy at the Museum of Vertebrate Zoology, Berkeley, CA (MVZ)
714 and Adam Ferguson at the Field Museum of Natural History, Chicago, IL (FMNH), and to the
715 original collectors. This work was supported by the National Science Foundation (DEB-1754096
716 to J.M.G), the Eunice Kennedy Shriver National Institute of Child Health and Human
717 Development of the National Institutes of Health (R01-HD094787 to J.M.G.). J.J.H. received
718 financial support from the Cornell Center for Vertebrate Genomics. J.-S.-B. was supported by the
719 University of Michigan Life Sciences Fellows Program and the Jean Wright Cohn Endowment
720 Fund at the University of Michigan Museum of Zoology. Computations for species tree
721 reconstruction were performed using the computer clusters and data storage resources of the
722 University of California Riverside HPCC, which were funded by grants from NSF (MRI-2215705,
723 MRI-1429826) and NIH (1S10OD016290-01A1), and the Cornell University Biotechnology
724 Resource Center BioHPC (RRID:SCR_021757) with help from Qi Sun. Bioinformatic analyses
725 for genomic discordance and selection tests were conducted using the University of Montana Griz
726 Shared Computing Cluster supported by grants from the NSF (CC-2018112 and OAC-1925267,

727 J.M.G. co-PI). Any opinions, findings, and conclusions or recommendations expressed in this
728 material are those of the authors and do not necessarily reflect the views of the NSF or the NIH.

729

For Peer Review

730 **Tables**

731 **Table 1:** All taxa whose genomes were included in this study, the source of the assembly, and
 732 the assembly level of each genome. For the six samples used in the genome-wide discordance
 733 analyses (column 5, except for mm10), we also generated reference-based pseudo-assemblies
 734 using the mouse genome (mm10) as the reference.

Taxon	Assembly source	Assembly level	No. UCEs	Used in genome-wide discordance analyses
<i>Apodemus speciosus</i>	GenBank: GCA_002335545.1	Scaffolds	2336	
<i>Apodemus sylvaticus</i>	GenBank: GCA_001305905.1	Scaffolds	2510	
<i>Arvicathis niloticus</i>	GenBank: GCA_011762505.1	Chromosomes	2563	
<i>Grammomys dolichurus</i>	Kumon et al., 2021: <i>de novo</i> assembled	Chromosomes	2395	*
<i>Hylomyscus allenii</i>	Kumon et al., 2021: <i>de novo</i> assembled	Chromosomes	2392	*
<i>Mastomys natalensis</i>	Kumon et al., 2021: <i>de novo</i> assembled	Chromosomes	2483	*
<i>Mus caroli</i>	GenBank: GCA_900094665.2	Chromosomes	2584	
<i>Mus musculus</i>	GenBank: GRCm38.p6/mm10	Chromosomes	2294	*
<i>Mus pahari</i>	GenBank: GCA_900095145.2	Chromosomes	2556	
<i>Mus spretus</i>	GenBank: GCA_001624865.1	Chromosomes	2578	
<i>Otomys typus</i>	This study: <i>de novo</i> assembled	Scaffolds	2627	
<i>Phodopus sungorus</i>	Moore et al., 2022: <i>de novo</i> assembled	Chromosomes	2633	
<i>Praomys delectorum</i>	Kumon et al., 2021: <i>de novo</i> assembled	Chromosomes	2549	*
<i>Rattus norvegicus</i>	GenBank: GCA_015227675.2	Chromosomes	2425	
<i>Rattus rattus</i>	GenBank: GCA_011064425.1	Chromosomes	2443	
<i>Rhabdomys dilectus</i>	Kumon et al., 2021: <i>de novo</i> assembled	Chromosomes	2546	*
<i>Rhombomys opimus</i>	GenBank: GCA_010120015.1	Scaffolds	2627	
<i>Rhynchosomys soricoides</i>	Kumon et al., 2021: <i>de novo</i> assembled	Chromosomes	2570	*

735

736

737

738

739 **Table 2: Prior node ages used in phylogenetic dating in millions of years before present.**

Clade	Minimum Age	Maximum Age	Citation
<i>Mus</i>	5.3	7.2	Steppan and Schenk, 2017
<i>Apodemus</i>	5.3	7.2	Schenk et al., 2013
<i>Rattus</i>	2.4	3.6	Steppan and Schenk, 2017
<i>Murinae</i>	12.1	14.05	Schenk et al., 2013

740

741 **Table 3: The most frequently recovered topologies across all 10kb windows. RS = *Rhyneomys***
742 ***soricoides*, GD = *Grammomys dolichurus*, RD = *Rhabdomys dilectus*, MM = *Mus musculus*,**
743 **HA = *Hylomyscus allenii*, MN = *Mastomys natalensis*, PD = *Praomys delectorum*.**

Rank	Topology	# of windows	Proportion of windows
1	(RS,((GD,RD),(MM,((HA,MN),PD))));	23864	0.146
2	(RS,((GD,RD),(MM,((HA,PD),MN))));	23836	0.146
3*	(RS,((GD,RD),(MM,(HA,(MN,PD)))));	21509	0.131
4	(RS,(MM,((GD,RD),((HA,MN),PD))));	14417	0.088
5	(RS,(MM,((GD,RD),((HA,PD),MN))));	14321	0.0874
6	(RS,(MM,((GD,RD),(HA,(MN,PD)))));	14044	0.0858
7	(RS,(((HA,PD),MN),(MM,(GD,RD))));	11723	0.0716
8	(RS,(((HA,MN),PD),(MM,(GD,RD))));	11308	0.0691

744 *The topology recovered from concatenation of genes or UCEs

745 **Table 4: Summaries of phylogenies per chromosome.**

Chromosome	# of unique topologies recovered
1	184
2	123
3	114
4	144
5	134
6	172
7	218
8	133
9	116
10	110
11	93
12	179
13	186
14	173

15	96
16	94
17	188
18	75
19	82
X	207

746

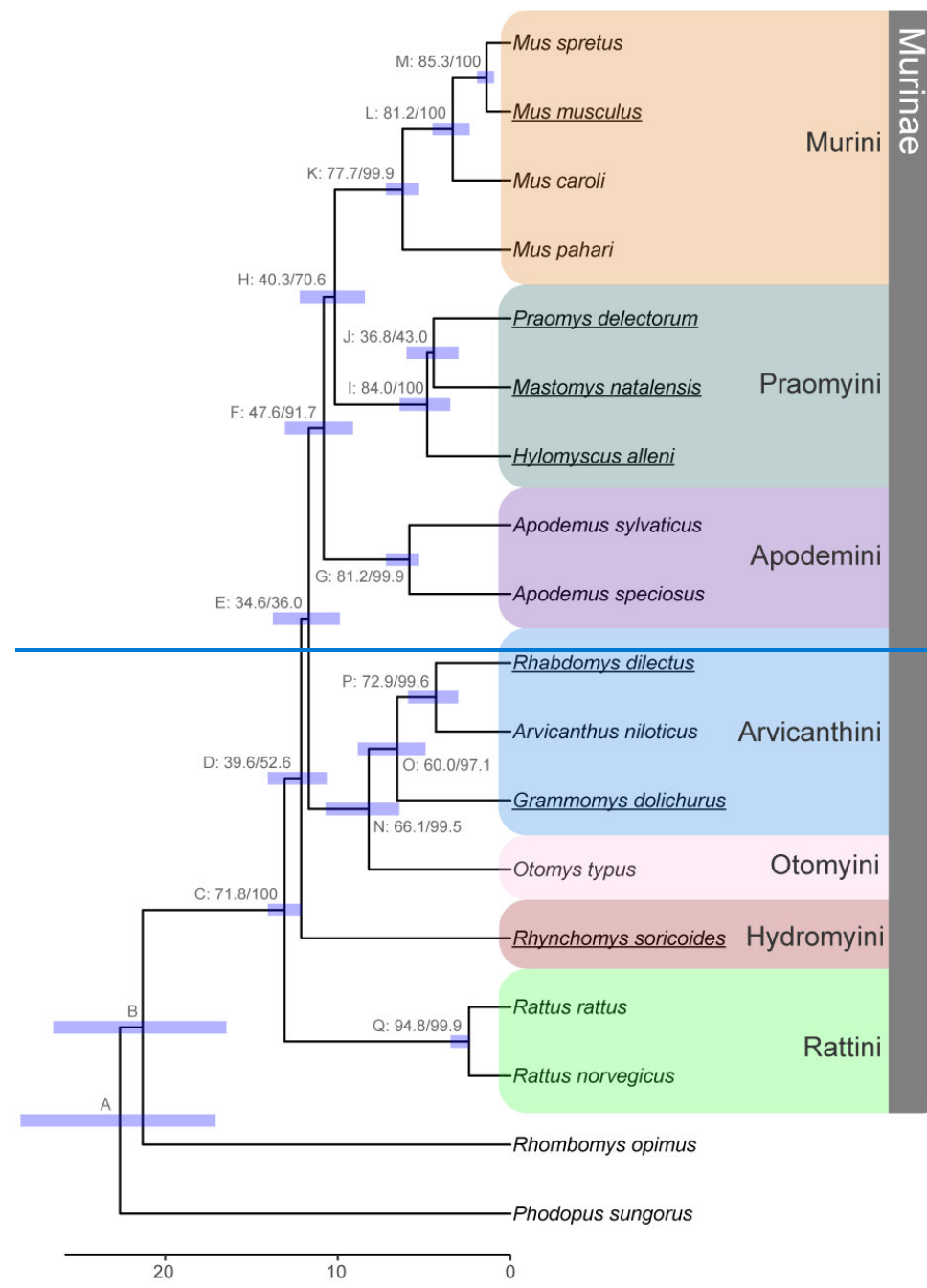
747 **Table 5.: Table 1.** Rates and types of error when using concatenated a single species trees for
748 gene-based selection tests. (Assuming the gene tree topology is the correct topology).

Test	False positive rate	False negative rate
BUSTED	0.45%	28.10%
aBSREL	0.41%	10.60%
M1a vs. M2a	2.66%	3.20%

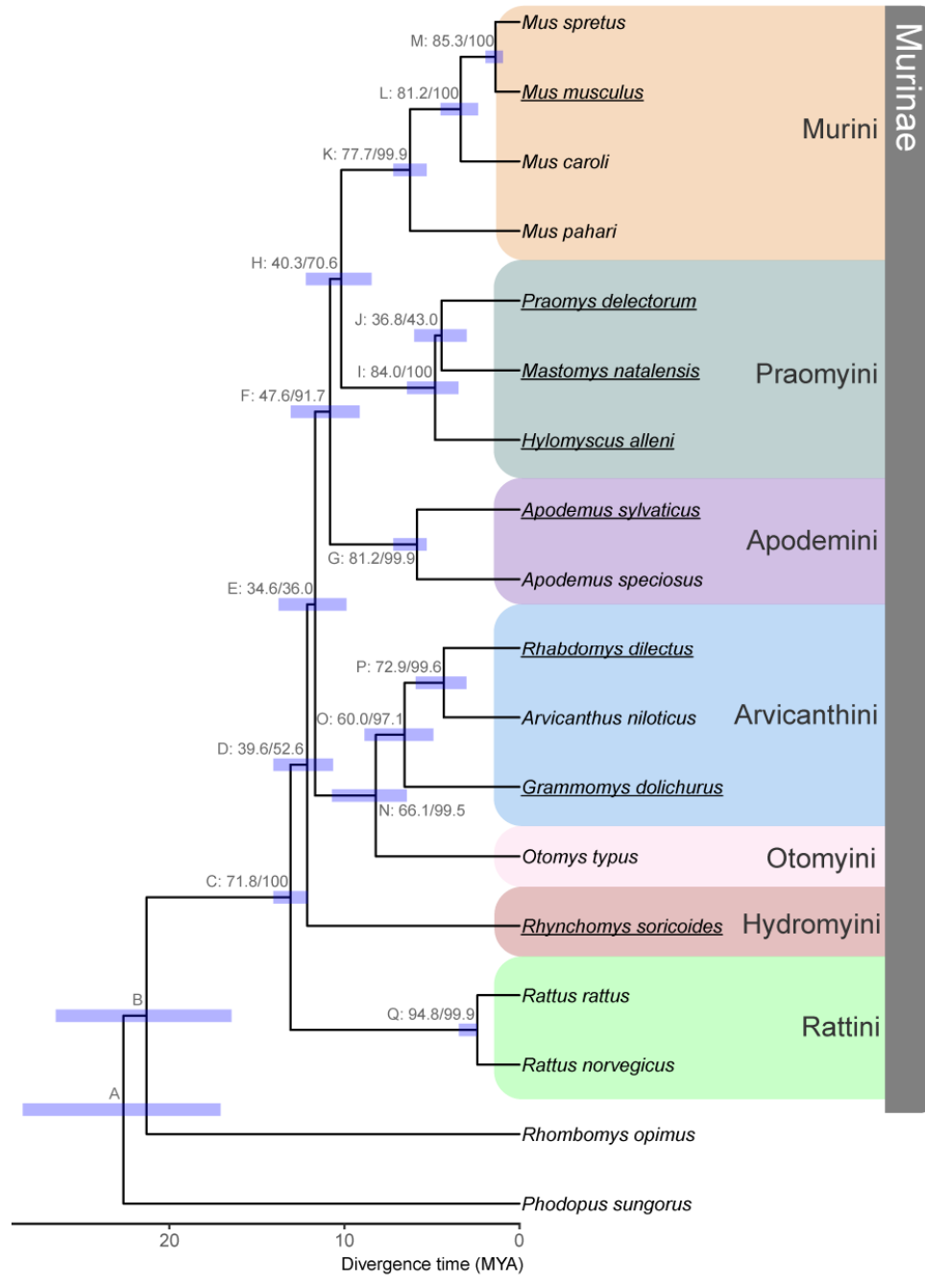
749

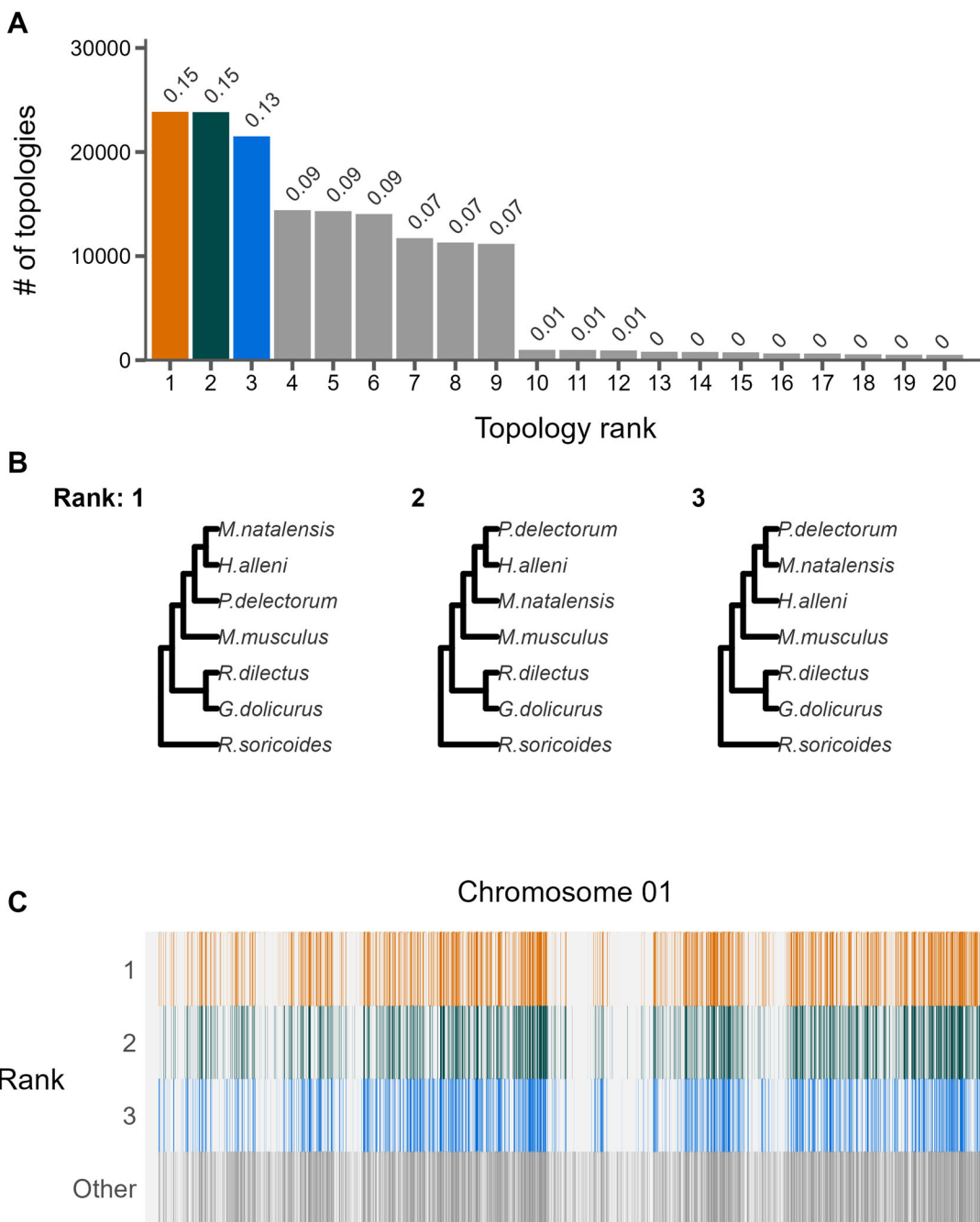
750

751

752 **Figures**753 **Figure 1**

754



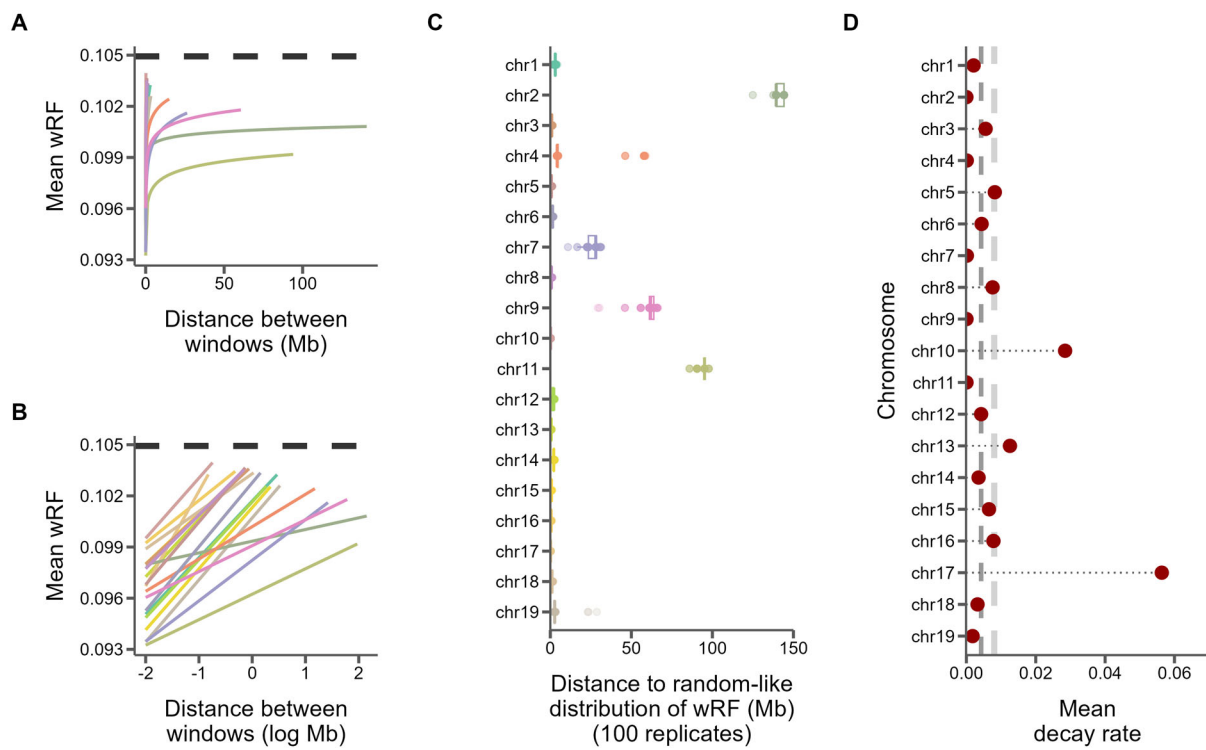
764 **Figure 2**

765

|766 **Figure 2**: The landscape and profile of phylogenetic discordance across non-overlapping 10kb
767 windows in murine genomes. A) Distribution of the 20 most frequent topologies recovered across
768 all windows. Numbers above bars indicate proportion of each topology. B) The top three
769 topologies recovered across all chromosomes 1. C) Distribution of the topologies recovered along

770 chromosome 1. The x-axis is scaled to the length of the chromosome and each vertical bar
771 represents one 10kb window. The three most frequent topologies occupy the first three rows while
772 all other topologies are shown in the bottom row. See Supplemental File S1 for individual
773 chromosome plots.

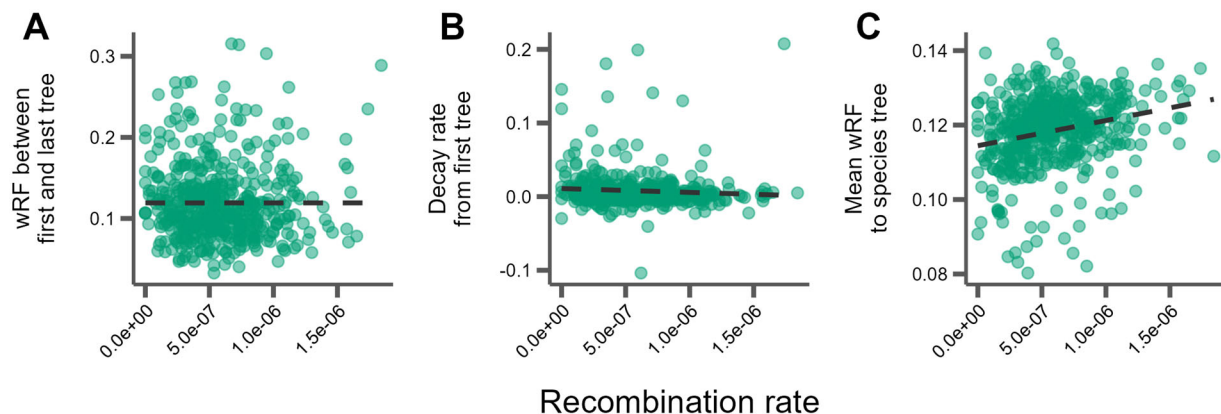
For Peer Review

774 **Figure 3**

775

776 **Figure 3**. Similarity between 10kb windows decays as genomic distance between windows
 777 increases. A) The log fit to the mean of distributions of weighted Robinson-Foulds distances
 778 between trees of windows at increasing genomic distance (10kb steps). Each line represents one
 779 chromosome. B) The same, but on a log scale with a linear fit. C) For every window on each
 780 chromosome, the genomic distance between windows at which tree distance becomes random for
 781 100 replicates of random window selection. D) The Points represent the slopes of the correlation
 782 between genomic distance and tree distance (lines from panel B represent), which is the rate at
 783 which tree similarity decays across the genome. Dark grey dashed line is median slope and light
 784 grey dashed line is mean.

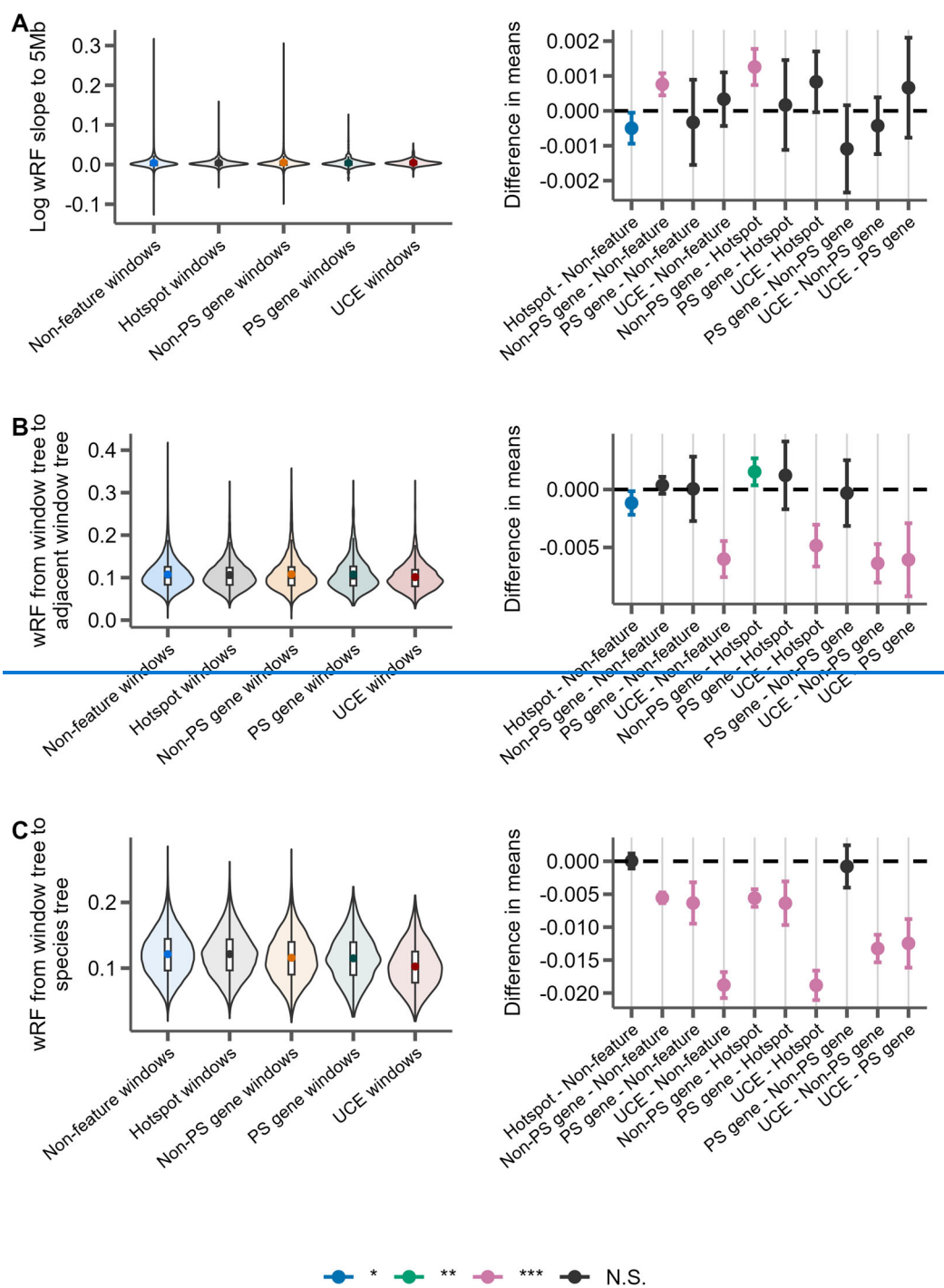
785

786 **Figure 4**

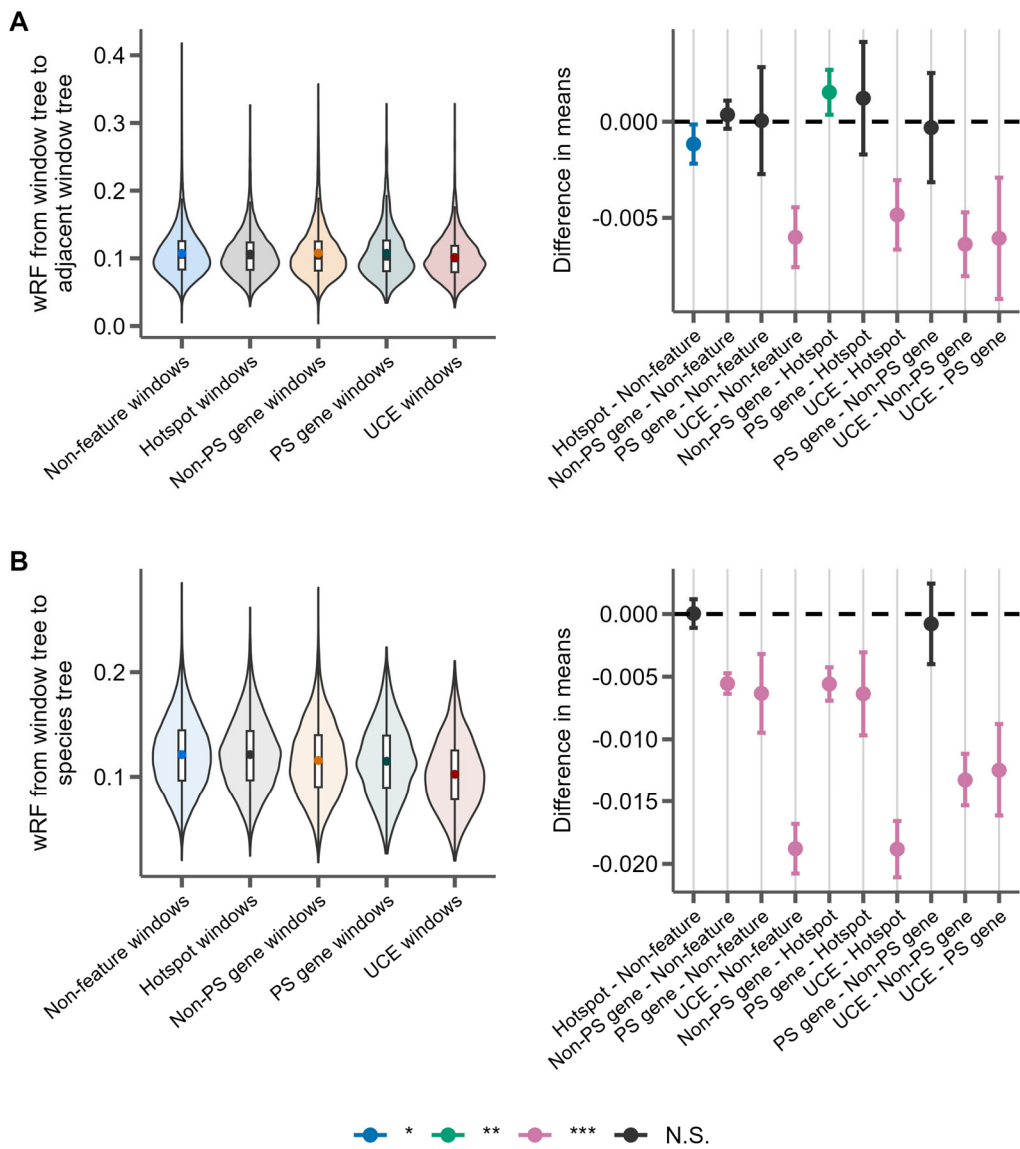
787

788 **Figure 4:** Correlations between tree similarity and recombination rate in 5Mb windows. A)
 789 Tree similarity as measured by the weighted Robinson-Foulds distance between the first and last
 790 10kb10 kb windows within the 5Mb window. B) The slopes of the linear correlation between
 791 the weighted Robinson-Foulds distances between the first 10kb10 kb window and every other
 792 10kb10 kb window within a 5Mb window represent the rate at which tree similarity decays
 793 over each 5Mb window. C) The mean wRF of all 10kb10 kb window trees within each 5Mb
 794 window compared to the species tree.

795

796 **Figure 5**

797



798

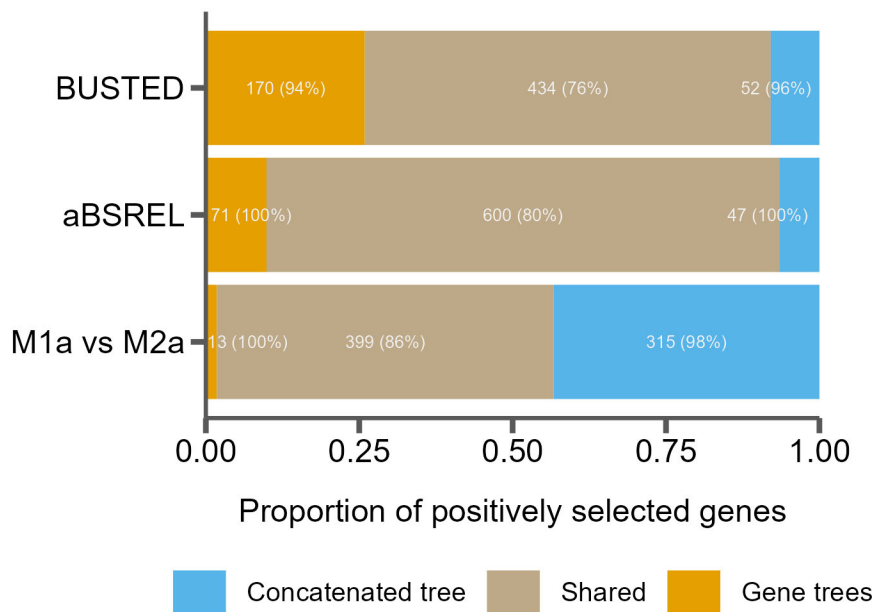
799 **Figure 5:** Distributions of weighted Robinson-Foulds distance from 10kb
800 windows either centered on recombination hotspots (Hotspot), protein-coding genes without
801 evidence for positive selection (Non-PS genes), protein coding genes with evidence for positive
802 selection (PS genes), UCEs, or containing none of these features (Non-feature). For each panel,
803 the left portion shows the distributions of the measure for each feature type and the right panel
804 shows the differences in means for each pairwise comparison of features with significance assessed
805 with Tukey's range test. The labels on the x-axis indicate the feature pairs being compared, with
806 the first feature being the reference (*i.e.* points above 0 indicate this feature has a higher mean). *P*-
807 value thresholds: * < 0.05, ** < 0.01, *** < 0.001. A) The rate of decay of phylogenetic similarity
808 is calculated as the slope of a linear regression between wRF and the log distance between each
809 window up to 5Mb away from the feature window. BA) The phylogenetic similarity of windows

|810 immediately adjacent to feature windows. **EB**) The phylogenetic similarity between the species
811 tree inferred from protein-coding gene trees and the feature window.

812

For Peer Review

813 **Figure 6**



814

|815 **Figure 6**: Tree misspecification leads to erroneous results in tests for positive selection. The
816 proportion of genes inferred to be under positive selection for three tests using either a single
817 species tree (concatenated tree) or individual gene trees, as well as those found in both cases
818 (shared). Numbers in the bars indicate raw counts, and percentages indicate the percent of genes
819 in that category that are discordant from the species tree.

820

821

822

823 **References**

- 824 PDB (The Paleobiology Database) [Internet]. 2011 January 21st, 2022]. Available from:
825 <http://paleodb.org/>
- 826
- 827 Aghova T, Kimura Y, Bryja J, Dobigny G, Granjon L, Kergoat GJ. 2018. Fossils know it best:
828 Using a new set of fossil calibrations to improve the temporal phylogenetic framework of murid
829 rodents (Rodentia: Muridae). *Mol Phylogenet Evol* 128:98-111.
- 830
- 831 Alda F, Ludt WB, Elias DJ, McMahan CD, Chakrabarty P. 2021. Comparing Ultraconserved
832 Elements and Exons for Phylogenomic Analyses of Middle American Cichlids: When Data Agree
833 to Disagree. *Genome Biol Evol* 13:evab161.
- 834
- 835 Alexander AM, Su YC, Oliveros CH, Olson KV, Travers SL, Brown RM. 2017. Genomic data
836 reveals potential for hybridization, introgression, and incomplete lineage sorting to confound
837 phylogenetic relationships in an adaptive radiation of narrow-mouth frogs. *Evolution* 71:475-488.
- 838
- 839 Avise JC, Robinson TJ. 2008. Hemiplasy: a new term in the lexicon of phylogenetics. *Syst Biol*
840 57:503-507.
- 841
- 842 Baudat F, Buard J, Grey C, Fledel-Alon A, Ober C, Przeworski M, Coop G, de Massy B. 2010.
843 PRDM9 is a major determinant of meiotic recombination hotspots in humans and mice. *Science*
844 327:836-840.
- 845
- 846 Baum DA. 2007. Concordance trees, concordance factors, and the exploration of reticulate
847 genealogy. *TAXON* 56:417-426.
- 848
- 849 Benjamini Y, Hochberg Y. 1995. Controlling the false discovery rate: a practical and powerful
850 approach to multiple testing. *Journal of the Royal statistical society: series B (Methodological)*
851 57:289-300.
- 852
- 853 Bloom BH. 1970. Space/time trade-offs in hash coding with allowable errors. *Commun. ACM*
854 13:422–426.
- 855
- 856 Böcker S, Canzar S, Gunnar WK. 2013. The Generalized Robinson-Foulds Metric. In: Darling A,
857 Stoye J, editors. *Algorithms in Bioinformatics*. Berlin, Heidelberg: Springer.
- 858
- 859 Bolger AM, Lohse M, Usadel B. 2014. Trimmomatic: a flexible trimmer for Illumina sequence
860 data. *Bioinformatics* 30:2114-2120.

- 861
862 Borowiec ML. 2016. AMAS: a fast tool for alignment manipulation and computing of summary
863 statistics. PeerJ 4:e1660.
- 864
865 Bradley RK, Roberts A, Smoot M, Juvekar S, Do J, Dewey C, Holmes I, Pachter L. 2009. Fast
866 statistical alignment. PLoS Comput Biol 5:e1000392.
- 867
868 Capella-Gutierrez S, Silla-Martinez JM, Gabaldon T. 2009. trimAl: a tool for automated alignment
869 trimming in large-scale phylogenetic analyses. Bioinformatics 25:1972-1973.
- 870
871 Carbone L, Harris RA, Gnerre S, Veeramah KR, Lorente-Galdos B, Huddleston J, Meyer TJ,
872 Herrero J, Roos C, Aken B, et al. 2014. Gibbon genome and the fast karyotype evolution of small
873 apes. Nature 513:195-201.
- 874
875 Chan KO, Hutter CR, Wood PL, Jr., Grismer LL, Brown RM. 2020. Target-capture phylogenomics
876 provide insights on gene and species tree discordances in Old World treefrogs (Anura:
877 Rhacophoridae). Proc Biol Sci 287:20202102.
- 878
879 Charlesworth B, Morgan MT, Charlesworth D. 1993. The effect of deleterious mutations on
880 neutral molecular variation. Genetics 134:1289-1303.
- 881
882 Chernomor O, von Haeseler A, Minh BQ. 2016. Terrace Aware Data Structure for Phylogenomic
883 Inference from Supermatrices. Syst Biol 65:997-1008.
- 884
885 Christmas MJ, Kaplow IM, Genereux DP, Dong MX, Hughes GM, Li X, Sullivan PF, Hindle AG,
886 Andrews G, Armstrong JC, et al. 2023. Evolutionary constraint and innovation across hundreds of
887 placental mammals. Science 380:eabn3943.
- 888
889 Cox A, Ackert-Bicknell CL, Dumont BL, Ding Y, Bell JT, Brockmann GA, Wergedal JE, Bult C,
890 Paigen B, Flint J, et al. 2009. A new standard genetic map for the laboratory mouse. Genetics
891 182:1335-1344.
- 892
893 Cunningham F, Allen JE, Allen J, Alvarez-Jarreta J, Amode MR, Armean IM, Austine-Orimoloye
894 O, Azov AG, Barnes I, Bennett R, et al. 2022. Ensembl 2022. Nucleic Acids Res 50:D988-D995.
- 895
896 Danecek P, Bonfield JK, Liddle J, Marshall J, Ohan V, Pollard MO, Whitwham A, Keane T,
897 McCarthy SA, Davies RM, et al. 2021. Twelve years of SAMtools and BCFtools. Gigascience
898 10:giab008.

- 899
900 Dapper AL, Payseur BA. 2017. Connecting theory and data to understand recombination rate
901 evolution. *Philos Trans R Soc Lond B Biol Sci* 372.
- 902
903 Daxner-Höck G. 2002. Cricetodon meini and other rodents from Mühlbach and Grund, Lower
904 Austria (Middle Miocene, late MN5). *Annalen des Naturhistorischen Museums in Wien. Serie A*
905 für Mineralogie und Petrographie, Geologie und Paläontologie, Anthropologie und
906 Prähistorie:267-291.
- 907
908 Degnan JH, Rosenberg NA. 2006. Discordance of species trees with their most likely gene trees.
909 *PLoS Genet* 2:e68.
- 910
911 Edwards SV. 2009. Is a new and general theory of molecular systematics emerging? *Evolution*
912 63:1-19.
- 913
914 Faircloth BC. 2013. illumiprocessor: a trimmomatic wrapper for parallel adapter and quality
915 trimming.
- 916
917 Faircloth BC. 2016. PHYLUCE is a software package for the analysis of conserved genomic loci.
918 *Bioinformatics* 32:786-788.
- 919
920 Faircloth BC, McCormack JE, Crawford NG, Harvey MG, Brumfield RT, Glenn TC. 2012.
921 Ultraconserved elements anchor thousands of genetic markers spanning multiple evolutionary
922 timescales. *Syst Biol* 61:717-726.
- 923
924 Feng S, Bai M, Rivas-Gonzalez I, Li C, Liu S, Tong Y, Yang H, Chen G, Xie D, Sears KE, et al.
925 2022. Incomplete lineage sorting and phenotypic evolution in marsupials. *Cell* 185:1646-1660
926 e1618.
- 927
928 Ferreira MS, Jones MR, Callahan CM, Farelo L, Tolesa Z, Suchentrunk F, Boursot P, Mills LS,
929 Alves PC, Good JM, et al. 2021. The Legacy of Recurrent Introgression during the Radiation of
930 Hares. *Syst Biol* 70:593-607.
- 931
932 Foley NM, Harris AJ, Bredemeyer KR, Ruedi M, Puechmaille SJ, Teeling EC, Criscitiello MF,
933 Murphy WJ. 2024. Karyotypic stasis and swarming influenced the evolution of viral tolerance in
934 a species-rich bat radiation. *Cell Genom* 4:100482.
- 935

- 936 Foley NM, Mason VC, Harris AJ, Bredemeyer KR, Damas J, Lewin HA, Eizirik E, Gatesy J,
937 Karlsson EK, Lindblad-Toh K, et al. 2023. A genomic timescale for placental mammal evolution.
938 Science 380:eab18189.
- 939
940 Fontaine MC, Pease JB, Steele A, Waterhouse RM, Neafsey DE, Sharakhov IV, Jiang X, Hall AB,
941 Catteruccia F, Kakani E, et al. 2015. Mosquito genomics. Extensive introgression in a malaria
942 vector species complex revealed by phylogenomics. Science 347:1258524.
- 943
944 Foote AD, Liu Y, Thomas GW, Vinar T, Alföldi J, Deng J, Dugan S, van Elk CE, Hunter ME,
945 Joshi V, et al. 2015. Convergent evolution of the genomes of marine mammals. Nat Genet 47:272-
946 275.
- 947
948 Gable SM, Byars MI, Literman R, Tollis M. 2022. A Genomic Perspective on the Evolutionary
949 Diversification of Turtles. Syst Biol 71:1331-1347.
- 950
951 Gibbs RA, Weinstock GM, Metzker ML, Muzny DM, Sodergren EJ, Scherer S, Scott G, Steffen
952 D, Worley KC, Burch PE, et al. 2004. Genome sequence of the Brown Norway rat yields insights
953 into mammalian evolution. Nature 428:493-521.
- 954
955 Good JM, Wiebe V, Albert FW, Burbano HA, Kircher M, Green RE, Halbwax M, Andre C,
956 Atencia R, Fischer A, et al. 2013. Comparative population genomics of the ejaculate in humans
957 and the great apes. Mol Biol Evol 30:964-976.
- 958
959 Green RE, Krause J, Briggs AW, Maricic T, Stenzel U, Kircher M, Patterson N, Li H, Zhai W,
960 Fritz MH, et al. 2010. A draft sequence of the Neandertal genome. Science 328:710-722.
- 961
962 Guindon S, Dufayard JF, Lefort V, Anisimova M, Hordijk W, Gascuel O. 2010. New algorithms
963 and methods to estimate maximum-likelihood phylogenies: assessing the performance of PhyML
964 3.0. Syst Biol 59:307-321.
- 965
966 Hahn MW, Nakhleh L. 2016. Irrational exuberance for resolved species trees. Evolution 70:7-17.
- 967
968 He B, Zhao Y, Su C, Lin G, Wang Y, Li L, Ma J, Yang Q, Hao J. 2023. Phylogenomics reveal
969 extensive phylogenetic discordance due to incomplete lineage sorting following the rapid radiation
970 of alpine butterflies (Papilionidae: Parnassius). Syst Entomol.
- 971
972 Hibbins MS, Breithaupt LC, Hahn MW. 2023. Phylogenomic comparative methods: Accurate
973 evolutionary inferences in the presence of gene tree discordance. Proc Natl Acad Sci U S A
974 120:e2220389120.

- 975
976 Hinrichs AS, Karolchik D, Baertsch R, Barber GP, Bejerano G, Clawson H, Diekhans M, Furey
977 TS, Harte RA, Hsu F, et al. 2006. The UCSC Genome Browser Database: update 2006. Nucleic
978 Acids Res 34:D590-598.
- 979
980 Hoang DT, Chernomor O, von Haeseler A, Minh BQ, Vinh LS. 2018. UFBoot2: Improving the
981 Ultrafast Bootstrap Approximation. Mol Biol Evol 35:518-522.
- 982
983 Hobolth A, Christensen OF, Mailund T, Schierup MH. 2007. Genomic relationships and speciation
984 times of human, chimpanzee, and gorilla inferred from a coalescent hidden Markov model. PLoS
985 Genet 3:e7.
- 986
987 Holm S. 1979. A simple sequentially rejective multiple test procedure. Scandinavian journal of
988 statistics:65-70.
- 989
990 Hu Z, Sackton TB, Edwards SV, Liu JS. 2019. Bayesian Detection of Convergent Rate Changes
991 of Conserved Noncoding Elements on Phylogenetic Trees. Mol Biol Evol 36:1086-1100.
- 992
993 Hudson RR. 1983. Testing the Constant-Rate Neutral Allele Model with Protein Sequence Data.
994 Evolution 37:203-217.
- 995
996 Hudson RR, Kaplan NL. 1988. The coalescent process in models with selection and
997 recombination. Genetics 120:831-840.
- 998
999 Hudson RR, Kaplan NL. 1995. deleterious background selection with recombination. Genetics
1000 141:1605-1617.
- 1001
1002 Huson DH, Klöpper T, Lockhart PJ, Steel MA. 2005. Reconstruction of Reticulate Networks from
1003 Gene Trees. In: Miyano S, Mesirov J, Kasif S, Istrail S, Pevzner PA, Waterman M, editors.
1004 Research in Computational Molecular Biology. RECOMB 2005. Lecture Notes in Computer
1005 Science: Springer, Berlin, Heidelberg.
- 1006
1007 Jackman SD, Vandervalk BP, Mohamadi H, Chu J, Yeo S, Hammond SA, Jahesh G, Khan H,
1008 Coombe L, Warren RL, et al. 2017. ABySS 2.0: resource-efficient assembly of large genomes
1009 using a Bloom filter. Genome Res 27:768-777.
- 1010
1011 Jarvis ED, Mirarab S, Aberer AJ, Li B, Houde P, Li C, Ho SY, Faircloth BC, Nabholz B, Howard
1012 JT, et al. 2014. Whole-genome analyses resolve early branches in the tree of life of modern birds.
1013 Science 346:1320-1331.

- 1014
1015 Jensen-Seaman MI, Furey TS, Payseur BA, Lu Y, Roskin KM, Chen CF, Thomas MA, Haussler
1016 D, Jacob HJ. 2004. Comparative recombination rates in the rat, mouse, and human genomes.
1017 Genome Res 14:528-538.
- 1018
1019 Jones MR, Mills LS, Alves PC, Callahan CM, Alves JM, Lafferty DJR, Jiggins FM, Jensen JD,
1020 Melo-Ferreira J, Good JM. 2018. Adaptive introgression underlies polymorphic seasonal
1021 camouflage in snowshoe hares. Science 360:1355-1358.
- 1022
1023 Junier T, Zdobnov EM. 2010. The Newick utilities: high-throughput phylogenetic tree processing
1024 in the UNIX shell. Bioinformatics 26:1669-1670.
- 1025
1026 Kalyaanamoorthy S, Minh BQ, Wong TKF, von Haeseler A, Jermiin LS. 2017. ModelFinder: fast
1027 model selection for accurate phylogenetic estimates. Nat Methods 14:587-589.
- 1028
1029 Kaplan NL, Hudson RR, Langley CH. 1989. The "hitchhiking effect" revisited. Genetics 123:887-
1030 899.
- 1031
1032 Kartje ME, Jing P, Payseur BA. 2020. Weak Correlation between Nucleotide Variation and
1033 Recombination Rate across the House Mouse Genome. Genome Biol Evol 12:293-299.
- 1034
1035 Katoh K, Standley DM. 2013. MAFFT multiple sequence alignment software version 7:
1036 improvements in performance and usability. Mol Biol Evol 30:772-780.
- 1037
1038 Katzman S, Kern AD, Bejerano G, Fewell G, Fulton L, Wilson RK, Salama SR, Haussler D. 2007.
1039 Human genome ultraconserved elements are ultraselected. Science 317:915.
- 1040
1041 Keane TM, Wong K, Adams DJ, Flint J, Reymond A, Yalcin B. 2014. Identification of structural
1042 variation in mouse genomes. Front Genet 5:192.
- 1043
1044 Kimura Y, Hawkins MT, McDonough MM, Jacobs LL, Flynn LJ. 2015. Corrected placement of
1045 Mus-Rattus fossil calibration forces precision in the molecular tree of rodents. Sci Rep 5:14444.
- 1046
1047 Kimura Y, Jacobs LL, Cerling TE, Uno KT, Ferguson KM, Flynn LJ, Patnaik R. 2013. Fossil mice
1048 and rats show isotopic evidence of niche partitioning and change in dental ecomorphology related
1049 to dietary shift in Late Miocene of Pakistan. PLoS One 8:e69308.
- 1050

- 1051 Kong A, Gudbjartsson DF, Sainz J, Jonsdottir GM, Gudjonsson SA, Richardsson B, Sigurdardottir
1052 S, Barnard J, Hallbeck B, Masson G, et al. 2002. A high-resolution recombination map of the
1053 human genome. *Nat Genet* 31:241-247.
- 1054
- 1055 Kowalczyk A, Meyer WK, Partha R, Mao W, Clark NL, Chikina M. 2019. RERconverge: an R
1056 package for associating evolutionary rates with convergent traits. *Bioinformatics* 35:4815-4817.
- 1057
- 1058 Kulathinal RJ, Stevison LS, Noor MA. 2009. The genomics of speciation in *Drosophila*: diversity,
1059 divergence, and introgression estimated using low-coverage genome sequencing. *PLoS Genet*
1060 5:e1000550.
- 1061
- 1062 Kumon T, Ma J, Akins RB, Stefanik D, Nordgren CE, Kim J, Levine MT, Lampson MA. 2021.
1063 Parallel pathways for recruiting effector proteins determine centromere drive and suppression. *Cell*
1064 184:4904-4918 e4911.
- 1065
- 1066 Calculating and interpreting gene- and site-concordance factors in phylogenomics [Internet]. The
1067 Lanfear Lab @ ANU2018 September 20, 2021]. Available from:
1068 http://www.robertlanfear.com/blog/files/concordance_factors.html
- 1069
- 1070 Lecompte E, Aplin K, Denys C, Catzeffis F, Chades M, Chevret P. 2008. Phylogeny and
1071 biogeography of African Murinae based on mitochondrial and nuclear gene sequences, with a new
1072 tribal classification of the subfamily. *BMC Evol Biol* 8:199.
- 1073
- 1074 Lewontin RC, Birch LC. 1966. Hybridization as a Source of Variation for Adaptation to New
1075 Environments. *Evolution* 20:315-336.
- 1076
- 1077 Li H. 2013. Aligning sequence reads, clone sequences and assembly contigs with BWA-MEM.
1078 arXiv preprint arXiv:1303.3997.
- 1079
- 1080 Li H. 2018. Minimap2: pairwise alignment for nucleotide sequences. *Bioinformatics* 34:3094-
1081 3100.
- 1082
- 1083 Liu X, Wei F, Li M, Jiang X, Feng Z, Hu J. 2004. Molecular phylogeny and taxonomy of wood
1084 mice (genus *Apodemus* Kaup, 1829) based on complete mtDNA cytochrome b sequences, with
1085 emphasis on Chinese species. *Mol Phylogenetic Evol* 33:1-15.
- 1086
- 1087 Lopes F, Oliveira LR, Kessler A, Beux Y, Crespo E, Cardenas-Alayza S, Majluf P, Sepulveda M,
1088 Brownell RL, Franco-Trecu V, et al. 2021. Phylogenomic Discordance in the Eared Seals is best

- 1089 explained by Incomplete Lineage Sorting following Explosive Radiation in the Southern
1090 Hemisphere. *Syst Biol* 70:786-802.
- 1091
1092 Lundrigan BL, Jansa SA, Tucker PK. 2002. Phylogenetic relationships in the genus *mus*, based on
1093 paternally, maternally, and biparentally inherited characters. *Syst Biol* 51:410-431.
- 1094
1095 Maddison WP. 1997. Gene Trees in Species Trees. *Systematic Biology* 46:523-536.
- 1096
1097 Martin Y, Gerlach G, Schlotterer C, Meyer A. 2000. Molecular phylogeny of European muroid
1098 rodents based on complete cytochrome b sequences. *Mol Phylogenet Evol* 16:37-47.
- 1099
1100 McKenzie PF, Eaton DAR. 2020. The Multispecies Coalescent in Space and Time.
1101 bioRxiv:2020.2008.2002.233395.
- 1102
1103 Mendes FK, Fuentes-Gonzalez JA, Schraiber JG, Hahn MW. 2018. A multispecies coalescent
1104 model for quantitative traits. *Elife* 7:e36482.
- 1105
1106 Mendes FK, Hahn MW. 2016. Gene Tree Discordance Causes Apparent Substitution Rate
1107 Variation. *Syst Biol* 65:711-721.
- 1108
1109 Mendes FK, Hahn Y, Hahn MW. 2016. Gene Tree Discordance Can Generate Patterns of
1110 Diminishing Convergence over Time. *Mol Biol Evol* 33:3299-3307.
- 1111
1112 Mendes FK, Livera AP, Hahn MW. 2019. The perils of intralocus recombination for inferences of
1113 molecular convergence. *Philos Trans R Soc Lond B Biol Sci* 374:20180244.
- 1114
1115 Mikula O, Nicolas V, Šumbera R, Konečný A, Denys C, Verheyen E, Bryjová A, Lemmon AR,
1116 Lemmon EM, Bryja J. 2021. Nuclear phylogenomics, but not mitogenomics, resolves the most
1117 successful Late Miocene radiation of African mammals (Rodentia: Muridae: Arvicanthini).
1118 *Molecular Phylogenetics and Evolution* 157:107069.
- 1119
1120 Minh BQ, Hahn MW, Lanfear R. 2020. New Methods to Calculate Concordance Factors for
1121 Phylogenomic Datasets. *Mol Biol Evol* 37:2727-2733.
- 1122
1123 Minh BQ, Schmidt HA, Chernomor O, Schrempf D, Woodhams MD, von Haeseler A, Lanfear R.
1124 2020. IQ-TREE 2: New Models and Efficient Methods for Phylogenetic Inference in the Genomic
1125 Era. *Mol Biol Evol* 37:1530-1534.
- 1126

- 1127 Mölder F, Jablonski KP, Letcher B, Hall MB, Tomkins-Tinch CH, Sochat V, Forster J, Lee S,
1128 Twardziok SO, Kanitz A, et al. 2021. Sustainable data analysis with Snakemake. F1000Res 10:33.
- 1129
- 1130 Moore EC, Thomas GWC, Mortimer S, Kopania EEK, Hunnicutt KE, Clare-Salzler ZJ, Larson
1131 EL, Good JM. 2022. The Evolution of Widespread Recombination Suppression on the Dwarf
1132 Hamster (*Phodopus*) X Chromosome. *Genome Biol Evol* 14:evac080.
- 1133
- 1134 Mouse Genome Sequencing C, Waterston RH, Lindblad-Toh K, Birney E, Rogers J, Abril JF,
1135 Agarwal P, Agarwala R, Ainscough R, Alexandersson M, et al. 2002. Initial sequencing and
1136 comparative analysis of the mouse genome. *Nature* 420:520-562.
- 1137
- 1138 Murrell B, Weaver S, Smith MD, Wertheim JO, Murrell S, Aylward A, Eren K, Pollner T, Martin
1139 DP, Smith DM, et al. 2015. Gene-wide identification of episodic selection. *Mol Biol Evol* 32:1365-
1140 1371.
- 1141
- 1142 Nilsson P, Solbakken MH, Schmid BV, Orr RJS, Lv R, Cui Y, Song Y, Zhang Y, Baalsrud HT,
1143 Torresen OK, et al. 2020. The Genome of the Great Gerbil Reveals Species-Specific Duplication
1144 of an MHCII Gene. *Genome Biol Evol* 12:3832-3849.
- 1145
- 1146 Pagès M, Fabre P-H, Chaval Y, Mortelliti A, Nicolas V, Wells K, Michaux JR, Lazzari V. 2016.
1147 Molecular phylogeny of South-East Asian arboreal murine rodents. *Zoologica Scripta* 45:349-364.
- 1148
- 1149 Pamilo P, Nei M. 1988. Relationships between gene trees and species trees. *Mol Biol Evol* 5:568-
1150 583.
- 1151
- 1152 Paradis E, Schliep K. 2019. ape 5.0: an environment for modern phylogenetics and evolutionary
1153 analyses in R. *Bioinformatics* 35:526-528.
- 1154
- 1155 Partha R, Kowalczyk A, Clark NL, Chikina M. 2019. Robust Method for Detecting Convergent
1156 Shifts in Evolutionary Rates. *Mol Biol Evol* 36:1817-1830.
- 1157
- 1158 Pease JB, Haak DC, Hahn MW, Moyle LC. 2016. Phylogenomics Reveals Three Sources of
1159 Adaptive Variation during a Rapid Radiation. *PLoS Biol* 14:e1002379.
- 1160
- 1161 Pease JB, Hahn MW. 2013. More accurate phylogenies inferred from low-recombination regions
1162 in the presence of incomplete lineage sorting. *Evolution* 67:2376-2384.
- 1163

- 1164 Platt RN, 2nd, Vandewege MW, Ray DA. 2018. Mammalian transposable elements and their
1165 impacts on genome evolution. *Chromosome Res* 26:25-43.
- 1166
- 1167 Pollard KS, Hubisz MJ, Rosenbloom KR, Siepel A. 2010. Detection of nonneutral substitution
1168 rates on mammalian phylogenies. *Genome Res* 20:110-121.
- 1169
- 1170 Pond SL, Frost SD, Muse SV. 2005. HyPhy: hypothesis testing using phylogenies. *Bioinformatics*
1171 21:676-679.
- 1172
- 1173 Poplin R, Ruano-Rubio V, DePristo MA, Fennell TJ, Carneiro MO, Auwera GAVd, Kling DE,
1174 Gauthier LD, Levy-Moonshine A, Roazen D, et al. 2018. Scaling accurate genetic variant
1175 discovery to tens of thousands of samples. *bioRxiv*:201178.
- 1176
- 1177 Ptak SE, Hinds DA, Koehler K, Nickel B, Patil N, Ballinger DG, Przeworski M, Frazer KA, Paabo
1178 S. 2005. Fine-scale recombination patterns differ between chimpanzees and humans. *Nat Genet*
1179 37:429-434.
- 1180
- 1181 Quinlan AR, Hall IM. 2010. BEDTools: a flexible suite of utilities for comparing genomic
1182 features. *Bioinformatics* 26:841-842.
- 1183
- 1184 R Core Team. 2021. R: A language and environment for statistical computing. Vienna, Austria.
- 1185
- 1186 Ranwez V, Douzery EJP, Cambon C, Chantret N, Delsuc F. 2018. MACSE v2: Toolkit for the
1187 Alignment of Coding Sequences Accounting for Frameshifts and Stop Codons. *Mol Biol Evol*
1188 35:2582-2584.
- 1189
- 1190 Revell LJ. 2012. phytools: an R package for phylogenetic comparative biology (and other things).
1191 *Methods in Ecology and Evolution* 3:217-223.
- 1192
- 1193 Rivas-Gonzalez I, Rousselle M, Li F, Zhou L, Dutheil JY, Munch K, Shao Y, Wu D, Schierup
1194 MH, Zhang G. 2023. Pervasive incomplete lineage sorting illuminates speciation and selection in
1195 primates. *Science* 380:eabn4409.
- 1196
- 1197 Robinson DF, Foulds LR. 1981. Comparison of phylogenetic trees. *Mathematical Biosciences*
1198 53:131-147.
- 1199
- 1200 Robinson DF, Foulds LR editors.; 1979 Berlin, Heidelberg.
- 1201

- 1202 Romanenko SA, Perelman PL, Trifonov VA, Graphodatsky AS. 2012. Chromosomal evolution in
1203 Rodentia. *Heredity (Edinb)* 108:4-16.
- 1204
- 1205 Rosenberg NA. 2002. The probability of topological concordance of gene trees and species trees.
1206 *Theor Popul Biol* 61:225-247.
- 1207
- 1208 Rowe KC, Achmadi AS, Fabre P-H, Schenk JJ, Steppan SJ, Esselstyn JA. 2019. Oceanic islands
1209 of Wallacea as a source for dispersal and diversification of murine rodents. *Journal of*
1210 *Biogeography* 46:2752-2768.
- 1211
- 1212 Roycroft E, Achmadi A, Callahan CM, Esselstyn JA, Good JM, Moussalli A, Rowe KC. 2021.
1213 Molecular Evolution of Ecological Specialisation: Genomic Insights from the Diversification of
1214 Murine Rodents. *Genome Biol Evol* 13:evab103.
- 1215
- 1216 Roycroft EJ, Moussalli A, Rowe KC. 2020. Phylogenomics Uncovers Confidence and Conflict in
1217 the Rapid Radiation of Australo-Papuan Rodents. *Syst Biol* 69:431-444.
- 1218
- 1219 Sarver BA, Keeble S, Cosart T, Tucker PK, Dean MD, Good JM. 2017. Phylogenomic Insights
1220 into Mouse Evolution Using a Pseudoreference Approach. *Genome Biol Evol* 9:726-739.
- 1221
- 1222 Scally A, Dutheil JY, Hillier LW, Jordan GE, Goodhead I, Herrero J, Hobolth A, Lappalainen T,
1223 Mailund T, Marques-Bonet T, et al. 2012. Insights into hominid evolution from the gorilla genome
1224 sequence. *Nature* 483:169-175.
- 1225
- 1226 Schenk JJ, Rowe KC, Steppan SJ. 2013. Ecological opportunity and incumbency in the
1227 diversification of repeated continental colonizations by muroid rodents. *Syst Biol* 62:837-864.
- 1228
- 1229 Schliep KP. 2011. phangorn: phylogenetic analysis in R. *Bioinformatics* 27:592-593.
- 1230
- 1231 Serizawa K, Suzuki H, Tsuchiya K. 2000. A phylogenetic view on species radiation in Apodemus
1232 inferred from variation of nuclear and mitochondrial genes. *Biochem Genet* 38:27-40.
- 1233
- 1234 Shifman S, Bell JT, Copley RR, Taylor MS, Williams RW, Mott R, Flint J. 2006. A high-resolution
1235 single nucleotide polymorphism genetic map of the mouse genome. *PLoS Biol* 4:e395.
- 1236
- 1237 Singhal S, Leffler EM, Sannareddy K, Turner I, Venn O, Hooper DM, Strand AI, Li Q, Raney B,
1238 Balakrishnan CN, et al. 2015. Stable recombination hotspots in birds. *Science* 350:928-932.
- 1239

- 1240 Slatkin M, Pollack JL. 2006. The concordance of gene trees and species trees at two linked loci.
1241 *Genetics* 172:1979-1984.
- 1242
1243 Smagulova F, Gregoretti IV, Brick K, Khil P, Camerini-Otero RD, Petukhova GV. 2011. Genome-
1244 wide analysis reveals novel molecular features of mouse recombination hotspots. *Nature* 472:375-
1245 378.
- 1246
1247 RepeatMasker Open-4.0 [Internet]. 2013-2015. Available from <http://www.repeatmasker.org>.
- 1248
1249 Smith BT, Merwin J, Provost KL, Thom G, Brumfield RT, Ferreira M, Mauck WM, Moyle RG,
1250 Wright TF, Joseph L. 2023. Phylogenomic Analysis of the Parrots of the World Distinguishes
1251 Artifactual from Biological Sources of Gene Tree Discordance. *Syst Biol* 72:228-241.
- 1252
1253 Smith JM, Haigh J. 1974. The hitch-hiking effect of a favourable gene. *Genet Res* 23:23-35.
- 1254
1255 Smith MD, Wertheim JO, Weaver S, Murrell B, Scheffler K, Kosakovsky Pond SL. 2015. Less is
1256 more: an adaptive branch-site random effects model for efficient detection of episodic diversifying
1257 selection. *Mol Biol Evol* 32:1342-1353.
- 1258
1259 Smith SA, Brown JW, Walker JF. 2018. So many genes, so little time: A practical approach to
1260 divergence-time estimation in the genomic era. *PLoS One* 13:e0197433.
- 1261
1262 Smith SA, Moore MJ, Brown JW, Yang Y. 2015. Analysis of phylogenomic datasets reveals
1263 conflict, concordance, and gene duplications with examples from animals and plants. *BMC Evol
1264 Biol* 15:150.
- 1265
1266 Stanyon R, Yang F, Cavagna P, O'Brien P, Bagga M, Ferguson-Smith M, Wienberg J. 1999.
1267 Animal Cytogenetics and Comparative Mapping—Reciprocal chromosome painting shows that
1268 genomic rearrangement between rat and mouse proceeds ten times faster than between humans
1269 and cats. *Cytogenetics and Cell Genetics* 84:150-155.
- 1270
1271 Stapley J, Feulner PGD, Johnston SE, Santure AW, Smadja CM. 2017. Variation in recombination
1272 frequency and distribution across eukaryotes: patterns and processes. *Philos Trans R Soc Lond B
1273 Biol Sci* 372.
- 1274
1275 Steppan SJ, Adkins RM, Spinks PQ, Hale C. 2005. Multigene phylogeny of the Old World mice,
1276 Murinae, reveals distinct geographic lineages and the declining utility of mitochondrial genes
1277 compared to nuclear genes. *Mol Phylogenetic Evol* 37:370-388.

- 1278
1279 Steppan SJ, Schenk JJ. 2017. Muroid rodent phylogenetics: 900-species tree reveals increasing
1280 diversification rates. PLoS One 12:e0183070.
- 1281
1282 Stevenson LS, Woerner AE, Kidd JM, Kelley JL, Veeramah KR, McManus KF, Great Ape Genome
1283 P, Bustamante CD, Hammer MF, Wall JD. 2016. The Time Scale of Recombination Rate
1284 Evolution in Great Apes. Mol Biol Evol 33:928-945.
- 1285
1286 Sun C, Huang J, Wang Y, Zhao X, Su L, Thomas GWC, Zhao M, Zhang X, Jungreis I, Kellis M,
1287 et al. 2021. Genus-Wide Characterization of Bumblebee Genomes Provides Insights into Their
1288 Evolution and Variation in Ecological and Behavioral Traits. Mol Biol Evol 38:486-501.
- 1289
1290 Suzuki H, Shimada T, Terashima M, Tsuchiya K, Aplin K. 2004. Temporal, spatial, and ecological
1291 modes of evolution of Eurasian *Mus* based on mitochondrial and nuclear gene sequences. Mol
1292 Phylogenet Evol 33:626-646.
- 1293
1294 Tange O. 2018. GNU Parallel.
- 1295
1296 To TH, Jung M, Lycett S, Gascuel O. 2016. Fast Dating Using Least-Squares Criteria and
1297 Algorithms. Syst Biol 65:82-97.
- 1298
1299 Treaster S, Deelen J, Daane JM, Murabito J, Karasik D, Harris MP. 2023. Convergent genomics
1300 of longevity in rockfishes highlights the genetics of human life span variation. Sci Adv
1301 9:eadd2743.
- 1302
1303 van der Valk T, Pecnerova P, Diez-Del-Molino D, Bergstrom A, Oppenheimer J, Hartmann S,
1304 Xenikoudakis G, Thomas JA, Dehasque M, Saglican E, et al. 2021. Million-year-old DNA sheds
1305 light on the genomic history of mammoths. Nature 591:265-269.
- 1306
1307 Vanderpool D, Minh BQ, Lanfear R, Hughes D, Murali S, Harris RA, Raveendran M, Muzny DM,
1308 Hibbins MS, Williamson RJ, et al. 2020. Primate phylogenomics uncovers multiple rapid
1309 radiations and ancient interspecific introgression. PLoS Biol 18:e3000954.
- 1310
1311 Wang LG, Lam TT, Xu S, Dai Z, Zhou L, Feng T, Guo P, Dunn CW, Jones BR, Bradley T, et al.
1312 2020. Treeio: An R Package for Phylogenetic Tree Input and Output with Richly Annotated and
1313 Associated Data. Mol Biol Evol 37:599-603.
- 1314
1315 White MA, Ane C, Dewey CN, Larget BR, Payseur BA. 2009. Fine-scale phylogenetic
1316 discordance across the house mouse genome. PLoS Genet 5:e1000729.

- 1317
1318 Yalcin B, Wong K, Agam A, Goodson M, Keane TM, Gan X, Nellaker C, Goodstadt L, Nicod J,
1319 Bhomra A, et al. 2011. Sequence-based characterization of structural variation in the mouse
1320 genome. *Nature* 477:326-329.
- 1321
1322 Yang Z. 2007. PAML 4: phylogenetic analysis by maximum likelihood. *Mol Biol Evol* 24:1586-
1323 1591.
- 1324
1325 Yekutieli D, Benjamini Y. 1999. Resampling-based false discovery rate controlling multiple test
1326 procedures for correlated test statistics. *Journal of Statistical Planning and Inference* 82:171-196.
- 1327
1328 Yu G. 2020. Using ggtree to Visualize Data on Tree-Like Structures. *Curr Protoc Bioinformatics*
1329 69:e96.
- 1330
1331 Yu G, Smith DK, Zhu H, Guan Y, Lam TT-Y. 2017. ggtree: an r package for visualization and
1332 annotation of phylogenetic trees with their covariates and other associated data. *Methods in
1333 Ecology and Evolution* 8:28-36.
- 1334
1335 Zhang C, Rabiee M, Sayyari E, Mirarab S. 2018. ASTRAL-III: polynomial time species tree
1336 reconstruction from partially resolved gene trees. *BMC Bioinformatics* 19:153.
- 1337
1338
1339